Effects of Tissue Mimetic Conditions on Antibiotic Interactions Against *Klebsiella pneumoniae*

A thesis submitted by

Yoelkys Morales

in partial fulfillment of the requirements for the degree of

PhD

in

Molecular Microbiology

Tufts University

Graduate School of Biomedical Sciences

May 2023

Advisor: Joan Mecsas, PhD

Abstract

Klebsiella pneumoniae is a Gram-negative bacterium that is the causative pathogen in infections such as bacteremia, pneumonia, urinary tract infections, and liver abscesses. While traditionally it has been associated with hospitalized and immunocompromised patients, increases in community-acquired infections have been observed. Most recently, *Klebsiella* has risen in notoriety due to high levels of drug resistance. Alarming rates of both multi-drug (MDR) and pan-drug resistant (PDR) infections have led organizations such as the Center for Disease Control and World Health Organization to classify *Klebsiella,* and other Gram-negative pathogens, as a global health threat. In an age where antibiotic discovery is at an all-time low, scientists and physicians have looked into alternative strategies to combat these infections. One of these methods is the repurposing of current antibiotics into combination therapies in hopes of taking advantage of complementary effects between drugs. Advantages such as broad coverage of organisms, shorter therapy duration, and reduced rates of resistance have been documented. Despite this, it is currently not recommended for MDR *Klebsiella.* This is due to the lack of clinical guidance and reliability of predicting which combinations improve clinical outcomes for a specific patient and infection. So far *in vitro* synergy testing has not yielded a strong correlation with improved clinical outcomes. However, combination therapy has shown significant reductions in mortality for patients suffering from the most critical and lethal forms of infection by *Klebsiella.* As rates of PDR infections rise so may the need for combination therapy as a reliable clinical tool.

In this dissertation, we hypothesize that a factor contributing to the discordance between *in vitro* testing and *in vivo* outcomes for drug combinations may the physiologic environment of the bacteria during infection and the influence these conditions have on drug combination interactions. By testing a panel of ten drugs in pair-wise combination using DiaMOND (Diagonal measurement of n-way Drug interactions) across three separate media we found that, for *Klebsiella,* tissue relevant media had a significant effect on drug interactions. Furthermore, using a mouse model for *Klebsiella* lung infections we found that media nutritionally similar to the mouse lung had stronger correlations with *in vivo* antibiotic interactions than a standard rich medium. Lastly, we developed a Δ*tdk* mutant in *Klebsiella* as a tool for testing the antibiotic trimethoprim-sulfamethoxazole (TMP:SMX) in a mouse model. Normally, elevated levels of thymidine found in mouse plasma, but not human, inhibit the effects of this commonly used antibiotic preventing researches from using mouse models, a critical tool for pharmacological studies, to explore anti-folate therapies such as TMP:SMX. Deletion of *tdk* sensitizes *Klebsiella* to TMP:SMX despite the presence of thymidine thus enabling a mouse model for testing anti-folate therapy. Collectively, by using DiaMOND we explore the potential for combination therapy for the treatment of *Klebsiella* and identify growth conditions as a key factor that needs to be considered. Through these efforts we also developed tools to help probe the potential for combination therapy for the treatment of multi-drug resistant *Klebsiella.*

Acknowledgements

I have been very fortunate to have completed my PhD here at Tufts. Over time, Tufts has become like a second home to me, where I have been able to find several wonderful mentors that have guided me along the way. I was first introduced to Tufts through a the Leadership Alliance through which I participated in the BDBS program while I was a rising Sophomore at Williams College. Coming to Tufts for a summer and working with Dr. Henry Wortis on babesiosis introduced me to the world of biomedical research and specifically host-pathogen interactions. Following my graduation from Williams, Henry was kind enough to put me in contact with Dr. Miguel Stadecker who took me in as a fresh college graduate to be a technician for his lab working on a different parasite, schistosomiasis. My work with Miguel was always at the interface of host-pathogens interactions and this is where I learned how to be a diligent and curious researcher. While in Miguel's lab I had the pleasure of working with Dr. Parisa Kalantari who helped me learn numerous techniques and guided me at the bench daily. Through my work with Miguel I then entered the PREP program at Tufts working with Dr. Stephen Bunnell across the hall. Although I continued to work on the same pathogen it was from a different lens, focusing on innate immunology and cell signaling. With Steve I was able to hone many of the skills that have led me to where I am today . I was continuously impressed with his ability to think about science and elegantly connect seemingly unrelated concepts. His dedication to teaching and spending time with me one-on-one will always be appreciated.

My scientific training at Tufts ultimately culminated in joining Dr. Joan Mecsas' lab as a MD/PhD student. Even before I applied to the Tufts MSTP I knew that I wanted to work with Joan. Despite having never met her, the kind words spoken by her students in regard to her mentorship spoke volumes for me. Together with her interest in host-pathogen interactions motivated me to rotate in her lab with hopes of joining two years later. Working with Joan on a rotation project confirmed that she would be an ideal mentor for me. She gave me the guidance to work on a current project in the lab but when I asked to work on something fully unrelated, and in hindsight rather ambitious, she fully supported me and joined me in my enthusiasm to connect neutrophil inflammasome activation to *Yersinia* and SKAP. I knew after that, regardless of the project I would enjoy my time in her lab. After joining the lab two years later Joan found the perfect project for me. I will forever be grateful that she was thoughtful in presenting a project that would combine my interest in microbiology, translational medicine, and host-pathogen interactions. All while helping me maintain a portion of my clinical knowledge.

During my time in the Mecsas lab I was in an environment that was supportive and conducive for learning how to be a scientist. I had the support to work independently pull from numerous resources while given the opportunity and encouragement to present my work in many different meetings and conferences. I would also like to thank all the members of the lab that helped create this environment and for being Escape Room champions. I personally want to thank Dr. Anne McCabe and Dr. Rebecca Silver, team Kleb, specifically for essentially teaching me microbiology and how to infect mice. Thank you Anne for staring at MatLab errors in confusion with me and to Rebecca for teaching me how mice breathe. Of course I would also thank Angel for your company

and shared suffering during COVID when we were the only lab members for some time. Against all odds we kept the lab running and functional for the new members there today. I hope to be at your defense soon!

I also thank my thesis chair committee, Dr. Aimee Shen, Dr. Linden Hu, Dr. Bree Aldrige, and Dr. Alysse Wurcel. Our meetings were always a pleasure and a great time discussing science. Your advice and guidance was invaluable during my time and I appreciated all of your clinical and scientific insights! I also want to specifically thank Alysse for being my clinical mentor. With her support I was awarded a GERM grant from IDSA to work on a project I cared deeply about. Outside of science I have a passion for social justice and this project, which we later published on, helped me explore those passions during my thesis work. A special thanks to Bree and the Aldridge lab for helping me understand DiaMOND, somewhat learning MatLab, and letting me use BARB. I personally thank Dr. Jonah Larkins-Ford for his help with DiaMOND and Yonathan Degefu for always helping me with my numerous Matlab struggles. Lastly, Dr. Kathleen Davis who started working on DiaMOND in Gram-negatives alongside me. We were truly in the trenches at the start learning both microbiology, MatLab, and DiaMOND. Your constant help and willingness to talk about science has been instrumental in my thesis work.

I also want to thank the MSTP program and all its members for continual support and friendship during my time here. It has been a long road with many obstacles along the way. I have been lucky to be surrounded by peers that exemplify what it means to be a physician scientist and I am glad to have met you all.

Thank you to the microbiology program, including all the administrators, program coordinators, and fellow students. Truly a well run and supportive program that has been extremely welcoming. In the wake of the events that occurred during my time here I was inspired by the commitment to DEI efforts and I look forward to seeing the differences it makes withing the program!

Lastly, I need to thank my family. My sister Melissa for following me up to Boston and going to Tufts undergrad. I am always proud of her and all she has accomplished! My mom Mayelin and my dad Juan are two of the most incredible people I know. They have sacrificed so much for me, and my sister and I owe them for the core values I hold today. Both of them are examples of hard work and dedication paying off in the long run and I love them all very much.

Table of Contents

List of Tables

List of Figures

List of Abbreviations

AAC	acetyltransferase
Ab	Acinetobacter baumanii
AMR	antimicrobial resistance
ANT	nucleotidyltransferase
APH	phosphotransferase
BAC	Bactrim
CAMHB	cation adjusted mueller hinton broth
CDC	center for disease control
CF	cystic fibrosis
CFP	cefepime
CFU	colony forming units
CFX	cefixime
CI	competetive index
COL	colistin
CTX	ceftriaxone
CTX-M	cefotaximase
DiaMOND	Diagonal measurement of n-way drug interaction
DTR	difficult to treat resistant
ESBL	extended spectrum beta-lactamase
FIC	fractional inhibitory concentration
GENT	gentamicin
hpi	hours post infection
IC90	inhibitory concnetraion 90%
IDSA	Infectious Disease society of america
Kp	Klebsiella pneumonia
KPC	Klebsiella produced carbapenemase
LEVO	levofloxacin
LPS	lippopolysaccaharides
M9Glu	minmal media + 0.5% glucose +0.6μM Fe(II)SO4
MBL	metallo beta-lactamase
MDR	multi-drug reistant
MERO	meropenem
MH	Mueller-Hinton
MIC	minimum inhibitory concentration
NDM-1	new dehli metallo protease
Pa	Pseudomonas aerugenosas
PDR	pan-drug resistant
PLA	propargyl-linked antifolates

RIF	rifampicin
RND	resistance nodulation divison
SBL	serine beta-lactamase
Tdk	thymidine kinase
THP	Tamm-Horsfall protein
TIG	tigecylcine
TMP:SMX	trimethoprim:sulfamethoxazole
UMM	urine mimetic media
UTI	urinary tract infection
VAP	ventillator associated pneumonia
VIM	Verona Imipenemase
WHO	world health organization
XDR	extensively drug resistant

Chapter 1: Introduction

1.1. *Klebsiella pneumoniae*

Klebsiella pneumoniae (Kp) is a Gram-negative encapsulated rod that is the causative pathogen of many infections, including pneumonia, urinary tract infections (UTIs), bacteremia, and liver abscesses (Paczosa & Mecsas, 2016). While each of these infections vary in their clinical presentation, Kp is known to cause high levels of inflammation and can be a persistent pathogen (Choby et al., 2020). As a member of the *Enterobacteriaceae* genus and ranked among the top 10 bacteria causing hospital-acquired infections. Concerningly, it is the most common pathogen isolated from intensive care units and a significant contributor to hospital outbreaks. It is typically transmitted through the gastrointestinal tract and hands of hospital staff (Al-Zalabani et al., 2020). While focal infections can vary, Kp is the second most common cause (behind *E. coli*) for bloodstream infections. Risk factors for mortality to Kp are increasing age, extra-urinary or biliary infection, heart disease, alcoholism, and diabetes (Meatherall et al., 2009). Clinical concern for Kp has continued to increase with new isolates that are continually more virulent or drug resistant (Choby et al., 2020).

1.1.1. History and Prevalence

Kp is a Gram-negative encapsulated rod that is the causative pathogen of many infections, including pneumonia, UTIs, bacteremia, and liver abscesses (Paczosa & Mecsas, 2016). It was first identified in 1882 by Carl Friedländer as a cause of pneumonia (Ashurst & Dawson, 2022). Historically Kp has been thought to primarily cause infections in immunocompromised or hospitalized individuals. However, with

increasing rates of newer and more virulent strains, referred to as hypervirulent strains, community acquired infections by Kp are becoming more common (Li et al., 2019). Kp often resides on the surface of medical devices but can also be isolated from soil, water, and food-based sources. Notably, Kp frequently colonizes the human gastro-intestinal tract and can be isolated as a commensal organism in about 6-8% of people in the USA and Australia, however this number increases to about 25% for people with a recent hospital exposure (Wyres et al., 2020). In fact, the primary reservoir of Kp are humans due to its ability readily colonize the human mucosal linings of the gut and airways, although it can be found in the stool of several other mammalian species (Wyres et al., 2020).

Even though Kp can act like a benign commensal member of the human mucosa, it is capable of severe infections and pathogenicity. Strikingly, Kp is responsible for about 12% of all hospital-acquired pneumonias, surpassed only by Pseudomonas which accounts for 17% of these infections (Walter et al., 2018). Rates of infection by Kp, in addition to other Gram-negative pathogens, have also seen a recent spike in incidence, linked to the global SARs-COV2 pandemic (Shbaklo et al., 2022). Patients suffering from COVID are at an increased risk of secondary infection by Kp, particularly once placed on a ventilator (Shbaklo et al., 2022). To make matters worse, rates of drug resistant Kp infections have also steadily risen in recent years (Effah et al., 2020). This spread of drug resistant stains of Kp is occurring in the backdrop of a public health crisis regarding antimicrobial resistant bacterial infections (Talebi Bezmin Abadi et al., 2019). In this dissertation, we examine the effectiveness of Kp as a pathogen while highlighting

the challenges in overcoming antimicrobial resistance. We then focus on two projects focusing on Kp that expand one strategy to combat this growing threat.

1.1.2. Virulence Factors

Despite being an effective and widespread pathogen Kp does not have many complex or sophisticated virulence factors (Paczosa & Mecsas, 2016). However, it does have several key element that allow it to grow in a wide variety of environments, evade the immune system, and cause severe disease. These include a capsule, lipid polysaccharide (LPS), siderophores, and fimbriae.

1.1.2.1. Capsule

Perhaps the most critical and studied strategy employed by Kp is the thick polysaccharide capsule surrounding the bacterium (Podschun & Ullmann, 1998). Over 79 different forms of this capsule have been described to date, with non-capsulated strains of the bacteria proving to be severely limited in their pathogenicity (Hansen et al., 1999; Walker & Miller, 2020). The capsule element masks many of the inflammatory antigens that would normally draw the immune system to a Gram-negative bacterium while also preventing many immunological or chemical assaults from harming Kp (Paczosa & Mecsas, 2016). It has been demonstrated that capsulated Kp attenuates the levels of IL-1ß, IL-8, IL-6, and TNF-a when compared to non-capsulated strains (Regueiro et al., 2011; Yoshida et al., 2000, 2001). This results in fewer neutrophils being recruited to the site of infection slowing the immune response to Kp. In addition to masking antigens, the capsule prevents immune cells from binding to the bacteria, which protects it from

phagocytosis (Bengoechea & Sa Pessoa, 2019; Yoshida et al., 2000). Lastly, the capsule is able to protect Kp from the host complement system as well as a variety of antimicrobial peptides (Merino et al., 1992).

1.1.2.2. Role of LPS

In addition to the polysaccharide capsule, like other Gram-negative bacteria, Kp has LPS coating the outer leaflet of the cell membrane (Choi et al., 2020). LPS is an endotoxin comprised of O antigen, lipid A, and core oligosaccharide and is a potent immune activator (Rossol et al., 2011). This has both detrimental and beneficial effects for Kp during infection. One of the primary recognition receptors for LPS is TLR4 (Rossol et al., 2011) and mice lacking this receptor have been found to be more susceptible infection by strains of Kp (Cai et al., 2009). This finding demonstrated the role of LPS as an inflammatory antigen that allows the immune system to detect and counteract infection by Kp. However, LPS is also an important virulence factor during infection, allowing the bacteria to avoid other humoral immune responses such as complement (Merino et al., 1992). In addition to protecting the bacteria from immune functions, LPS enhances the systemic spread of Kp during infection (Paczosa & Mecsas, 2016). This is thought to occur through the increased inflammation in surrounding tissues allowing for leakage of the bacterium into the bloodstream and into other tissue sites (Ohno et al., 1995). This process also enables easier acquisitions of essential nutrients, such as iron, from the surrounding environment (Ganz & Nemeth, 2015).

1.1.2.3. Iron acquisition and siderophores

An additional virulence factor for Kp are the various siderophores it can produce (Paczosa & Mecsas, 2016). During infection, a non-specific innate immune response is the sequestration and limitation of iron (Ganz & Nemeth, 2015). This leads to very low levels of free iron in plasma with the majority of iron bound to proteins such as transferrin or lactoferrin (Ganz & Nemeth, 2015). To bypass this host response, many bacteria including Kp release siderophores which have higher affinity to iron than these host proteins (Miethke & Marahiel, 2007). This allows the bacteria to scavenge iron from the host and utilize it for growth. Interestingly, Kp employs a wide variety of siderophores during infection, both allowing for evasion of host immune responses as well as adapting to different infection sites (Lan et al., 2021). This includes the siderophore yersiniabactin, first identified in Yersinia, which is overrepresented in Kp strains isolated from respiratory infections (Bachman et al., 2011). Yersiniabactin expression increases during lung infection is able to avoid innate immune responses that would normally neutralize siderophore activity (Bachman et al., 2011). In conjunction with enterobactin, this allows Kp to grow to high bacterial burdens in the lung environment.

1.1.2.4. Fimbriae aid with colonization and virulence.

Another well studied virulence factor for Kp is the presence of type 1 and 3 fimbriae which mediate adhesion of the bacteria (Paczosa & Mecsas, 2016). Type 1 fimbriae are thin protrusions on the surface of the bacterium and are considered mannose sensitive, due to its ability to bind to D-mannosylated glycoproteins (Knight &

Bouckaert, 2009) present on specific tissue cell linings. One location where type 1 fimbriae expression is often upregulated is the urinary tract (Klemm & Schembri, 2000). Kp strains isolated from a UTI are found to express high levels of type 1 fimbriae, which has also been associated to bladder colonization and biofilm formation (Struve et al., 2009). Unlike type 1, type 3 fimbriae are able to bind in a mannose independent manner and instead adhere to extracellular proteins such as collagen (Murphy & Clegg, 2012; Struve et al., 2009). However, neither type 1 or 3 fimbriae have been found to be essential for the colonization of the GI tract or lung environments (Paczosa & Mecsas, 2016). Instead, the role of fimbriae seems to be more involved with formation of biofilm and adhesion to non-biological surfaces, such as indwelling catheters (Struve et al., 2009). This is a critical component of Kp pathogenicity since these complex infections are often the most long lasting and difficult to treat.

Overall, the thick capsule, LPS, siderophores, and presence of fimbriae are the most well characterized and studied virulence factors for Kp. Unlike other pathogens, Kp does not utilize sophisticated virulence factors such as a type III secretion system or exotoxins (Johnson, 2018). Instead Kp relies on a simple, but effective, strategy of evading host immune factors and having the capacity to grow in a diverse set of environments with limited resources. This has led to a hearty pathogen that can cause many kinds of infections, which unfortunately, are becoming more difficult to treat with the emergence of both hypervirulent and drug-resistant strains. Next, we examine how a simple pathogen such as Kp has adapted beyond hospital acquired infections to cause infections in healthy individuals.

1.1.3. Emergence of hypervirulent strains

Classically, Kp has been considered a pathogen that mainly affects people who are immunocompromised, diabetic, or hospitalized (Paczosa & Mecsas, 2016). While increases in drug resistance have made it more difficult to treat these infections, drug resistance has not been associated with virulence. Since the 1980's however, newer strains have been identified that have been able to cause more serious infections in otherwise healthy individuals (Choby et al., 2020). These strains are referred to as hypervirulent strains when compared to classical strains. Hypervirulent strains infect both immunocompromised and healthy people because they are more invasive, and thus are likely to cause bacteremia, and established a replicative niche in tissues such as the liver (cheng et al., 1991; Choby et al., 2020). It was thought that hypervirulent strains have been mainly endemic in regions of Taiwan and Southeast Asia (Shon et al., 2013). More recent reports suggest that these strains have spread globally with cases in North America, Europe, and Australia (Serban et al., 2021). For now, hypervirulent strains remain mostly drug sensitive, with only 17% of hypervirulent strains being classified as ESBL (Li et al., 2014). While there have been some reports of carbapenemase-producing hypervirulent strains, fortunately these remain the minority (Arcari & Carattoli, 2022; Paczosa & Mecsas, 2016). Despite a low incidence of drug resistance in these strains there is a growing threat that drug resistance will continue to rise in hypervirulent strains leading to highly pathogenic and drug resistant strains of Kp. This looming public health threat has led to an increased interest in Kp and a need for novel therapeutics.

1.1.3.1. Distinction between classical and hypervirulent strains

Some key differences between hypervirulent strains and classical Kp strains are the kinds of infections they can cause. In addition to the tissues which classical strains are capable of invading, hypervirulent strains can also lead to pyogenic liver abscess, cellulitis, necrotizing fasciitis, and meningitis (Ko et al., 2002; Patel et al., 2018). A defining feature of hypervirulent strains is the hypercapsule serotype K1, which comprises 93% of hypervirulent strains (Yu et al., 2008). This hypercapsule is referred to as hypermucoviscous due to the polysaccharide components in the capsule when compared to classical Kp isolates (Yu et al., 2008). The thicker capsule also contributes to increased virulence as it may enhance many of the features that enable the classical capsule to contribute to pathogenicity during infection (Paczosa & Mecsas, 2016). More so than the classic capsule, the hypercapsule is a key component to complement resistance in hypervirulent strains (J. Zhu et al., 2021). Specifically, the hypercapsule protects the bacteria from the antimicrobial peptides HBD-1-3, lactoferrin, and neutrophil protein 1 (Fang et al., 2004). In addition to protecting the bacterial cell from humoral responses, the hypercapsule also further prevents phagocytosis of the cell by neutrophils and macrophages (J. Zhu et al., 2021). This has been linked to increased levels of fructose in the capsule (Panjaitan et al., 2021). Fructose production is enhanced in hypervirulent strains via upregulation of the *wcaG* gene, and its presence is critical for both capsule production and virulence during mouse infection models (Paczosa & Mecsas, 2016). By further evading the immune system, protecting from humoral responses such as complement, and limiting phagocytosis it may allow the bacterium to grow in a wider variety of tissues while infecting immunocompetent hosts.

1.1.3.2.Genetic markers for hypervirulent strains

The genes necessary for this hypercapsule are typically located on a large virulence plasmid, pLVPK (Lee, 2017), alongside the siderophore related genes aerobactin (*iutA, iucABCD*), yersiniabactin (*ybt*) and samochelin (*iroBCDN*) which together enable this hypervirulent phenotype (Patel et al., 2014; Walker & Miller, 2020). This plasmid also includes genes that enhance the regulation of capsule production such as regulator of mucoid phenotype A (*rmpA*) and *rmpA2*. This is coupled with increased production of regulation of capsule synthesis A and B (*rscA, rscB*) (Patel et al., 2014; Walker & Miller, 2020). Several experiments have linked the presence of *rmpA* to hypervirulence. While not all *rmpA* positive strains are hypervirulent, all hypervirulent strains are *rmpA* positive (Struve, 2015). In addition to *rmpA* and *rscA/B*, the gene *magA* (also known as *wyz_K1*) is also required for the hypercapsule production (Struve et al., 2015). Collectively, the presence of several of these genes within pLVPK enables both a hypercapsule and hypervirulent phenotype.

Alongside this increase in capsule production, hypervirulent plasmids also carry siderophores that are thought to enhance the virulence of Kp in various tissue types. Both siderophores yersiniabactin and salmochelin and been observed as overrepresented in hypervirulent strain of Kp compared to classical strains (Paczosa & Mecsas, 2016). Yersiniabactin has been linked to increased virulence in the lungs due to its resistance to lipocalin-2 which is expressed by neutrophils to sequester iron from bacteria (Miethke & Marahiel, 2007). Meanwhile, salmochelin is a modified enterobactin, through c-glucosylation, which enhances colonization of the nasopharynx by Kp (Paczosa & Mecsas, 2016). Salmochelin, similar to yersniabactin, is resistant to lipocalin-2 and is

present in over 90% of hypervirulent strains of Kp (Lan et al., 2021). The combined effects of yersniabactin and salmochelin lead to increased virulence in immunocompetent host where neutrophils are present and actively attempting to sequester iron from bacteria. Yet, the strongest association between a siderophore and hypervirulent strains is the presence of aerobactin. Aerobactin is a citrate-hydroxamate siderophore found in 93-100% of hypervirulent strains (Lan et al., 2021; Vernet et al., 1995). In fact, presence of aerobactin is always associated to a hypercapsule, although not all hypercapsule expressing strains also express aerobactin (Paczosa & Mecsas, 2016). This observation is primarily caused by the presence of the aerobactin gene cluster, *iucABCD*, on the virulence plasmid encoding *rmpA* (Nassif & Sansonetti, 1986; Walker & Miller, 2020). Together, these three siderophores: yersinabactin, salmochelin, and aerobactin enable virulence of Kp during many kinds of infections while creating robust redundancy for the acquisition of iron.

The presence of both the hypercapsule and additional siderophores greatly enhances the virulence of these Kp strains. While antibiotic resistance rates in hypervirulent strains have remained relatively low, this could change if rates of infection by hypervirulent strains continue to rise. As cases of hypervirulent Kp become more common globally, it could present a unique challenge of an infectious and drug resistant pathogen requiring global efforts to combat. The growing presence of pan-resistant strains of Kp coupled with rising cases of hypervirulent Kp infections make this crisis scenario a possibility that needs to be considered (Arcari & Carattoli, 2022).

1.1.4. Diversity in growth enviornments

One of the more interesting aspects of Kp, that often further complicates management of infections, is its ability to infect and replicate in a wide variety of tissues (Paczosa & Mecsas, 2016). While it was first isolated from patients with pneumonia, cases of Kp infections in nearly all tissue types have been reported (Sahly & Podschun, 1997). Some of the other common sites of infection besides the include the urinary tract, blood stream, and liver. However, there have also been cases of cellulitis, kidney abscess, myositis, meningitis, necrotizing fasciitis, osteomyelitis, and septic arthritis (Dourakis et al., 2006; Escudero Siosi et al., 2021; Fang et al., 2000; Kishibe et al., 2016; Paczosa & Mecsas, 2016; Rahim et al., 2019; Yen et al., 2018). While these sites of infection are far less common, when cases of Kp occur in these tissue sites it can be quite severe and devastating for the patient. In fact, cases of osteomyelitis caused by Kp are some of the most damaging, often leading to the full destruction of the bone and need for amputation (Prokesch et al., 2016). This high severity stems from the fact that once Kp establishes a replicative niche it is effective at evading the immune system while also being difficult to treat with antibiotics. The rates of these secondary infections caused by classical strains of Kp remain low, however hypervirulent strains of Kp are much more likely and capable of invading these tissue spaces in healthy individuals (Choby et al., 2020; Sahly & Podschun, 1997). With the increasing prevalence and spread of hypervirulent Kp strains the incidence and relevance of these infections will likely rise as well (Choby et al., 2020).

1.1.4.1. Adaptations for growth environments

The ability for Kp to grow in such diverse environments is a testament to the bacteria's ability to both scavenge for nutrients and have metabolic flexibility to use various carbon sources as a resource (Paczosa & Mecsas, 2016). Kp has even been considered by some as a potential microbial cell factory to produce several commercial bio-products (Kumar & Park, 2018). While the preferred carbon source for Kp is glucose, a possible link between Kp infection and diabetic patients, Kp is capable of using gluconate, glycerol, creatinine, starch, and many other sugars as primary sources of carbon (Kumar & Park, 2018). Additionally, Kp can utilize some lipids and even cholesterol as an energy source or signaling factor during lung and gastrointestinal infections (Lery et al., 2014). Lastly, it is able to extract nitrogen from urea allowing it to colonize the urinary tract as well as joint spaces where urea may be readily available (Collins & D'Orazio, 1993).

1.1.4.2.The lung environment experienced by Kp

Of the many tissue sites that Kp is able to infect the two most well-known and characterized infections are pneumonias and UTIs (Paczosa & Mecsas, 2016; Wang et al., 2020). Kp is one of the leading causes of hospital acquired pneumonia, in particular ventilator associated pneumonia (VAP) (Alp & Voss, 2006; Garcia-Menino et al., 2021; Rivera-Espinar et al., 2020). Within the lungs, the primary carbon source is glucose, for a healthy individual this is typically around 0.4mM or 12 times lower than the blood glucose level (Baker & Baines, 2018). This level of glucose is restricted primarily by tight junctions but can increase due to either an infection, increasing diffusion across tight

junctions, or hyperglycemia, increased plasma glucose levels lead to increased basal diffusion of glucose into the alveolar space (Baker & Baines, 2018). These factors place people with a viral infection, such as influenza, or diabetics at an increased risk of infection by Gram-negative bacteria such as Kp (Grousd et al., 2019). In addition to low levels of glucose found in the healthy lung the dominant protein is the lipoprotein surfactant which coats the alveolar lining and maintains the surface tension of the alveolar space (Ryan et al., 2006). Surfactants, specifically SP-B, have been shown to bind to some bacteria and have some antimicrobial effects in conjunction with nitric oxide species (Ryan et al., 2006). However, Kp can respond to and metabolize the lipids from surfactants to increase capsule production or fimbriae expression (Willsey et al., 2018). This response to surfactants has been linked to increase virulence of Kp in the lungs and a contributor towards biofilm formation (Willsey et al., 2018). Lastly, while there is a basal level of proteins in the alveolar space, including both surfactants and albumin, there are only trace levels of free amino acids in the lung space that could be utilized by bacteria for growth (Silver et al., 2019). Together, this creates a harsh environment for bacteria to establish a replicative niche. However, it is one that changes during infection and through inflammation to be more suitable for the bacteria (Baker & Baines, 2018).

1.1.4.3. Conditions experienced by Kp during a UTI

Similar to the lung environment, the urinary tract is a harsh nutrient starved environment that Kp must overcome to establish an infection. In contrast to the lung environment, the bladder and urinary tract has several obstacles for Kp to overcome in

addition to limited resources. These include a high osmolarity, variable pH, low levels of iron, and a low-nutrient environment where the free short chain amino acids are the major source of energy (Alteri & Mobley, 2012). Despite these limitations, Kp is one of leading causes of UTIs, making up about 4-6% of community acquired UTIs (Linhares et al., 2013) and up to 17% of hospital acquired UTIs (Polse et al., 2020). Establishing an infection in this environment requires the bacteria to be metabolically flexible, in particular by shifting to the appropriate respiratory chain acceptors (Alteri & Mobley, 2012). Additionally, Kp must contend with several host defense factors present in the urinary tract. These consists of urea, organic acids, salts, and high osmolarity. These stressors work in conjunction with humoral responses such as lactoferrin, Tamm-Horsfall protein (THP) (antimicrobial peptide produced in the distal loop of Henle), and various oligosaccharides with antimicrobial effects to restrict bacterial growth (Sobel, 1997). Furthermore, inflammation of the urinary tract leads to an influx of neutrophils which, when paired with the metabolic activity of the bacteria, leads to an acidic shift in pH and the disruption of normal glomerular functions that modulate the water and salt content of the urine (Alteri & Mobley, 2012). Cumulatively, these factors make it difficult for bacteria to infect the urinary tract. Despite this, Kp can overcome these obstacles. Kp is a urease-positive bacterium able to break down urea and utilize it as a nitrogen source (Collins & D'Orazio, 1993). Its siderophores overcome iron sequestration by lactoferrin, while the capsule protects Kp from several of the antimicrobial peptides in the urinary tract, including THP (Tarkkanen et al., 1992). Several risk factors lead to an increased incidence of UTIs caused by Kp. Of note is diabetes (likely due to an increase in the glucose content of the urine (Cristea et al., 2017), presence of an in-dwelling catheter in

the hospital setting, and an immuno compromised state increases risk of UTIs caused by Kp (Miftode et al., 2021). In particular, the presence of an in-dwelling catheter creates an abiotic surface that Kp, and other bacteria, can attach to and form a biofilm (Clegg & Murphy, 2016). This leads to persistent infections that can be very difficult to treat, often requiring several courses of treatments to fully eradicate.

In summary, both lung and bladder environments present several barriers that normally inhibit the colonization of these spaces by bacteria. Host defenses limit nutrient availability and accumulate antimicrobial peptides that deter the growth of pathogens. Through metabolic flexibility to utilize limited resources, capsule production protecting the cell from antimicrobial peptides, and inducing inflammation to increase resource availability, Kp can establish replicative niches in these harsh environments leading to severe infections (Paczosa & Mecsas, 2016). This has placed a spotlight on the need to understand how Kp can grow in various tissues, including both its abilities to use different energy sources and bypass the host defenses that normally prevent bacterial growth.

1.2. History of antibiotic use and observed resistance.

Since the discovery of penicillin by Alexander Fleming in 1928 there have been numerous classes of antibiotics discovered (Mohr, 2016). The period between 1940 and 1960 was considered the “golden age” of antibiotic discovery, with many of the antibiotics being used to this day being developed during this time (Mohr, 2016). Yet some of the earliest documentations of resistance was in 1940, 12 years after the discovery of penicillin, with identification of bacterial strains producing enzymes capable

of breaking down the drug (Davies & Davies, 2010). As newer antibiotics entered the market and use of antibiotics rose dramatically, so have rates of resistance. In particular, the time between implementation of a new drug and observed resistance has dramatically decreased with resistance to newer drugs arising in less than a year after discovery in some cases (Graham et al., 2017). This has created several challenges for researchers and has contributed to the lack of new antibiotics being developed.

The rise of antimicrobial resistance is not unique to Kp, but the increased incidence of MDR Kp infections has been alarming (Navon-Venezia et al., 2017). Recently, the awareness of Kp as a serious cause of infections has increased. This is mainly due to rising rates of drug resistance which render otherwise treatable infections as severe and life threatening. This coupled with a dearth of new therapeutic options has alarmed clinicians worldwide (Lewis, 2020). One study in the United Sates found that the rates of drug resistance in Kp have steadily increased from 2000 to 2007 with the highest increased resistance to the beta-lactam aztreonam, rising from 7.7 to 22.2% (Sanchez et al., 2013). These trends have led to the recognition of Kp by the Center for Disease Control (CDC) as both an urgent and serious threat (CDC 2019) due to the high rates and rapid spread of drug resistance. Additionally, the World Health Organization (WHO) has classified Kp amongst a group of pathogens capable of being pan-resistant. Collectively, these pathogens are referred to as "ESKAPE" pathogens comprised of *E. faecium, S. aureus, K. pneumoniae, A. baumannii, P. aeruginosa*, and Enterobacter (Pendleton et al., 2013) and are considered a global public health threat.

1.2.1. Evolution and spread of antimicrobial resistance.

Kp, like many other bacterial species acquire resistance to antibiotics through several mechanisms. Some examples of acquired resistance are through genetic mutations, genetic transfer of material, and selective pressure by antibiotics (Pendleton et al., 2013). These strategies result in modification of antimicrobial targets, presence and/or upregulation of efflux pump, or modification enzymes that break down antibiotics (Calfee, 2017).

1.2.2. Acquired resistance through genetic mutation.

Genetic mutation of an antimicrobial target is perhaps the most studied and reproducible mechanism of acquiring resistance in the laboratory setting. While resistance to virtually any drug can be selected for through experimental technique, they may not always be the most relevant mechanisms of resistance observed clinically. Nonetheless, mutational resistance is observed for some drug classes, namely rifampicin, fusidic acid, streptomycin, fluoroquinolones, and oxazolidinones (Woodford & Ellington, 2007). For Kp, this is most relevant for fluoroquinolones as the use of antibiotics such as ciprofloxacin have risen in recent years (Woodford & Ellington, 2007). The target of these fluoroquinolones is DNA topoisomerase II and IV which are required for DNA replication (Woodford & Ellington, 2007). Resistance to this class of antibiotics is most often caused through an accumulation of mutations in *gyrA*, *gyrB*, *parC*, and *parE* (Woodford & Ellington, 2007). Often these occur in a stepwise fashion with additional mutations leading to increased resistance. In a study conducted in tertiary hospitals in

India, about 20% of Kp clinical isolates were resistant to ciprofloxacin, with genetic mutation accounting for 54% of these isolates (Aditi Priyadarshini et al., 2019).

1.2.3. Modification of off-target cellular factors

In addition to genetic modification of antimicrobial targets, modification of other factors has been shown to contribute to antibiotic resistance. This includes genetic regulation of efflux pumps and porins on the cell membrane that normally play a role in virulence or nutrient acquisition (Langevin et al., 2020; Paczosa & Mecsas, 2016). Either the upregulation of these efflux pumps or modifications which allow them to bind and transport antibiotics has been observed (Blanco et al., 2016). One of the most characterized is the ABC transporter ArcAB-TolC efflux system (Langevin et al., 2020; Paczosa & Mecsas, 2016). As part of a two-component system it contributes both to virulence, by exporting several host factors encountered during infection, as well as resistance to several beta-lactams, quinolinone, and tetracyclines (Brown et al., 2022; Hasdemir et al., 2004). Expression of ArcAB is increased during infection as well as exposure to antibiotic stress (Brown et al., 2022). In addition to ArcAB, the porins OmpK35 and OmpK36 have been implicated in resistance to β-lactam antibiotics including carbapenems (Pacsoza, 2016, Joshi, 2021). OmpK35/36 have also been shown to contribute towards virulence in Kp mouse models, with deletion of OmpK36 decreasing levels of lung colonization (Chen, 2010). At the cost of virulence, down regulation of these porins leads to an increase in resistance (Joshi et al., 2021; Paczosa & Mecsas, 2016). The presence of efflux pumps is a significant contribution to the forms of resistance observed in clinical isolates of Kp. A study in Turkey, a hotspot for MDR Kp,

found that 39% of isolates had high levels of drug efflux activity contributing to the levels of drug resistance observed (Hasdemir et al., 2004).

1.2.4. Antibiotic resistance genes on mobile genetic elements

A significant portion of resistance mechanism are carried on transferrable plasmids (Calfee, 2017). Since Kp is a commensal in the gut microbiome in about 4% of healthy people, it is believed that transfer of the antibiotic resistance plasmids between strains of Kp or between Kp and other species of bacteria in the GI tract may contribute to the rise in antibiotic resistance (Gomez et al., 2021; McInnes et al., 2020). Antimicrobial resistance plasmids can carry a wide variety of genes that contribute towards resistance. This includes efflux pumps specific to certain classes of antibiotics (quinolinone efflux pump, QepA (Yamane et al., 2007)), antibiotic modification enzymes (aminoglycoside N-acetyltransferases, AAC (Ramirez & Tolmasky, 2010)), and perhaps the most well-known are enzymes that degrade antibiotics (ß-lactamase enzymes such as New Dehli metallo-ß-lactamase, NDM-1 (Tooke et al., 2019)).

1.2.5. Efflux pumps on mobile genetic elements.

Of the efflux pumps that reside on transmissible plasmids some of the more relevant for Kp are fluoroquinolone efflux pumps (Aathithan & French, 2011). The spread of these efflux pumps has significantly contributed to the high levels of resistance to fluoroquinolones such as ciprofloxacin worldwide (Li et al., 2019). A study in London found that over 90% of Kp isolates had ciprofloxacin efflux activity, and further showed that efflux was sufficient to contribute to resistance even in isolates with no other

resistance mechanisms to ciprofloxacin (Aathithan & French, 2011). A specific plasmid-encoded pump that has wide-spread implications is OqxAB (Li et al., 2019). OqxAB is a resistance nodulation division (RND) efflux pump, first identified within a plasmid isolated in 2004 from a strain of *E. coli* in a pig farm (Li et al., 2019). This pump has since been implicated in the efflux of several additional antibiotic classes such as nitrofurantoin, tigecycline, and chloramphenicol, although for Kp, its effects on quinolone resistance has been the most profound (Bharatham et al., 2021). Evidence suggests that *oqxAB* has undergone several instances of horizontal gene transfer and is now found among strains of Kp, *Salmonella* and *E. coli* (Li et al., 2019). As of 2019 the prevalence of *oqxAB* in Kp ranges from as low as 10% in Seoul to 100% in areas of Ohio (Li et al., 2019). Newer efforts to better understand this efflux pump and identify possible compound inhibitors are ongoing to combat this form of resistance (Bharatham et al., 2021).

1.2.6. Antibiotic modifying enzymes.

After an antibiotic enters a bacterial cell, several other mechanisms can lead to resistance. Enzymes that neutralize antibiotics through modifications, referred broadly as antibiotic modification enzymes, can chemically modify essential functional groups of an antibiotic to render them ineffective (Wright, 1999). A relevant and well-studied category of these enzymes are the aminoglycoside modifying enzymes (Wright, 1999). These represent a diverse set of enzymes that typically reside on mobile plasmids and catalyze the modification of -OH and NH2 on core functional groups or sugar moieties. They can be grouped into three categories that vary by the kind of modification they catalyze:

acetyltransferase (AAC), nucleotidyltransferase (ANTs), or phosphotransferase (APH) (Ramirez & Tolmasky, 2010). Of these, the most widespread in Kp are AACs, specifically AAC(3) (Ramirez & Tolmasky, 2010). AACs are part of a super family of proteins containing over 10,000 proteins. They catalyze the acetylation of -NH2 groups using coenzyme A as a donor molecule (Ramirez & Tolmasky, 2010). Different classes of AACs confer resistance to different aminoglycosides. However, the most common amongst Enterobacteriaceae is AAC(3)-I/II, which confer resistance to gentamicin, tobramycin, and dibekacin (Ramirez & Tolmasky, 2010). The prevalence of these AACs continues to rise and spread world-wide. A study in Egypt found that 58% of Kp clinical isolates were positive for aac(3)-II (El-Badawy et al., 2017). Due to the diversity and variability in AACs and other aminoglycoside modifying enzymes, it has been difficult to develop inhibitors of these enzymes. Newer aminoglycosides, such as amikacin, have been developed with hopes of being resistant to the effects of AACs, but modifications to existing AACs have already led to emerging resistance (Xiao & Hu, 2012).

1.2.7. B-lactamases and their dissemination.

Although all mechanisms of resistance that reside on mobile genetic elements have been of great concern, ß-lactamases are some of the most worrisome and well-characterized. ß-lactams have been a staple of antibiotic therapy since the discovery of penicillin in 1928 (Mohr, 2016). ß-lactams inhibit bacterial growth by preventing the transpeptidation of peptidoglycan, a critical step for cell wall synthesis (Bush & Bradford, 2016). Often, ß-lactams have broad coverage of both Gram-positive and Gram-negative bacteria. A common feature across all ß-lactams is the beta-lactam ring at the

core of the structure (Bush & Bradford, 2016). Currently there are three main categories of ß-lactams: penicillin and its derivatives, cephalosporins, and carbapenems (Bush & Bradford, 2016). Key differences between these drugs classes are their ability to enter different bacterial species, binding preferences to penicillin binding proteins (DD transpeptidases), and perhaps most importantly, their resistance to hydrolyzation by ß-lactamase enzymes (Bush & Bradford, 2016).

ß-lactamases are enzymes, often encoded by mobile genetic elements, that can hydrolyze the amide bound in the 4-member beta-lactam ring at the core of every ß-lactam (Tooke et al., 2019). Hydrolyzation of this ring disables the ability of the antibiotic to function allowing the bacteria to grow in the presence of high concentration of these drugs. The first ß-lactamase capable of degrading penicillin was identified in E. coli in the 1940s (Tooke et al., 2019). Since then, chemists and bacteria have been in an arms-race between the development of new ß-lactams and evolution of new ß-lactamases that can degrade novel drugs.

1.2.7.1. Classification of β-lactamases

ß-lactamases can be categorized into four main groups; three serine ß-lactamases, A, C and D (SBL A/C/D) groups, and the class B group, metallo(zinc)-ß-lactamases (MBLs) (Tooke et al., 2019). While SBLs utilize the active-site serine, similar to serine proteases, as a nucleophile for hydrolyzation, MBLs utilize a water activated metal to drive this reaction (Tooke et al., 2019). Class A enzymes are the most widely distributed SBLs and include TEM, SHV (sulfhydryl variant), CTX-M (cefotaximase), and notably K. pneumoniae carbapenemase (KPC). Variants of TEM, SHV, and CTX-M have been

recently identified with activity to a broad array of ß-lactams and are now considered extended spectrum beta-lactamases (ESBLs) (Tooke et al., 2019). Unlike class A ß-lactamases, class C ß-lactamases are mainly found on the chromosome of *Enterobacterecea* and are denoted as *ampC*. These typically do not have carbapenemase activity and often confer resistance of penicillins and some cephalosporins (Took, 2019). The class B ß-lactamases, or MBLs, are part of a super family of metallohydrolases found predominantly in prokaryotes. Some notable members of this category that have spread amongst Kp isolates are the carbapenemases NDM-1 and VIM (Verona Imipenemase) (Tooke et al., 2019). The spread NDM-1 in particular has been supported by multiple genetic elements to epidemic levels and is now a major contributor to carbapenem resistance seen today in many Gram-negative pathogens. In fact, resistance to the carbapenem, imipenem, was less than 1% in 2000 and rose to over 8% by 2007 for Kp isolates (Sanchez et al., 2013). More recently, a study in Portugal found carbapenem resistance in 25-34% of Kp isolates (Oliveira et al., 2022). The last class of ß-lactamases are the class D or OXA enzymes. These are the least understood but most diverse class of ß-lactamases. Originally, they were identified on a plasmid in 1960 and had the capacity to degrade penicillin (Tooke et al., 2019). Now, this protein family has expanded and includes ESBLs and carbapenemases. OXA-48 is of particular concern due to its spread amongst Kp isolates and is often the cause of carbapenem treatment failure (Tooke et al., 2019).

1.2.7.2. Development of β-lactamase inhibitors

The primary strategy to combat this rapid spread of ß-lactamases has been the development of ß-lactamase inhibitors. Traditionally, these compounds mimic the structure of ß-lactams and irreversibly inhibit ß-lactamases. Two of the first members of this class of compounds are clavulanate acid and sulbactam with tazobactam later being added to this list (Bush & Bradford, 2019). While these compounds proved highly effective at re-sensitizing pathogens to certain ß-lactams, their activity is mainly limited to class A ß-lactamases. More recent developments have given rise to Avibactam, which is capable of inhibiting class A, C, and a subset of class D enzymes. Importantly this includes some KPC enzymes (Tooke et al., 2019). Ceftazidime-avibactam has shown some potential; demonstrating efficacy against 99.6% of KPC positive Kp isolates during a two-year study in Greece (Galani et al., 2016). Overall, studies investigating the potential for ceftazidime-avibactam have been very positive with reduced mortality and morbidity in patients with KPC positive Kp bloodstream infections (Giamarellou & Karaiskos, 2022). Unsurprisingly, resistance to this novel drug has already been detected in some PDR clinical isolates. Novel variants of ß-lactamases with specific point mutations are unaffected by avibactam and have caused treatment failures (Galani et al., 2020).

Some other classes of ß-lactamase inhibitors have been developed in hopes of offering new therapeutic options specifically for class B MBL positive infections. This includes both meropenem-vaborbactam and imipenem-cilastatin-relebactam (Bush & Bradford, 2016; Patel et al., 2018). Unfortunately, while these new generation beta-lactamase inhibitors have strong activity for class A and C beta-lactamases, they have no

activity to the class B MBLs such as NDM-1 (Maraki et al., 2021). Neither meropenem-vaborbactam nor imipenem-cilastatin-relebactam have been extensively tested clinically, particularly against PDR infections. Both have shown strong *in vitro* results, sensitizing over 90% of KPC positive Kp isolates. However, in phase III clinical trials comparing meropenem-vaborbactam to best available therapy there was a significant increase in cure rates while 28-day mortality and microbiological cure (lack of growth from bacterial samples) were not significantly different (Wunderink et al., 2018). Meanwhile, imipenem-cilastatin-relebactam is still in being tested for clinical safety, although results seem promising so far, with favorable outcomes in 71% of cases (Motsch et al., 2020). While neither of these therapies have been thoroughly tested against PDR Kp and despite their lack of activity for MBL positive Kp, they remain the only recommended option for patients with MBL positive Kp infections according to the Infectious Disease Society of America (IDSA) (Tamma PD, 2022).

1.3. Multi-drug and pan-drug resistant *Klebsiella* infections.

Many of the mechanisms of antimicrobial resistance described above have spread globally within strains of Kp. As of 2022, alongside *A. baumannii* and *P. aeruginosa*, Kp is ranked in the highest priority for new treatment strategies (Giamarellou & Karaiskos, 2022). Traditionally multi-drug resistant (MDR) infections were those that were resistant to at least one agent across three separate classes. The extensive spread of antimicrobial resistance has led to further classification of these infections by the level of resistance found. Infections that are resistant to all but two or fewer antibiotic classes are considered extensively drug resistant (XDR). While infections that are resistant to all antibiotics in

all classes are labeled as pan-drug resistant (PDR) (Giamarellou & Karaiskos, 2022). An even newer definition is for those that are difficult to treat resistance (DTR). These pathogens are limited in treatment options and resistant to all first line therapies. Both PDR and DTR infections are linked with incredibly high mortality rates, between 20-71% (Giamarellou & Karaiskos, 2022).

A contributor to this high mortality rate is the lack of therapeutic options. When faced with these infections some of the few options available are trial of novel antibiotics such as new beta-lactamase inhibitors, an optimized regimen of a current drug, or synergistic combinations (often based on *in vitro* or mouse studies) (Giamarellou & Karaiskos, 2022). Unfortunately, new classes of antibiotics that function in Gram-negatives have not been developed since the advent of the synthetic fluroquinolones in 1960s (Butler & Buss, 2006; Mohr, 2016). Instead, optimized dosing of current antibiotics, such as carbapenems, is implemented even in cases of KPC positive isolates. The goal of this strategy is the optimization and increased dosing schedule of the carbapenem to achieve drug levels above the minimum inhibitory concentration (MIC) of the drug (Calfee, 2017). This requires achieving free drugs levels above the MIC for at least 40% of the dosing interval and has proven successful in several cases caused by Kp isolates with levels of carbapenem resistance below 16μg/ml (Bulik et al., 2010). Conversely, when specifically looking at KPC-positive isolates, treatment failure occurred in 40% of cases even when the meropenem MIC was 8μg/ml (Bulik et al., 2010). One of the challenges for this therapeutic strategy is the rapid hydrolysis that occurs with meropenem, leading to difficulties reaching high enough levels of the drug for long enough periods of time. Additionally, these treatments require frequent high-rate

infusions of these potent antibiotics. This places a high risk of adverse effects on the patient due to either side effects related to the drug itself or vascular stress of continuous high-rate infusions (Calfee, 2017).

1.3.1. Double carbapenem therapy

Alternatively, double carbapenem therapy has shown some benefits for treating KPC positive Kp infections. Typical combinations involve ertapenem, which has a high affinity for most carbapenemase enzymes, with either meropenem or doripenem, both having low affinity for carbapenemase enzymes (Calfee, 2017). The rationale behind this treatment is that ertapenem consumes or titrates most of the carbapenemase activity while allowing the other drug to impose its antimicrobial effects (Calfee, 2017). This has been demonstrated using a mouse model to be the effective against both KPC and NDM-1 producing strains of Kp with the best outcomes in moderately resistant strains with carbapenem MICs ranging from 4-16μg/ml (Wiskirchen et al., 2013). Limited case series using this strategy has shown some promise in humans to treat bacteremia and UTIs (Calfee, 2017).

1.4. Combination therapy for the treatment of *Klebsiella pneumoniae*

Another tool that clinicians have at their disposal when faced with infections caused by carbapenem-resistant Kp infections is the repurposing of current antibiotics as combination therapies. Here the strategy involves combining antibiotics in hopes of taking advantage of potential interactions between two or more drugs to overcome the resistances (Agyeman et al., 2020). While the IDSA does not recommend the use of

multiple antibiotics for the empiric treatment of drug susceptible or MDR infections by Kp, it can be considered for XDR or PDR cases of Kp infections (Tamma PD, 2022). Currently, most retrospective studies that have compared monotherapy to combination therapy for treating carbapenem-resistant Kp have found a reduction in mortality for the combination therapy groups (Calfee, 2017). One meta-analysis comparing monotherapies to combinations therapies found that across 29 studies including 3019 antibiotic-treated patients infected with carbapenem-resistant Kp there was a reduced mortality in patients given combination therapy (odds ratio of 1.45 for mortality when comparing monotherapy to combination therapy) (Agyeman et al., 2020). This analysis focused on studies between 2007-2018 in seven different countries (USA, Greece, Italy, Brazil, China, Spain, and Israel). This same meta-analysis also found that there was no difference between combinations involving either two or more than two antibiotics. Moreover, no significant differences were observed between combinations that included specific agents such as a carbapenem, polymyxin, or tigecycline. While this large meta-analysis did find reductions in mortality with combination therapy, there was no significant difference in rates of culture negative infections (Agyeman et al., 2020). The authors note that more well-designed randomized control studies are needed to better compare the differences between these treatment strategies. It should also be emphasized that studies that include meropenem-vaborbactam or imipenem-relebactam have not been performed and may prove beneficial (Agyeman et al., 2020).

1.4.1. Recommendations for antibiotic combinations.

Currently, there are no clear recommendations or guidelines for combinations of specific antibiotics that can be used to treat MDR Kp infections (Tamma PD, 2022). In fact, studies that looked at cases of carbapenem-resistant Kp infections found no significant differences in clinical outcomes between specific combinations (Agyeman et al., 2020; Scudeller et al., 2021). However, analyses that focused on cases with the highest mortality, often involving bloodstream infections, found that combinations involving a carbapenem with a polymyxin seemed to perform best (Tumbarello et al., 2015). In fact, when looking at all patients, combination therapy of any kind reduced mortality by 8% ($p<0.05$), but when narrowing to patients in the ICU or those with septic shock this difference increases to 23% ($p<0.001$) and 37% ($p<.001$) respectively (Tumbarello et al., 2015). This study concluded that several clinical factors should be accounted for when considering combination therapy, but for critically ill patients there was a significant reduction in mortality rates with combination therapy compared to monotherapy.

The most well studied antibiotics used in combination for the treatment of carbapenem-resistant Kp have been carbapenems, colistin, and tigecycline. These last-resort drugs are only considered for the severely ill patients when other therapies have failed (Jacobs et al., 2017). Combinations that involve a carbapenem and either colistin or tigecycline, dependent on drug susceptibility profiles, have proven the most effectful (Calfee, 2017). However, *in vitro* studies have highlighted other potentially beneficial combinations as well. Notably, colistin + rifampin, carbapenems + aminoglycosides, and lastly ceftazidime-avibactam + aztreonam (Scudeller et al., 2021). Studies found that this

combination had some key advantages over their respective monotherapies including higher bactericidal effects and lower re-growth rates (Scudeller et al., 2021).

1.4.2. Limitations of drug combination therapy.

Combination therapy has shown some distinct benefits for treating cases of carbapenem-resistant Kp infections, in particular for critically ill patients (Agyeman et al., 2020; Tumbarello et al., 2015). There are however some limitations to combination therapy. For one, while several meta-analyses have identified the benefits of combination therapy, some randomized control trials have not identified significant advantages to combination therapy, with some reporting increased levels of adverse effects leading to worse clinical outcomes for patients (Agyeman et al., 2020). This is not necessarily surprising given that the common drugs used in combination therapy, colistin and tigecycline, have severe side effects including nephrotoxicity (Elgazzar et al., 2022; Spapen et al., 2011). This is compounded by the fact that combination therapy is often turned to in critically ill and unstable patients when other treatments have failed making these adverse effects less tolerable for the patients. In addition, there is little clinical guidance on drugs or doses to use for combination therapy in the literature stemming from a lack of well controlled randomized trials. This is likely due to the challenges and nature of the illness being studied. It is difficult to justify and recruit for a traditional trial in patients who are critically ill and often implementing combination therapy as a last resort.

Another limitation to combination therapy is observed when they involve the use of carbapenems such as meropenem. Combinations involving meropenem are most effective when there is only moderate levels of resistance to carbapenems (Calfee, 2017). For Kp, the best responses occurs in isolates with meropenem MICs between <8-16µg/ml (Daikos et al., 2014). For isolates with much higher levels of carbapenem resistance, combination therapy involving a carbapenem does not have added benefits compared to monotherapies (Calfee, 2017). This may be due to either highly expressed carbapenemase or multiple carbapenemase enzymes that degrade the drug and reduce potential synergistic effects it may have within the combination. Ultimately, combination therapy is an important, yet understudied, tool for clinicians when combating MDR infections.

As the rates of DTR and PDR infections continue to rise leading to increased incidence and prevalence of bloodstream infections caused by these pathogens there may be a need for the use of combination therapy in conjunction with novel compounds. A more complete understanding of which drug combinations are most appropriate for different specific Kp isolates and infections is needed to fully incorporate combination therapy as standard practice.

1.5. Testing drug combinations

While there has recently been an increased interest in the potential for combination therapy, the idea of using multiple antibiotics to treat an infection was first documented in 1950 (Acar, 2000). It was observed that the rate of relapse for enterococcal endocarditis was reduced when the aminoglycoside streptomycin was added to the standard course of penicillin G (Jawetz & Gunnison, 1952). Since then,

understanding how antibiotics interact in combination has been an interest to microbiologists. These studies have led to the identification of several promising combinations, some of which have become standard of care. This includes the combination of a cell wall inhibitor, such as penicillin, with an aminoglycoside. In several bacterial species, including Kp, the uptake of aminoglycosides is increased in the presence of these cell wall inhibitors (Moellering & Weinberg, 1971). Of more clinical relevance, the combination of trimethoprim and sulfamethoxazole was approved by the FDA in 1973. This is one of the only combinations of antibiotics that demonstrated clear synergy *in vitro* that is used clinically to this date (Estrada et al., 2016). Since then, there has been an interest in identifying novel compound combinations that prove to be synergistic and capable of inhibiting bacterial growth.

1.5.1. Classifying antibiotic interactions

When considering antibiotic combinations, it is important to understand the kind of interactions the two drugs are having when affecting the same bacterial cell. The two primary kinds of interactions are synergistic or antagonistic interactions (Doern, 2014). Synergy is when the combined effects of two or more drugs is greater than the sum of the individual effects of the drugs. On the other hand, antagonism is when the effect of the combination is less than the sum of the effects of the individual drugs (Doern, 2014). Synergism has conventionally been the goal of combination studies as it has been thought to offer benefits for treating bacterial infections. However, thus far very few studies have shown that testing for synergy from patient samples correlates with improved patient outcomes (Doern, 2014). Some limitations to these studies are the inconsistent use of

various methods for testing synergy as well the difficulties of recapitulating the complexity of these infections in the laboratory setting (Doern, 2014). For Kp specifically, traditional media used for antibiotic testing involves a rich media, with Mueller-Hinton (MH) (EUCAST, 2022) or cation adjusted Mueller-Hinton broth (CAMHB) (Matuschek et al., 2022)While rich media allows for robust bacterial growth, it may not be representative of how drug combinations interact in specific tissues.

1.5.2. Models to quantify antibiotic interactions.

To better understand the potential of combination therapy for treating complex Kp infections accurate and reliable *in vitro* testing of drug combinations is critical. Several laboratory techniques have been developed to test antibiotic combinations for their effectiveness as a therapeutic regiment. These include the checkerboard method, kill curve comparison, disk diffusion, and paper strip diffusion (Acar, 2000). Outputs from these various techniques can be used to model antibiotic interactions and classify if they behave in either synergistic or antagonistic manners. While there are many models that can be used to quantify these interactions, the two most used and relevant are the Loewe additivity model and Bliss independence model (Yadav et al., 2015). Both are commonly used to quantify how drugs interact with each other. However, there are several key differences between them which may make one model more favorable than the other. Most importantly, while both models have similar definitions for synergism and antagonism they significantly differ in the null-hypothesis and what the expected outcome is if the there is no interaction between the drugs (Yadav et al., 2015).

1.5.2.1. Loewe additivity model

The Loewe additivity model defines the expected effect of a drug combination as if a drug was added to itself. This assumes that a 1X dose of drug A has the same effect as ½ X + ½ X of drug A. It then compares this expected effect to the measured effect of drugs ½ A + ½ B. The net effect of these comparisons is compiled to generate a fractional inhibitory concentration (FIC) that can be used to categorize combinations as synergistic, antagonistic, or additive (Yadav et al., 2015). A limitation to the Loewe model is that the concentration of each drug experienced by the bacteria that correlates with specific levels of inhibition must be known (Yadav et al., 2015). This can be difficult to accurately measure reliably in some experimental designs. However, this model allows for the identification and comparison of drug interactions at multiple levels of growth inhibition.

1.5.2.2. Bliss model of independence.

On the other hand, the Bliss model of independence assumes that two drugs have independent effects and uses probabilities to calculate expected effects of a combination (Yadav et al., 2015). The Bliss model uses the measured effect of drug A and drug B and assumes that drug A will exert its effect on the bacterial population and then drug B will have its independent effect on the remaining surviving population (Demidenko, 2019). This difference between the expected and observed effects of the combination is used to calculate a Bliss score which categorizes drugs combinations as synergistic, antagonistic, or independent (Demidenko & Miller, 2019). A limitation of Bliss is that the model assumes that both drugs interact with an individual cell at separate times. Additionally, the Bliss model does not account for differing magnitudes in effects between different

drugs (Yadav et al., 2015). One advantage of the Bliss model is the ability to use a small number of doses to predict the behavior of a drug combination. This allows for testing models with fewer measurements where the drug concentration may not be known (Demidenko & Miller, 2019).

1.5.3. Checkerboard method for measuring drug interactions.

The most frequently used method for measuring drug interactions is the checkerboard analysis where two drugs are added in increasing concentrations and levels of bacterial growth are used as the output (Acar, 2000). It is important to note that this often does not differentiate between bacteriostatic, inhibition of growth, and bacteriolytic, lysing of bacteria, activities (Acar, 2000) unless follow up outgrowth assays are used. Some more rapid and qualitive techniques are the disk diffusion and paper strip diffusion methods. While not as quantitative as the checkerboard, these tests are faster and may offer the ability to test a higher number of combinations in a shorter amount of time (Acar, 2000). Even though checkerboard analysis has been the gold standard for accurately testing antibiotic combination, it does not have great potential for scaling experiments to test a high number of antibiotics across multiple condition. This problem only grows when considering higher order combination above two-drug combinations (Doern, 2014).

1.5.4. Diagonal measurement of n-way drug interactions

To overcome these challenges and increase the scale and potential for synergy testing, a geometric optimization of the checkerboard assay was developed by Dr. Bree

Aldridge at Tufts University (Cokol, 2017, Larkins-Ford, 2021). This method is referred to as Diagonal Measurement of n-way drug interactions (DiaMOND). By utilizing a subset of the checkerboard comprising of equipotent doses it is possible to model drug interactions for a higher number of drugs across many more experimental designs. Read outs from DiaMOND can be used to quantify drug interactions through either the Loewe or Bliss models. Lastly, a key advantage of DiaMOND is the ability to model higher order drug combinations such as three or more drugs in a single combination. This was taken advantage to measure drug interactions across a panel of nine antibiotics used for the treatment of M. tuberculosis in both pairwise and three-way drug combinations (Cokol et al., 2017). Subsequent studies utilized DiaMOND to investigate the effects of various growth conditions on drug interactions in M. tuberculosis and formulate predictions on in vivo outcomes (Doern, 2014).

1.6. Aims of work

In this dissertation we aimed to utilize DiaMOND to explore the combinatorial space of Kp. We hypothesized that past efforts to correlate *in vitro* synergy testing with in vivo outcomes have not accounted for the physiological state of the bacteria during infection of various tissues. By measuring drug interactions in physiologically relevant media conditions, we aimed to identify synergistic drug combinations in tissue mimetic medias that would not be present in standard rich media, such as CAMHB. For this, we focus on the two most common forms of Kp infections, pneumonia and UTIs. We then optimized a mouse model for lung infection with Kp to incorporate antibiotic combination therapy. This would allow us to identify potential correlations between in vivo data and *in vitro* measurements taken in different media conditions.

Chapter 2: Critical role of growth medium for detecting drug interaction in Gram-negative bacteria that model *in vivo* responses[1]

[1]Davis K., Morales Y., McCabe A., Mecsas J., and Aldridge Bree., Submitted to *PLOS Pathogens* 09/25/2022

2.1. Introduction

The rise in antimicrobial resistant (AMR) infections is a global health crisis that threatens the ability to treat many bacterial, viral, and fungal infections (Antimicrobial Resistance, 2022). The rate of multi-drug resistant (MDR) bacterial infections has been steadily increasing for the past 20 years and was boosted by the recent SARS-CoV2 pandemic, which saw a significant increase in MDR related secondary bacterial infections leading to increased rates of morbidity and mortality (Khurana et al., 2021). Among MDR infections, some of the most harmful and difficult to treat are those caused by Gram-negative bacteria within the category of ESKAPE pathogens (*Enterococcus faecium*, *Staphylococcus aureus*, *Klebsiella pneumoniae* (Kp), *Acinetobacter baumannii* (Ab), *Pseudomonas aeruginosa* (Pa), and *Enterobacter* species). This group of bacteria is recognized by the World Health Organization (WHO) as capable of pan-resistance (De Oliveira et al., 2020). Clinicians and scientists have responded by investing in antibiotic stewardship and novel therapies to combat these infections (Hernando-Amado et al., 2019).

Treatment of infections caused by MDR pathogens often involves the use of a combination of antibiotics to limit the emergence of antibiotic resistance (Sullivan et al., 2020). Though current meta-analyses and clinical trials sometimes support the use of combination therapy for Gram-negative MDR infections, these studies are often inconclusive (Bassetti et al., 2018). Limitations to our understanding of drug combination therapies for the treatment of MDR infections inhibits our ability to effectively predict *in vivo* efficacy using *in vitro* assays (Pranita D. Tamma*, 2022). Therefore, therapy is reliant on clinical reasoning by individual physicians on a case-by-case basis. Another

barrier for combination therapy testing is the resources required to test combinations of antimicrobial in a traditional plate-based checkerboard assay due to the exponential cost of testing multiple drugs in high-order combinations (Sun et al., 2013). Understanding the potential for combination therapy is further complicated by the fact that these Gram-negative bacteria can cause infections at multiple sites (De Oliveira et al., 2020). Thus, standard rich media conditions (as defined by the European Committee on Antimicrobial Susceptibility Testing and the International Organization for Standardization) used for *in vitro* assays may not effectively predict how a combination will interact in various distinct *in vivo* environments where bacterial metabolism can differ (Davis et al., 2021). Here, we hypothesize that environmental effects on bacterial physiology influence drug interactions and that measurements taken using tissue mimetic media will be better able to predict *in vivo* outcomes.

To test this hypothesis, we undertook a systematic study of pairwise antibiotic interactions in different growth environments focused on three Gram-negative ESKAPE pathogens, Ab, Kp, and Pa, which together are among the major worldwide causes of nosocomial infections (De Oliveira et al., 2020). We measured synergistic, additive, and antagonistic antibiotic interactions in standard rich medium and compared these to measurements made in media designed to simulate lung or urine environments, to model two common sites of infection for these three pathogens. Generating this large dataset of antibiotic interaction measurements allowed us to interrogate the combinatorial space for these species through several lenses. We first asked whether antibiotic combinations behave similarly across all species and media conditions. After finding only one instance where the outcome of an antibiotic combination was similar for all three species grown in

all three media, we next teased out both media-specific and species-specific contributions to this observation. Comparisons between different species grown within the same media conditions generally showed poor correlations. However, we did observe reasonable correlations for Pa between the three different media conditions, and a strong correlation between Ab responses in CAMHB and the lung-like condition. By contrast, Kp had very poor correlations across all three conditions. We then assessed the capacity to translate *in vitro* measurements made using medium predicted to simulate the lung nutritional environment or standard rich medium to results found in mouse lung infections. For Kp, *in vitro* measurements in a lung mimetic medium were significantly more predictive of *in vivo* results. This work demonstrates that antibiotic interactions are highly variable when comparing across three gram-negative ESKAPE pathogens and highlights the importance of growth medium by showing a superior correlation between *in vivo* interactions and *in vitro* interactions in a tissue mimetic growth medium.

2.2. Results

2.2.1. Systematic survey of condition-specific drug interaction in three Gram-negative pathogens

To determine the dependence of drug interactions on growth conditions and bacterial species, we generated a dataset of pairwise drug interaction measurements from a panel of drugs that were tested against Ab, Pa, and Kp (Figure 2.1A). We chose well-characterized strains of each species – Ab strain ATCC 17978, Pa strain PaO1, and Kp strain ATCC 43816. Each of these strains was grown in three different growth conditions (Fig. 2.1A) and tested against clinically relevant drugs that cover a range of classes and

mechanisms of action (Table 2.1) (Tamma et al., 2021). The drugs trimethoprim-sulfamethoxazole (BAC) and cefixime were tested only with Kp because of their clinical relevance specific to Kp (11). We systematically measured drug interactions among strains and media conditions by leveraging the efficiency of a methodology called diagonal measurements of n-way drug interactions (DiaMOND), which implements a geometric optimization of the standard checkerboard assay (Cokol, Kuru et al. 2017, Larkins-Ford, Greenstein et al. 2021.

Table 2.1: Antibiotics used in this study.

Antibiotic	Abbreviation	Class	Mechanism of Action
trimethoprim-sulfamethoxazole	BAC	antifolate antibacterial (trimethoprim); sulfonamide (sulfamethoxazole)	folate synthesis inhibition
cefepime	CEF	cephalosporin	cell wall synthesis inhibition
cefixime	CFX	cephalosporin	cell wall synthesis inhibition
colistin	COL	Polymyxin	cell membrane disruption
ceftriaxone	CTX	cephalosporin	cell wall synthesis inhibition
gentamicin	GEN	aminoglycoside	protein synthesis inhibition
levofloxacin	LEV	fluoroquinolone	inhibition of DNA replication and transcription
meropenem	MER	Carbapenem	cell wall synthesis inhibition
rifampicin	RIF	antimycobacterial	RNA synthesis inhibition
tigecycline	TIG	glycylcycline	protein synthesis inhibition

Class, mechanism of action and 3-letter abbreviation of all antibiotics used in this study.

Each of these species can cause infection at multiple sites in the body, which have different growth conditions that may influence bacterial metabolism (Poudel et al., 2019; Weber et al., 2020) and drug response (Foster, 2017; Mead et al., 2019; Nagy et al., 2020). However, to our knowledge the effect of growth conditions on drug interactions

across different species has not been tested systematically. To directly evaluate whether different growth conditions impact pairwise drug interactions, we employed three media conditions – Cation-Adjusted Mueller Hinton Broth (CAMHB), M9 + 0.5% Glucose + Fe(II)SO4, pH 7.0 (M9Glu), and Urine Mimetic Media (UMM), which has a pH of 6.4 with creatinine and urea as the predominate carbon sources (see Methods). We chose CAMHB because it is a standard for microbiological susceptibility testing, and it is a rich medium that is high in amino acids and vitamins (Schofield, 2012). M9 supplemented with 0.5% glucose and 0.6μM $Fe(II)SO_4$ is a minimal medium that lacks amino acids yet still produces consistent reproducible bacterial growth. Additionally, M9Glu reflects the low amino acid availability observed in bronchoalveolar lavage fluid from mice (Paczosa et al., 2020; Silver et al., 2019) making it a better mimic for bacterial infection in the lungs and other amino acid deficient environments. Finally, we used a Urine Mimetic Media based Brooks & Keevil (1997) to approximate the growth environment experienced by the bacteria during a urinary tract infection (Brooks & Keevil, 1997).

We generated a drug interaction dataset using DiaMOND (Cokol et al., 2017; Van et al., 2021) by measuring the three most information-rich dose response curves: the combination dose responses of increasing equipotent doses of two drugs, and the dose responses of each single drug. We use these dose response curves to calculate the fractional inhibitory concentration (FIC), a measure of drug interactions. The FIC is the ratio of the observed combination dose that results in a certain level of growth inhibition compared to the expected combination dose if the two drugs are additive (see Materials and Methods). Here, we report log transformed FIC scores; $\log_2 FIC_{50}$ scores close to zero indicate additivity, more negative scores indicate synergy (e.g., the drugs combined are

more effective than expected based on their efficacies alone), and more positive scores indicate antagonism between drug pairs. The efficiency of DiaMOND enabled us to create a dataset of >300 unique combinations of species, medium, and pairwise drug interactions.

2.2.2. Drug interactions are dependent on species and growth environment.

The drug interaction data for 28 drug pairs tested for three species, each grown in three media conditions, is shown in a heatmap with hierarchical clustering in Fig. 2.1B (log_2FIC_{50}). We observed that for each medium (color-coded above the clustergram), drug combinations varied in their log_2FIC_{50} scores among different species. Furthermore, within individual species, drug combinations often varied in their log_2FIC_{50} scores across the three media conditions (three columns within a black box), although the extent of this variation is different for different species. The three Pa growth conditions cluster together (Cluster I), indicating their similarity to each other and differences from Ab and Kp. On the other hand, Ab CAMHB and M9Glu cluster together with Kp M9glu (Cluster III), while Ab UMM is in an adjacent cluster (Cluster IV). Kp CAMHB and Kp UMM make up Cluster II. These clustering patterns suggest that drug interactions are influenced by differences between species while the impact of media is more pronounced in some species versus others.

Pearson correlation coefficients were derived to quantify changes in drug interactions between different species in the same growth conditions (Fig 2.1D) and between different growth conditions within each species (Fig 2.1E). The outcome of drug pair interactions between species within the same medium was extremely variable; all

nine Pearson coefficients were below 0.6 and eight of the nine were below 0.4 (Fig. 2.1D). Thus, species-specific attributes impact drug interactions under these conditions. Curiously, despite the overall low Pearson coefficients, the correlation between species was consistently highest in M9Glu and lowest in UMM (Fig. 2.1D). In contrast to differences in drug interactions between species within the same medium, drug interactions in Pa between all three media showed high and significant correlations, with all three correlations above 0.64 (Fig. 2.1E). This was also reflected visually by the clustergrams (Fig. 2.1B). Likewise, drug interactions in Ab between CAMHB and M9Glu showed a high and significant correlation (Fig. 2.1E). On the other hand, Kp had low correlations in medium-to-medium comparisons, with all three correlations below 0.4 (Fig. 2.1E). In summary, drug interactions varied widely across different species, while media conditions had larger effects on drug interactions in some species compared to others.

2.2.3. Drug interactions are overall biased towards antagonism, but synergy is more prevalent in some species in nutrient-depleted media.

Efforts to develop clinically impactful combination therapies are focused on identifying synergistic combinations. Though we did not find combinations that were synergistic across all species and conditions tested, one combination, ceftriaxone + gentamicin (#22), was synergistic in a single medium (UMM) across all three species. Additionally, two combinations, colistin + rifampicin (#13) in Ab and gentamicin + tigecycline (#3), were synergistic across all three growth conditions for Kp.

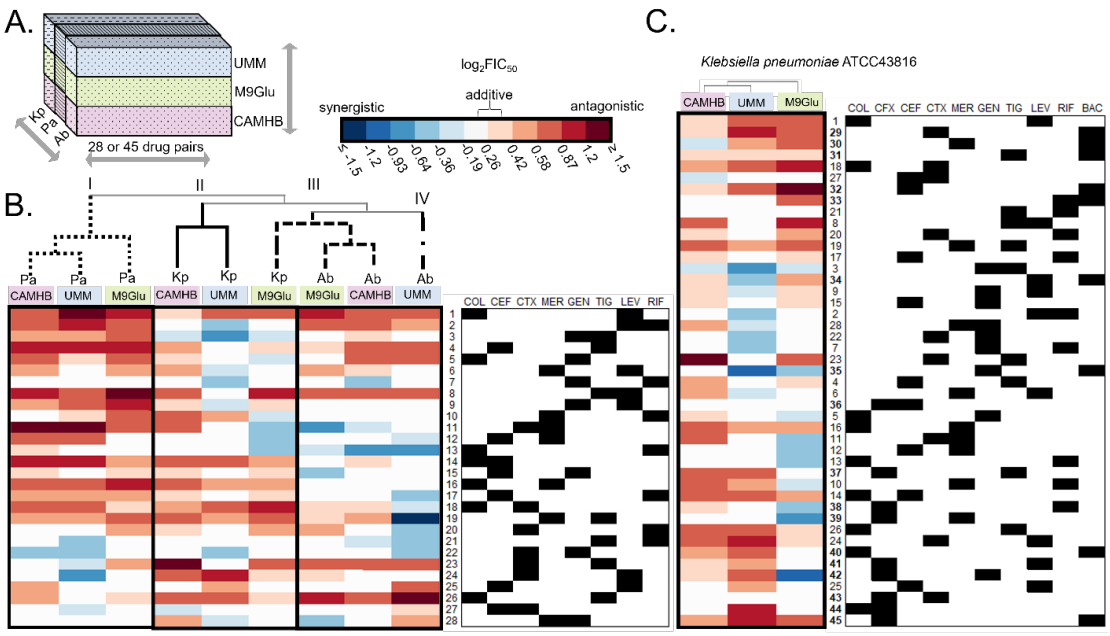

D.

Correlation by Species	CAMHB			M9Glu			UMM		
	Ab vs. Pa	Ab vs. Kp	Pa vs. Kp	Ab vs. Pa	Ab vs. Kp	Pa vs. Kp	Ab vs. Pa	Ab vs. Kp	Pa vs. Kp
Pearson r	0.36	0.24	0.26	0.38	0.54	0.38	0.095	0.11	0.18
p value	6.2E-02	2.2E-01	1.9E-01	4.5E-02	2.7E-03	4.6E-02	6.3E-01	5.8E-01	3.6E-01

E.

Correlation by Media	*Pseudomonas aeruginosa* (Pa)			*Acinetobacter baumanii* (Ab)			*Klebsiella pneumoniae* (Kp)		
	CAMHB vs. M9Glu	CAMHB vs. UMM	M9Glu vs. UMM	CAMHB vs. M9Glu	CAMHB vs. UMM	M9Glu vs. UMM	CAMHB vs. M9Glu	CAMHB vs. UMM	M9Glu vs. UMM
Pearson r	0.64	0.83	0.68	0.75	0.57	0.43	0.33	0.38	0.33
p value	2.1E-04	4.1E-08	6.7E-05	4.7E-06	1.5E-03	2.2E-02	2.7E-02	1.0E-02	2.6E-02

Figure 2.1: Variation in drug interaction across species and media. (A) Study design involved testing 28 pairs of antibiotics against *A. baumannii* ATCC17978 (Ab) and *P. aeruginosa* PaO1 (Pa), and 45 pairs against *K. pneumoniae* ATCC 43816 (Kp). Testing was done with all strains grown in three different growth conditions: cation-adjusted Mueller-Hinton Broth (CAMHB); M9 minimal medium + 0.5% glucose supplemented with 0.6µM iron (II) sulfate, and with 10mM sodium acetate for Ab and Pa; and urine mimetic medium (UMM) (Brooks & Keevil, 1997) supplemented with 0.01% glucose and 0.6µM iron (II) sulfate for Kp. (B) Clustergram of the $\log_2 FIC_{50}$ values of the 28 drug pairs tested across all three species and media, with each row representing a drug combination (indicated by black squares under the drug abbreviations in the table on the right) and each column representing a species tested in a particular medium. Each drug-pair number is maintained throughout the manuscript for ease of comparison. Hierarchical clustering was performed using average linkage between clusters and Pearson correlation distance metric between columns. Each value represents an average of at least three replicates (C) Clustergram of the $\log_2 FIC_{50}$ values of all 45 drug pairs tested against Kp in all three media (columns). Hierarchical clustering, notation of drug pairs, and representation of $\log_2 FIC_{50}$ is the same as for (B). (D) The Pearson correlation coefficient (r) and p value were determined for each species-to-species comparison of mean $\log_2 FIC_{50}$ values in the three media conditions. (E) The Pearson correlation coefficient (r) and p value was determined for each medium-to-medium comparison of mean $\log_2 FIC_{50}$ values in the three species.

However, combinations that were synergistic against one species in a particular growth condition were often not synergistic against other species in that growth condition nor in a different growth condition for the same species (e.g., meropenem plus tigecycline (#19) was synergistic for Ab in UMM, but antagonistic for Ab in the other growth conditions, and antagonistic for Pa and Kp in UMM). One combination was antagonistic across all species and media, colistin + levofloxacin (#1). The tendency towards antagonism was dependent on growth conditions, with combinations in UMM less likely to be antagonistic than those in CAMHB or M9Glu. Specifically, nine combinations were antagonistic across all three species in CAMHB (#'s 1, 4, 5, 6, 8, 14, 18,19, and 26), eight in M9Glu (#'s 1, 4, 8,18, 19, 20, 23, and 26), and one in UMM (#1) (Fig. 2.1B).

Despite the overall predominance of antagonism, the number of combinations that were additive or antagonistic in CAMHB but synergistic in one or both nutrient-depleted media differed for the three species (Fig. 2.2, gray regions of graphs). For Pa, four combinations that were additive in CAMHB were synergistic in UMM (Fig. 2.2B). For Ab, more combinations shifted from additive or antagonistic in CAMHB to synergistic in a nutrient-depleted media: two synergies were identified in M9Glu (Fig. 2.2C gray region) and six synergies were found in UMM (Fig. 2.2D gray region). For Kp, among the drug pairs tested in all three species, five combinations were synergistic in M9Glu but not in CAMHB (Fig. 2.2E gray region), and six combinations were synergistic in UMM but not in CAMHB (Fig. 2.2F gray region). Among the drug pairs tested only in Kp (the 8 core drugs against trimethoprim-sulfamethoxazole or cefixime), four were synergistic in M9Glu but not CAMHB, and two were synergistic in UMM but not CAMHB. Thus, for Ab and Kp tissue mimetic conditions revealed additional synergistic combinations

and may yield different predictions than measurements made in CAMHB. On the other hand, it may be sufficient to test drug pairs in rich media alone for Pa.

2.2.4. Specific antibiotics were associated with synergistic interactions in nutrient-depleted media.

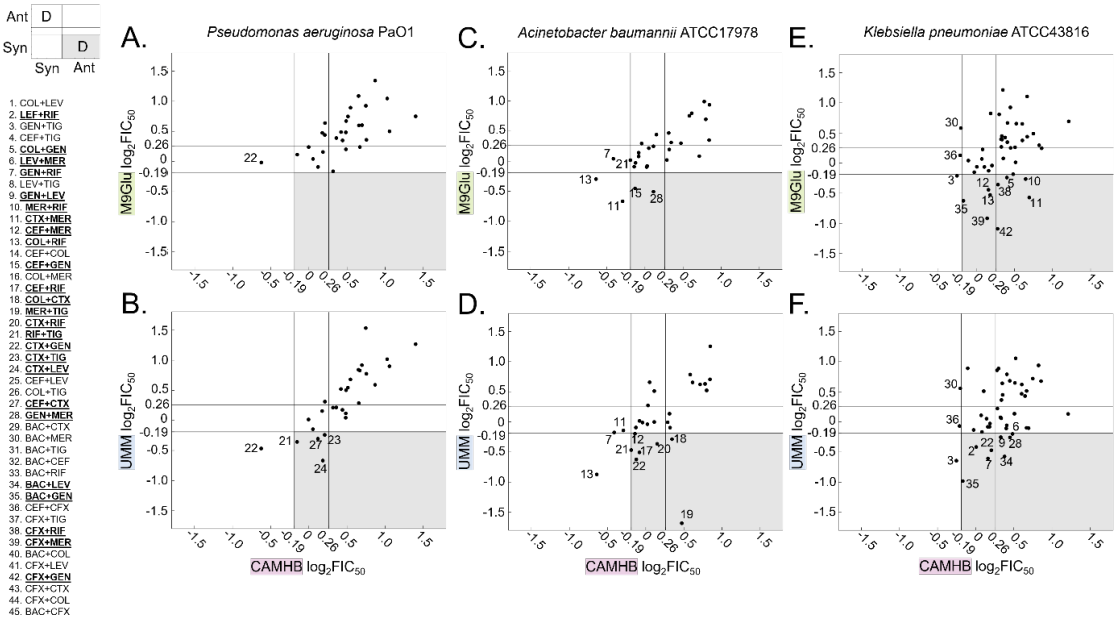

Figure 2.2: Nutrient-depleted media (M9Glu, UMM) reveal more synergistic combinations than standard rich media (CAMHB) for some species. (A-F) Scatterplots of log_2FIC_{50} values for all 28 drug pairs tested against (A, B) *Pa* PaO1, (C, D) *Ab* ATCC17978 and (E, F) 45 drug pairs tested against *Kp* ATCC43816. X-values represent log_2FIC_{50} in CAMHB, while y-values represent log_2FIC_{50} value in nutrient-depleted media, (A, C, E) M9Glu and (B, D, F) UMM. Lines parallel to the x-axis and y-axis indicate the boundaries of additivity (log_2FIC_{50} from -0.19 to 0.26, see Materials and Methods). Combinations that fall in the upper-left and lower-right sections of each graph indicate discordant interactions between results in CAMHB and results in the nutrient-depleted medium (marked with a D in the key on the left). Combinations that fall in the gray shaded regions are synergistic in nutrient-depleted media but additive or antagonistic in CAMHB; combinations for which this occurs in one or more species are bold-faced and underlined in the list of combinations on the left.

We next evaluated if specific antibiotics were more likely to be impacted by changes in media and if single drugs were responsible for higher rates of synergistic interactions dependent on growth medium. To investigate this, we first determined which combinations showed significant differences in log_2FIC_{50} scores in different media conditions with the same species. The results are shown in Fig. 2.3 with statistically significant differences between combinations indicated with a teardrop.

First, we considered the 28 drug pairs that we tested in all three species (Fig. 2.3B). For Ab (Fig. 2.3B middle ring), there were 4 instances of significant differences between interaction measurements, and in all 4 cases the type of interaction (synergy, additivity, antagonism) for a combination switched between two media (yellow teardrops). For Pa (Fig. 2.3B, inner ring), there were nine instances of significant differences between interaction measurements in two media, but in five of those cases the interaction type did not change between the two media (green teardrops).

Finally, for Kp (Fig. 2.3B, outer ring), there were nine instances of significant differences, and in all cases the interaction type switched (yellow teardrops). Among the additional combinations tested in Kp (Fig. 2.3C), we saw sixteen significant differences, and the interaction type changed for fourteen of those cases (yellow teardrops) and stayed antagonistic for two cases (green teardrops). Thus, significantly different interaction type switches between media were more frequent in Kp than Ab or Pa, mirroring the same trend observed with the Pearson correlation coefficients where there was the poorest correlation for Kp when comparing impact of antibiotics between different media types (Fig. 2.1E).

Next, we evaluated whether some drugs were over-represented among significantly different combinations that had instances of switching interaction type among media (e.g., additive to antagonistic or synergistic to antagonistic, Fig. 2.3, yellow teardrops). Because two drugs in the dataset (trimethoprim-sulfamethoxazole and cefixime) were tested only against Kp, we converted the actual number of interaction switches to a percentage of the total possible interaction switches between media types, for combinations containing that drug. The total number of possible interaction switches was 27 for trimethoprim-sulfamethoxazole and cefixime and 69 for the other eight drugs (see Materials and Methods). The results for all ten drugs are shown in Fig. 2.4A (yellow bars). Combinations involving trimethoprim-sulfamethoxazole, cefixime, meropenem, and gentamicin were more likely to show a significant difference in interaction type switch between media. We also calculated what subset of the instances of switching involved synergy - i.e., they were not a switch from additivity to antagonism (Fig. 2.4A, black bars). Of these, over 80 percent of the switches with gentamicin and meropenem involved a change to or from synergy (little differences between black bars and yellow bars, Fig. 2.4A).

We determined the subset of instances that involved switching from additivity or antagonism in CAMHB to synergy in a nutrient-depleted media for each antibiotic (Fig. 2.3B and 2.3C, yellow teardrops). To do so, the percentage of switches to synergy by dividing by the total number of potential switches between CAMHB and M9Glu and between CAMHB and UMM was calculated. Trimethoprim-sulfamethoxazole and cefixime had the highest percentage of significant switches to synergy in a nutrient-depleted media (Fig. 2.4B), with the caveat that they were only tested in Kp. Of the eight

drugs tested in all three species, meropenem and gentamicin had the highest percentage of significant switches to synergy in nutrient-depleted media (five switches for meropenem and five for gentamicin). Thus, when testing combinations involving meropenem, gentamicin, as well as trimethoprim-sulfamethoxazole and cefixime in Kp, nutrient-depleted media revealed synergies not observed in CAMHB.

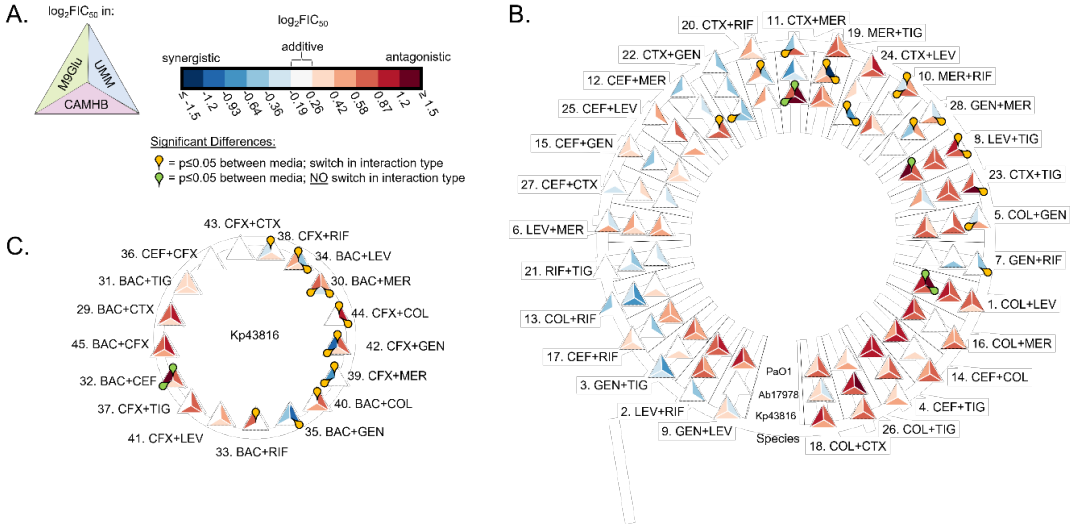

Figure 2.3: Different species show different degrees of variation across media conditions. (A) Triangle diagram represents how the log_2FIC_{50} data is depicted in (B) and (C) with UMM value on the top right, M9glu value on top left and CAMHB on the bottom. Log_2FIC_{50} values are reported as in Figure 2.1. (B, C) Yellow teardrops indicate significant differences ($p \leq 0.05$) between media where combinations change interaction type (ex. switch from synergy to antagonism between media); green teardrops indicate significance for combinations that do not change interaction type. Significance was based on a 2-way ANOVA using Tukey's multiple comparison post-test ($\alpha = 0.05$), using the log_2FIC_{50}. (B) The outer ring of triangles represent log_2FIC_{50} data of combinations tested in Kp, the middle ring represents combinations tested in Ab, and the inner ring represents the combinations tested in Pa. (C) The log_2FIC_{50} data for combinations only tested against Kp.

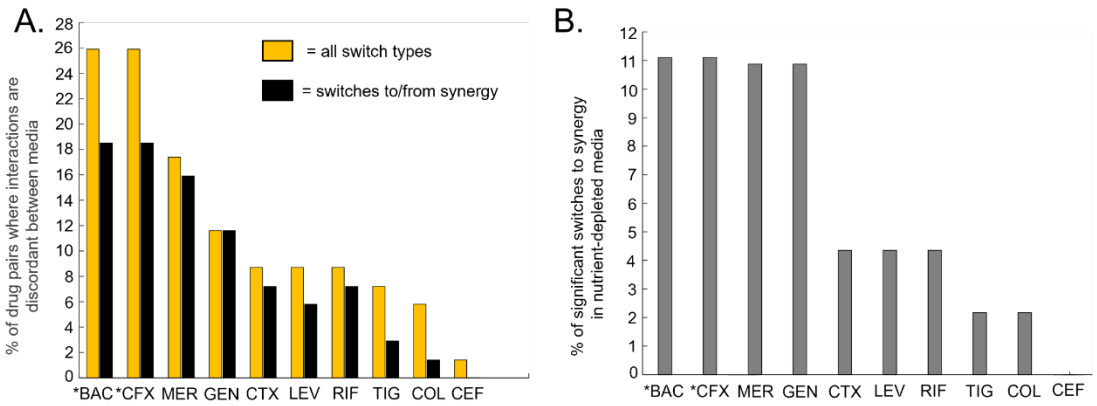

Figure 2.4: Some drugs were more frequently observed in combinations that show a significant difference in interaction between media. An asterisk indicates a drug that was only tested against Kp. (A) Yellow bars: the percentage of combinations involving each drug that showed a statistically significant $\log_2 FIC_{50}$ interaction type switch (ex. synergistic to antagonistic) in different media conditions (yellow bars). Black bars: the percentage of combinations involving each drug that showed a statistically significant $\log_2 FIC_{50}$ interaction type switch to or from synergy. (B) The percentage of combinations involving each drug that switched from additivity or antagonism in CAMHB to synergy in nutrient-depleted media (M9Glu or UMM).

Our *in vitro* data indicate that growth conditions influence the likelihood of observing synergy in combinations. The dependency on growth condition was stronger in Ab and Kp (Figs. 2.2, 2.3, 2.4A). Furthermore, certain antibiotics were more likely to impact medium-dependent synergies. This raises the question of whether *in vitro* data from specific media better reflect in vivo outcomes of drug combinations for specific infection types.

2.2.5. Drug interaction in M9 glucose medium correlated with *in vivo* outcomes for Ab and Kp.

For some species, *in vitro* media conditions had varied influence on drug interaction. For example, there was a strong correlation for Ab between M9Glu and CAMHB whereas there was a poor correlation for Kp between these two media (Figs

2.1B, C and E). Therefore, we postulated that certain media conditions may better reflect in vivo drug interactions or efficacy for Kp. To determine whether measurements of drug interactions in specific media are more predictive of in vivo outcomes, we investigated whether drug interactions in Ab or Kp grown in CAMHB or M9Glu better replicated in vivo observations of drug combinations in lung infections. We analyzed a set of studies in which drug combinations were tested against Ab or Kp lung infections in mice or rats (Tables 2.2-3, first column) and interpreted the in vivo results using the following criteria and strategies (Tables 2.2-3, second column). We only evaluated animal studies where data was shown for each antibiotic used alone and in combination, and where CFU was measured from lung tissue (Tables 2.2-3, column 1). If the combination reduced the bacterial burden substantially more than both the single antibiotics used in monotherapy, we interpreted the result as 'synergistic' (Tables 2.2-3, column 2). Alternatively, if CFUs were similar or worse, we called the combination 'not more effective' or 'less effective'. In some cases, one antibiotic was ineffective against Ab or Kp while a second antibiotic was effective. When the ineffective antibiotic further reduced the killing by the effective antibiotic, we considered this 'potentiating' and analogous to synergy for this comparison (Tables 2.2-3, column 2). In several cases, the antibiotic combinations used in the animal studies were not the same as ones used in our dataset (Tables 2.2-3, columns 1, 3). In these cases, we compared antibiotics within the same class as those in our *in vitro* analyses (Table 2.1). For example, Zhang et al, use a combination of polymyxin B + meropenem, which we compared to our *in vitro* results with colistin + meropenem (#16).

To evaluate whether *in vitro* data in CAMHB or M9Glu better predicts in vivo outcomes, we compared the outcome categories from the animal studies with our *in vitro*

measures (Tables 2.2-3, column 5 derived from data from Figs. 2.2-3). We found that for Kp, M9Glu correlated with all in vivo interpretations whereas *in vitro* data from CAMHB would have only predicted one of the combinations (Table 2.3). By contrast, in Ab, both CAMHB and M9Glu predicted in vivo outcomes at similar frequencies (Table 2.2). Collectively, these results are consistent with the poor Pearson co-efficient comparison for Kp and the high co-efficient for Ab between these media (Fig 2.1E).

To account for the possibility that drug interactions may vary depending on specific clinical isolates and their individual drug susceptibility patterns, three Ab clinical isolates with a range of resistance profiles (Ab5075, EGA355, and EGA368) were grown in CAMHB and M9Glu and tested against 8 antibiotics combinations (Fig. 2.5A, B). Ab5075 was highly resistant to gentamicin and meropenem, while EGA355 was highly resistant to levofloxacin resulting in unobtainable IC50 values for these drugs. Thus, for these drugs we tested for potentiation in the relevant strain by adding a constant amount of the resistant drug along with increasing amounts of the sensitive drug and measuring shifts in IC50 of the sensitive drug. This shift was reported as a $\log_2$ fold-change in IC50, with negative $\log_2 Fold_{50}$ scores indicating that addition of the resistant drug lowered the IC50 of the sensitive drug, despite the resistant drug showing no growth inhibition on its own (Fig 2.5A, B).

To evaluate the possibility that drug interactions may vary depending on specific clinical isolates and their individual drug susceptibility patterns, we expanded the number of Ab strains evaluated and compared their responses *in vitro* to our interpretation of the in vivo. Three Ab clinical isolates with a range of resistance profiles (Ab5075, EGA355, and EGA368) grown in CAMHB and M9Glu were tested against nine antibiotics

combinations (Fig. 2.5A). Ab5075 was highly resistant to gentamicin and meropenem, whereas EGA355 was highly resistant to levofloxacin resulting in unobtainable IC50 values for these drugs. Thus, for these drugs we tested for potentiation in the relevant strain by adding a constant amount of the resistant drug along with increasing amounts of the sensitive drug and measuring shifts in IC50 of the sensitive drug. This shift was reported as a $\log_2$ fold-change in IC50, with negative $\log_2 Fold_{50}$ scores indicating that addition of the resistant drug lowered the IC50 of the sensitive drug, despite the resistant drug showing no growth inhibition on its own (Fig 2.5A, blocks marked with asterisks). Drug combinations are listed in same order as Table 2.2 with the 4 'in vivo synergistic' combinations on top. Collectively for all 4 strains, more synergistically combinations were observed in the top 4 drug-pairs (10/15 for CAMHB and 10/14 for M9glu) than in the bottom 4 (4/16 for each medium).

To compare the drug responses of these isolates *in vitro* more quantitatively to our interpretation of the in vivo, we grouped combination pairs by whether they were predicted to be synergistic or not in vivo and compared the $\log_2 FIC_{50}$ scores between M9Glu and CAMHB from all strains (Fig 2.5B-C). There was a greater difference between the $\log_2 FIC_{50}$ scores of combinations that were annotated as synergistic (blue) or not (red) in vivo when the combinations were measured in M9Glu ($p = 0.001$) compared to CAMHB ($p=0.02$). This suggests that M9Glu may be more predictive than CAMHB for Ab strains, but that CAMHB was also predictive. These results are concurrent with the Pearson coefficient observed between M9Glu and CAMHB for Ab (Fig. 2.1E, R=0.75, p=4.7 x 10-7) as well as the clustering of drug interactions for Ab in M9Glu and CAMHB (Fig. 2.1B, subgroup III).

Table 2.2. Annotations from *in vivo* lung studies of antibiotic combinations used in Ab infections and comparisons to *in vitro* results

Source(s), combination, animal model[1]	Interpretation of *in vivo* interaction[2]	Combination (#) from our dataset[3]	Observed *in vitro* interaction for Ab17978 in	
			CAMHB	M9Glu
Fan et al. 2016 (colistin + meropenem, mouse) Zhang et al. 2021 (polymyxin B +meropenem, mouse)	synergistic or potentiating	COL+MER (#16)	additive	additive
Pantopoulou et al. 2007 (colistin + rifampicin, rat) Fan et al. 2016 (colistin + rifampicin, mouse) Song et al. 2009 (colistin + rifampicin, mouse) Zhang et al. 2021 (polymyxin B + rifampicin, mouse)	synergistic or potentiating	COL+RIF (#13)	synergistic	additive
Montero et al. 2004 (imipenem + tobramycin, mouse)	synergistic or potentiating	GEN+MER (#28)	antagonistic	synergistic
Sun et al. 2014 (meropenem + rifampicin, mouse) Montero et al. 2004 (imipenem + rifampicin, mouse) Song et al. 2009 (imipenem + rifampicin, mouse)	synergistic or potentiating	MER+RIF (#10)	additive	additive
Yilmaz et al. 2012 (colistin + tigecycline, rat) Fan et al. 2016 (colistin + tigecycline, mouse)	not more effective together	COL+TIG (#26)	antagonistic	antagonistic
Joly-Guillou et al. 2000 (amikacin + levofloxacin, mouse)	less effective in combination	GEN+LEV (#9)	additive	antagonistic
Montero et al. 2004 (rifampicin + tobramycin, mouse) Song et al. 2009 (rifampicin + amikacin, mouse)	less effective in combination	GEN+RIF (#7)	synergistic	additive
Joly-Guillou et al. 2000 (amikacin + levofloxacin, mouse)	less effective in combination	LEV+MER (#6)	antagonistic	antagonistic

1. Studies using combinations of antibiotics in a mouse lung infection model or thigh model and CFU in lung were evaluated (Fan et al., 2016; Joly-Guillou et al., 2000; Montero et al., 2004; Pantopoulou et al., 2007; Song et al., 2009; Sun et al., 2014; Yilmaz et al., 2013; Zhang et al., 2021).
2. Our interpretation of the interaction of the combination based on the data in these studies. Classified as either synergistic when the combination is more effective than either monotherapy, or if the combination did not significantly reduce lung bacterial burden it is listed as being not more effective than monotherapies. In most animal studies, individual antibiotic doses were combined to make the combination therapy resulting in higher total drug levels for the combination therapies compared to the monotherapies. Thus, increased killing could be considered additive or synergistic.
3. The combination in our data set (Fig. 2.2) that is being compared to for similar drug class as the ones used in the study

Table 2.3. Combinations that were synergistic or antagonistic in mouse *Klebsiella pneumoniae* lung infections

Source(s), combination, animal model[1]	Interpretation of *in vivo* interaction[2]	Combination (#) from our dataset[3]	Observed *in vitro* interaction for Kp43816 in	
			CAMHB	M9Glu
Hirsh et al. 2012 (amikacin + doripenem, mouse) Ota et al. 2020 (meropenem + amikacin, mouse)	synergistic	GEN+MER (#28)	antagonistic	synergistic
Huang et. Al 2021 (gentamicin + ceftazidime, mouse)	synergistic	CTX+GEN (#22)	additive	synergistic
Huang et. Al 2021 (gentamicin + cefepime, mouse)	synergistic	CEF+GEN\ (#42)	antagonistic	synergistic
Hirsh et al. 2012 (doripenem + levofloxacin, mouse)	not more effective than monotherapies	LEV+MER (#6)	antagonistic	additive
Hirsh et al. 2012 (amikacin + levofloxacin, mouse)	not more effective than monotherapies	GEN+LEV (#9)	antagonistic	antagonistic

1. Studies that used combinations of antibiotics in a mouse lung infection model (Hirsch et al., 2013; Huang et al., 2021; Ota et al., 2020)
2. Our interpretation of the interaction of the combination based on the data in these studies. Classified as either synergistic when the combination is more effective than either monotherapy or if the combination did not significantly reduce lung bacterial burden it is listed as being not more effective than monotherapies. In most animal studies, individual antibiotic doses were combined to make the combination therapy resulting in higher total drug levels for the combination therapies compared to the monotherapies. Increased killing could be considered additive or synergistic.
3. The combination in our data set (Fig. 2.2) that is being compared to for similar drug class as the ones used in the study.

In summary, for this collection of Ab strains, *in vitro* testing in M9Glu was slightly more predictive of in vivo outcomes. However, both M9Glu and CAMHB reflected in vivo outcomes even when the isolate being tested was highly resistant to one of the drugs in the combination. By contrast, retrospective analyses for Kp strongly suggest that a test medium of M9Glu more clearly differentiates between combinations that are synergistic or antagonistic in vivo against Kp lung infection, compared to CAMHB.

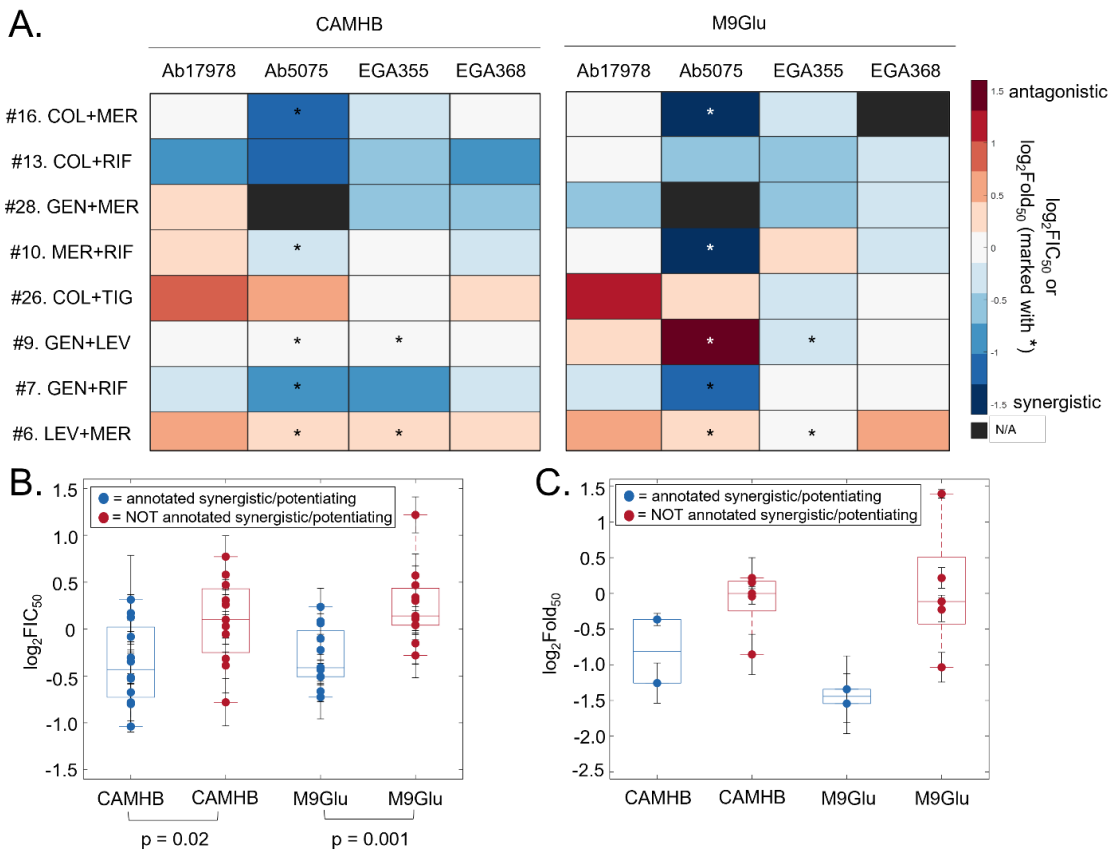

Figure 2.5: In Ab clinical isolates and lab strain (Ab17978), drug interactions in M9Glu correlate better than those in CAMHB with in vivo studies. (A) log_2FIC_{50} and log_2Fold_{50} values for combinations tested against Ab clinical isolates and lab strain (Ab17978) grown in CAMHB and M9Glu. The log_2Fold_{50} values are indicated with an asterisk. All values are averages of at least three biological replicates. (B-C) Box-and-whisker plots sorted by whether the combinations were annotated synergistic/potentiation (blue) or not (red) for the (B) log_2FIC_{50} values in CAMHB and in M9Glu or (C) the log_2Fold_{50}. The log_2FIC_{50} values and log_2Fold_{50} values are each shown as mean +/- S.E.M. For both comparisons in (B) a two-sample t-test was used with a significance level of $\alpha < 0.05$.

2.2.6. Drug combinations outcomes in a Kp mouse lung infection model were predicted by *in vitro* measurements in M9+glucose but not CAMHB

To further probe the ability of *in vitro* media conditions to predict the efficacy of a drug combination *in vivo,* we adapted a mouse model for Kp lung infection to incorporate antibiotic therapy (Paczosa et al., 2020; Silver et al., 2019). Though

traditional drug therapy is designed with the goal of eliminating bacterial burden, we used subtherapeutic doses of antibiotics with the goal of capturing potential synergies in the treatment of tissue infection by Kp. Specifically, we sought doses of single antibiotics (monotherapy) that reduced the lung bacterial burden significantly compared to a vehicle control, but where the bacterial burden remained at detectable levels. If combination treatments were more effective, we would expect fewer colony forming units (CFUs) recovered versus the single doses.

We tested the hypothesis that M9Glu is better able to predict *in vivo* outcomes by testing two combinations of antibiotics that were synergistic in M9Glu, cefixime + meropenem (#39) and cefixime + gentamicin (#42), but additive or antagonistic, respectively, in CAMHB. These combinations were chosen because they were statistically significant *in vitro* (Fig. 2.3). Initial testing was done to identify roughly equipotent doses that met the criteria for subtherapeutic doses. Doses of 10mg/kg of meropenem, 5mg/kg of cefixime, and 2 mg/kg of gentamicin given at 14 hours post-infection resulted in a lung bacterial burden between 10^5 and 10^6 CFUs 22 hours post-infection after intranasal inoculation of 10,000 CFU whereas untreated controls ranged between 10^7-10^8 CFUs. This bacterial burden in treated mice was significantly lower than the non-treated vehicle control while still being 2-3 logs higher than the limit of detection for this assay (Fig. 2.6).

To translate the additivity model used in DiaMOND and compare drug combination therapies to monotherapies *in vivo*, roughly equipotent doses of antibiotics were used for monotherapies and compared to combinations of two drugs each used at half the equipotent dose. For example, 5mg/kg of meropenem + 2.5 mg/kg cefixime was

compared to 10 mg/kg meropenem as well as 5 mg/kg cefixime. When either cefixime + meropenem (#39) or cefixime + gentamicin (#42) was used to treat Kp-infected mice, the combination therapy significantly reduced lung bacterial burden compared to their respective monotherapies (Fig. 2.6A, B). In addition, the inclusion of the individual components of the antibiotic combination doses on their own allowed for the quantification of drug interaction via a modified Bliss independence score (Liu et al., 2018) using $\log_{10}$ transformed values for CFU (see Materials and Methods). In brief, the Bliss independence model compares the observed effect of the combination to an expected inhibitory effect of the combination which assumes the two drugs act independently; positive scores indicate synergistic interactions while negative Bliss scores indicate antagonistic interactions. Using this log-transformed Bliss independence statistic, synergistic Bliss interactions scores of 0.11±0.02 for cefixime + meropenem (#39) and 0.24±0.07 for cefixime + gentamicin (#42) were calculated. Taken together, the significant reduction in lung bacterial burden by the combinations in addition to the positive Bliss scores indicate that these two combinations were acting synergistically in the mouse lung. Therefore, the drug interactions *in vivo* are more closely correlated with the *in vitro* measurements in M9Glu rather than the additive or antagonistic interactions measured in CAMHB.

To evaluate whether combination therapies broadly acted more effectively than monotherapies in this model regardless of drug interactions measured *in vitro*, cefepime + levofloxacin (#25) was used for *in vivo* testing – a combination that acted additively in both M9Glu and CAMHB. Doses of 10mg/kg for both drugs were chosen for monotherapy and 5 mg/kg of each for combination therapy. The combination of cefepime

+ levofloxacin (#25) was not significantly different from either monotherapy alone and had an antagonistic log-transformed Bliss interaction score of -0.22± 0.07 (Fig. 2.6C). Together, these experiments demonstrate that by using subtherapeutic antibiotic doses, the mouse model resolved differences in single versus combination drug therapy. Additionally, these data demonstrate that for both the combinations of cefixime + meropenem (#39) and cefixime + gentamicin (#42) M9Glu medium, an *in vitro* medium more nutritionally restricted similar to the lung environment, was better able to predict *in vivo* behavior when compared to a standard rich media.

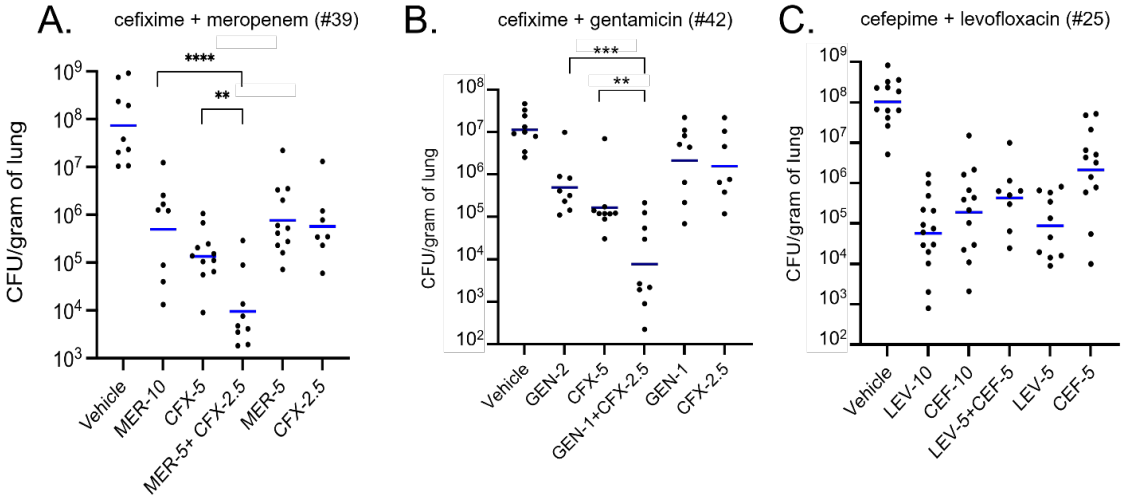

Figure 2.6. Drug combinations identified as synergistic in M9+Glucose, but not CAMHB, significantly reduce lung bacterial burden during mouse lung infection by *K. pneumoniae.* (A-C) Swiss Webster wild-type mice (black circles) were infected via intranasal route with 10,000 CFUs of Kp43816 and infection was allowed to proceed for 14 hours at which point mice were treated with either DMSO or indicated doses of drugs (in mg/kg) via intraperitoneal injection. Mice receiving meropenem were given a second dose at 18hr due to its short *in vivo* half-life (Louie et al., 2015). Lungs were harvested after 22 hours post infection and plated for bacterial burden (CFU/gram of lung). Blue lines indicate geometric means. Data for each drug combination group was compiled from n = 3 independent experiments with 3-4 mice in each group. Statistical analysis was done by two-way ANOVA with Bonferroni corrections.

2.3. Discussion

Our results demonstrate that drug interactions differ considerably across species. Within species, drug interactions also vary amongst growth conditions. Furthermore, among the panel of drug combinations tested, we observed little to no correlation between three Gram-negative species, in any of the media tested (Fig. 2.1D) and no drug combination was synergistic across all three species and growth conditions. This discordance in response to drug combinations across different species raises the important and unanswered question of what the best way to assess combination therapies is. Our observation that one cannot extrapolate from one bacterial species to another has also been observed by other investigators. Brochado and colleagues tested pairwise combinations from a broad array of antibiotics classes against *E. coli*, *S. Typhimurium* and Pa grown in Lysogeny Broth, and found that more than 70% of their tested drug interactions were species-specific (Brochado et al., 2018). This variation in response to antibiotic combinations amongst different species could be due to differences in antibiotic uptake (Chevereau & Bollenbach, 2015; Dillon et al., 2019), cell wall permeability (Berlanga et al., 2004), and/or cellular processes when grown in complex nutrient environments (Nichols et al., 2011). Consistent with the latter idea is our observation that differences in drug interactions between species were the least evident in the simplest medium, M9Glu (Fig. 2.1D). Collectively, our findings indicate that there may not be a "golden" combination that will be synergistic across a range of species and infection sites. Given the impact of species-specific physiology on drug interactions, a more tailored strategy focused on the pathogen and sites of infection may need to be considered.

Among our systematic drug interaction measurements, antagonism was overall more frequent than synergy (Fig. 2.1B, 2.1C), which is in agreement with studies of other species (Brochado et al., 2018; Chandrasekaran et al., 2016; Cokol et al., 2011; Larkins-Ford et al., 2021; Mason et al., 2017; Yeh et al., 2006) as well as with cancer therapies (Richards et al., 2020). However, ceftriaxone + gentamicin was synergistic across all three species in UMM (Fig. 2.1B). There are other *in vitro* and clinical evidence of synergy for combinations of beta-lactams and aminoglycosides in both Gram-positive and Gram-negative bacteria. For example, synergy was observed in the more rapid clearance of *Staphylococcus aureus* from cardiac vegetations in a rabbit endocarditis model by penicillin combined with gentamicin, compared to either drug alone (Sande & Johnson, 1975); a similar effect was also observed with *Streptococcus sanguis* in the rabbit endocarditis model (Sande & Irvin, 1974). Synergy was also observed with amoxicillin in combination with gentamicin when used to treat various strains of *Streptococcus pneumoniae* in a mouse pneumonia model that varied in their penicillin susceptibility (Darras-Joly et al., 1996). In these cases, the cephalosporin is believed to weaken the cell wall allowing better penetration of the aminoglycoside (Hancock et al., 1981; Miller et al., 1987; Moellering et al., 1971). Some *in vitro* studies with Pa have shown synergy with a beta-lactam and aminoglycoside (Giamarellou et al., 1984), but in the case of Pa synergy appears to depend on the strain as well as the specific identity of the beta-lactam with an aminoglycoside in combination (Drusano et al., 2009; Heineman & Lofton, 1978). Though we did not detect synergistic interactions in every case between gentamicin and the beta-lactams tested, their overall interactions skewed towards additivity/synergy (22 pairs) rather than antagonism (8 pairs). This is in stark contrast to

the overall skew towards antagonism in the data set (158/303 possible combinations). These observations further support the idea that these antibiotics may be particularly beneficial for the treatment of complex urinary tract infections.

Our dataset allowed us to take an in-depth look at how drug interactions vary across growth conditions and in different species. Though we focused on statistically significant interaction differences (Fig. 2.3, 2.4), we reported all media-to-media interaction differences (Fig. 2.1) for consideration. Drug interactions may be dependent on media for a variety of reasons, including differences in metabolic state (Meylan et al., 2017; Stokes et al., 2019), the activity of efflux pumps (Jain & Saini, 2016; Ma et al., 1996), and stress response pathways which can change depending on media condition (Brauner et al., 2016; Bryan & Kwan, 1983). For Kp and Ab, combinations that included gentamicin or meropenem were more likely to change to synergistic when moving from a rich medium (CAMHB) to non-rich media (M9Glu or UMM) (Fig. 2.4B). This highlights the importance of testing combinations involving these drugs in non-rich growth conditions which may better reflect *in vivo* outcomes for some types of Kp and Ab infections. However, this trend with gentamicin and meropenem was not observed in Pa. For Pa, the overall trend toward antagonism has been observed in at least one other study of a broad range of antibiotics (Brochado et al., 2018). The relatively low discordance in drug interaction across media for Pa may be explained by its metabolic adaptability, minimal nutritional requirements, and ability to grow in a variety of different environments (Meylan et al., 2017). These features combined with a wide array of innate resistance mechanisms (Livermore, 2002) suggest that *Pseudomonas* can face challenges from multiple antibiotics concurrently, along with environmental stressors. In contrast,

Kp undergoes shifts in metabolism upon growth in glucose or other changes in carbon sources (Lin et al., 2013; Lin et al., 2018), and exposure to subinhibitory amounts of meropenem also shifts the metabolism of Kp (Foschi et al., 2018). It would stand to reason that a reverse of this also occurs, that changes in Kp metabolism will exert an effect on drug interaction.

We used two approaches to evaluate which, if any, *in vitro* medium would best predict *in vivo* efficacy. For Ab and Kp, we compared our *in vitro* measurements of drug interactions to results from mouse and rat lung infection studies (Tables 2.2, 2.3, Fig. 2.5). For Ab, we additionally compared our results with ATCC 17978 to a panel of clinical isolates. In the case of Kp, results in M9Glu aligned with clinical findings whereas for Ab, both M9Glu and CAMHB were correlated with *in vivo* results. However, even for Ab, drug interactions in M9Glu tended to better recapitulate *in vivo* findings compared with interactions in CAMHB (Fig. 2.5B), even though M9glu is not an exact mimetic of lung conditions. For example, lungs contain detectable, albeit low and insufficient, levels of amino acids but there are no amino acids in M9Glu (Silver et al., 2019). To further explore the predictive power of *in vitro* measurements, we directly tested whether drug interactions in M9Glu or CAMHB better reflected results for a Kp mouse lung infection model. By using drugs at subtherapeutic levels, we had the resolution to detect enhanced clearance in lung bacterial burden when drugs were used in combination compared to as a monotherapy. This model permitted us to experimentally confirm that M9Glu better predicted drug combinations than CAMHB. Collectively, these analyses indicate that for Kp, M9Glu is better able to predict *in vivo* outcomes in the lungs when compared to CAMHB (or UMM). This further implies that Kp is using a

glycolytic program during its growth in the lungs and that these drug combinations are more effective under these conditions. Additionally, our results for cefixime + meropenem (#39) are in accord with previous clinical trial results, providing further evidence for the efficacy of double beta lactam therapy for multi-drug resistant Kp (Ji et al., 2015).

Traditional drug therapy in mice is often designed with the goal of eliminating the bacterial burden utilizing full doses of each drug together. Our dosing strategy, which uses combinations with half the dose of the monotherapy, was designed to measure *in vivo* drug interactions relative to additivity as a null model (Berenbaum, 1989; Greco et al., 1995). This allowed for a more direct comparison between a combination and its respective monotherapies. A potential strength of using subtherapeutic concentrations is the resolution to detect both decreases and increases in bacterial burden when giving a combination of drugs. Although we weighted our drug doses to detect further decreases in bacterial burden when using combinations, this model can be optimized to better capture antagonistic interactions by altering both the doses. Additionally, this dosing strategy using subtherapeutic concentrations can be adapted to test whether other infection site-specific mimetic media can achieve the same recapitulation observed here. For example, do results in UMM better recapitulate interactions in a Kp mouse model for cystitis compared to results in CAMHB? Future work will explore if this is the case. If so, then not only could tissue mimetic media be used to better predict *in vivo* outcomes in corresponding infection sites, but results of a panel of tissue mimetic media could be used to identify combinations that perform well across multiple sites in more complex infections.

Together, our findings have several implications. First, it should not be assumed that a drug combination will behave the same way in different growth conditions. However, for some species such as Pa, testing different media conditions may not be necessary, while for other species such as Kp infection sites may need to be carefully considered when choosing an appropriate combination therapy. For multi-site infections, choosing a combination that performs well across a range of growth conditions might be the best strategy. In addition, there is no consistent pattern of media-to-media variation between species; for Kp and Pa, responses in CAMHB and UMM were more similar, and for Ab, responses in CAMHB and M9Glu were more closely related (Fig. 2.1E). Thus, even for species like Ab and Kp for which changes in media affect drug combination response, there is variation between species in the magnitude of the effect that a specific media will have on drug responses. Our study suggests that informed use of combination therapies should take account of species and infection sites, and furthermore, that for some species growth conditions may have an outsized effect on combination interactions, as we have started to observe with this work. More studies are needed to further characterize the effect of species and growth conditions on drug interactions, to inform the design of better combination therapy.

2.4. Materials and Methods

2.4.1. Strains, antibiotics, and growth conditions

Strains used in this paper include Ab ATCC 17978 (a generous gift from the lab of Ralph Isberg at Tufts University), Pa PaO1 (a generous gift from the lab of Paul Blainey at the Broad Institute), and Kp ATCC 43816, as well as three Ab clinical isolates.

Ab5075 is a well-characterized, extensively drug resistant (XDR) isolate from a Walter Reed Army Medical Center patient between 2008 and 2009 (Jacobs et al 2014, Thompson et al 2014, Zurawski et al 2012). Susceptibility and resistance information for this strain was obtained from Wu et al. (2015) and Jacobs et al. (2014). EGA355 and EGA368 (obtained from Eddie Geisinger in the lab of Ralph Isberg at Tufts University) are two Ab strains that were isolated from patient sputum samples in 2013 and 2014, respectively, by the Tufts Medical Center Microbiology Laboratory. Species confirmation and MLST strain type (ST2) were determined by whole-genome sequencing.

Ten antibiotics were used in this study. Cefepime, colistin, ceftriaxone, gentamicin, levofloxacin, trimethoprim, sulfamethoxazole, cefixime, and meropenem were obtained from Sigma. Rifampicin and tigecycline were obtained from T.C.I. Chemicals. For *in vitro* studies trimethoprim and sulfamethoxazole were mixed at a 1:20 ratio. Cation-Adjusted Mueller Hinton II Broth (CAMHB) was purchased from Becton-Dickinson (BBL, Sparks, MD, USA) and prepared according to the manufacturer's instructions. M9 Minimal Salts 5x was purchased from Becton-Dickinson (Difco, Sparks, MD, USA), and M9 Minimal Medium (M9Glu) was prepared according to the manufacturer's instructions (including addition of 0.5% glucose). M9 was supplemented with 0.6μM Fe(II)SO4 for growing all strains, and with 10mM NaC2H3O2 for growing Ab and Pa strains. Urine mimetic media (UMM) was prepared according to the recipe of Brooks and Keevil (1997) and supplemented with 0.6μM Fe(II)SO4 and 0.01% glucose when used for growing Kp ATCC 43816.

2.4.2. Drug interaction measurements with DiaMOND assays

First dose centering experiments were performed to determine the IC90 values of each antibiotic for each strain in each medium. The same experimental protocol was used for both DiaMOND and dose centering experiments: a culture was grown overnight to saturation in the medium to be tested at 37°C with shaking, then 6µl of culture was used to inoculate 3ml fresh media, and this day culture was grown at 37°C with shaking until it reached mid-log (OD_{600}=0.2-0.5). This day culture was then diluted to OD_{600}=0.001, and 50µl culture was added to each of the non-edge wells of 384-well microplates, which had drugs dissolved in DMSO (ceftriaxone, levofloxacin, meropenem, rifampicin, tigecycline, trimethoprim, sulfamethoxazole and cefixime), or 0.1% Triton-X100 in water (cefepime, colistin, and gentamicin), pre-added to the plates using the HP D300E Digital Dispenser. Increasing amounts of single drugs and increasing total amounts of pairs of drugs were used to generate dose response curves for single drugs and pairs of drugs. For each plate, ≥ 4 wells were left untreated (no drug added), and 4-8 wells were treated positive controls, which received 3x MIC of one of the drugs tested. These controls were used for calculating the Z score, see Data Processing and Quality Control below. Then 50µl sterile media was added to each edge well of the 384-well plates. Plates were grown overnight (18-20 hours) with 37°C with shaking. The OD_{600} of each well was measured using a Biotek Synergy HT Microplate Reader. One biological replicate was performed for the dose centering for each species and growth condition, and ≥ 3 biological replicates were performed for each single drug and pairwise combination tested against each strain and medium (Fig. 2.7 and 2.8).

2.4.3. Data processing and quality control

All data analysis was performed in Matlab. The data for each biological replicate was analyzed separately, and $\log_2 FIC_{50}$ values and $\log_2 FIC_{90}$ for each biological replicate that passed quality control (see below) are reported in Figs.2.7 and 2.8, respectively. Each reported $\log_2 FIC_{50}$ value is the arithmetic mean of $\log_2 FIC_{50}$ values reported in Fig. 2.7. Processing the OD_{600} data by background-subtraction of the median of medium-only edge wells, normalization to the mean of untreated wells in each plate, fitting of the single and pairwise dose response curves with a three-parameter hill function, and calculation of inhibitory concentration (IC) values based on hill curve parameters was performed as described previously (Larkins-Ford et al., 2021). Determination of FIC_{50} scores using the IC_{50} value of the drug pair as well as the IC_{50} values of the component single drugs following the model of Loewe additivity was done as described previously (Larkins-Ford et al., 2021). The Ab clinical isolate Ab5075 was highly resistant to gentamicin and meropenem, and the Ab clinical isolate EGA355 was highly resistant to levofloxacin. So, for combinations including gentamicin or meropenem for Ab5075 (gentamicin + meropenem was not tested for Ab5075) and combinations including levofloxacin for EGA355, the drug to which the strain was highly resistant was treated as a sensitizer, and for the combination dose response curve a constant amount of the sensitizer drug was added to an increasing amount of the other drug in the pair. Instead of calculating the FIC50 score for the drug pair, the fold-change between the combination IC50 and the non-sensitizer drug IC50 was calculated as a measure of potentiation, and in data processing instead of normalizing to the mean of the untreated wells, the wells for the combination dose response curve were normalized to wells treated with only the

sensitizer drug. We consider potentiation analogous to synergy because both involve the combination of two drugs showing greater efficacy than the sum of the drugs' individual effects. Otherwise, we categorized the drug interaction as 'not more effective' if killing appeared similarly to the single doses or 'less effective' if more CFU were recovered in the combination dose compared to one or both single doses.

To ensure accuracy and consistency, all biological replicates included in the dataset had to pass the following series of quality control criteria. For single drug dose response curves, the R^2 of the fitted curve (from which we calculated IC values) had to be ≥ 0.9, and the 384-well plate on which the dose response curve was measured had to have a Z score of ≥ 0.4, to ensure sufficient difference between untreated and treated positive control wells requiring consistent growth in the untreated wells and growth inhibition in the positive control wells. The equation we used for Z score calculations is $Z = 1 - \frac{3 \times (\hat{\sigma}_p + \hat{\sigma}_n)}{|\hat{\mu}_p - \hat{\mu}_n|}$ In this equation, $\hat{\mu}_n$ and $\hat{\mu}_p$ are the average OD_{600} of the untreated and positive control wells, respectively, and $\hat{\sigma}_n$ and $\hat{\sigma}_p$ are the standard deviation of the untreated and positive control wells, respectively. We used the same requirements for combination dose response curves for which FIC50 was calculated, with the added criteria that these requirements also had to be met for the component single drugs' dose response curves, and the angle score for the combination (a measure of how close the single drugs doses were to achieving equipotency) had to be between 23° and 68° (no more than 22° degrees away from 45°, indicating equipotency and exact measurement along the diagonal).

2.4.4. Determination of additivity range, synergy and potentiation

To experimentally determine the window of additivity in our assays, the range of log2FIC50 scores obtained by measuring 3-5 drugs from the panel individually in the DiaMOND format with themselves (e.g., a mock combination experiment) against Ab17978, PaO1 and Kp43816 each grown in CAMHB and in M9Glu. For each species in each medium, at least two biological replicate measurements were performed for each drug tested with itself, and the resulting $\log_2 FIC_{50}$ scores were used to calculate a 95% confidence interval for additivity for each species in each media. All six of these 95% confidence interval ranges (three species in two media) were within the range of log2FIC50 = 0.26 and log2FIC50 = -0.19. Thus, log2FIC50 scores between -0.19 and 0.26 were considered additive, while scores less than that were considered synergistic and scores greater than that were considered antagonistic.

2.4.5. Statistical analysis

For each species, we identified the combinations with statistically significant differences in interaction type between growth conditions by performing a 2-way ANOVA with multiple comparisons using Tukey's multiple comparison post-test (α = 0.05), with the log2FIC50 scores from all combinations in CAMHB, M9Glu and UMM. Combinations were considered statistically significant if $p \leq 0.05$ in log2FIC50 between two growth conditions.

For each of the 10 drugs tested, we counted the total number of combinations involving that drug that switched interaction type (ex. synergy to antagonism) between two growth conditions, across all the growth conditions and species tested. For

comparisons between drugs (Fig. 2.4), we converted each total to a percentage of all the possible switches in interaction type between growth conditions, across all growth conditions and species. Since trimethoprim-sulfamethoxazole and cefixime were only tested in Kp, there are 27 possible switches for each of these two drugs: 1 species x 3 possible media-to-media comparisons x 9 combinations. For the other 8 drugs, there are 69 possible switches: 2 species (Ab, Pa) x 3 possible media-to-media comparisons x 7 combinations, plus 1 species (Kp) x 3 possible media-to-media comparisons x 9 combinations (since any of these other eight drugs was also tested with trimethoprim-sulfamethoxazole and cefixime in Kp).

2.4.6. Mouse Infections

For infections, 8-12 week old female or male Swiss Webster mice (Taconic) were anesthetized with isoflurane and infected via the intranasal route with 50ul containing 10,000 CFU of stationary phase Kp (ATCC43816) grown overnight in L broth and diluted in sterile PBS (Paczosa et al., 2020). Prior to infection, mice were weighed to ensure accurate doses of antibiotic(s). Infection was allowed to proceed for 14 hours. At which point, stated concentrations of antibiotics diluted in 100µl of DMSO were administered via intraperitoneal injection. For combination doses, antibiotics were mixed in 100 µl DMSO. A cohort of mice were given 100µl of DMSO at 14 hours post infection. (Antibiotic concentrations used were based on preliminary experiments (not shown) that identified antibiotic concentrations that reduced bacterial burden 50-500 fold compared to vehicle). Due to the short half-life of meropenem, a 2nd dose was given at 18 hours post infection. All other antibiotics have longer half-lives in mice (Louie et al., 2015). Mice were euthanized at 22 hours post infection. Lungs were collected, weighed,

and homogenized. Homogenates were diluted, plated on L agar plates, and grown at 37˚C overnight. CFUs were counted and used to calculate lung bacterial burden per gram of lung. A 2-way ANOVA with Bonferroni's multiple comparison corrections ($\alpha = 0.05$) was done on $\log_{10}$ transformed data to determine statistical significance using GraphPad Prism. All infections were done at least three times with groups of 2-4 mice/condition and data compiled. To calculate Bliss interaction scores, $\log_{10}$ CFU/gram of lung was used to calculate the relative inhibition for each treatment group. These values allowed for the implementation of the Bliss independence model to calculate the expected inhibition if there was no interaction between the two drugs being used (Liu et al., 2018). To calculate the expected inhibition Eq1 was used, where y_A and y_B is the observed fractional growth inhibition by drug A and drug B respectively at ½ the dose used for the combination therapy (for example 2.5mg/kg of cefixime and 5mg/kg of meropenem), y_B is the observed growth inhibition by drug B. Fractional growth inhibition was calculated by $\log_{10}$ transforming the geometric means of the CFU/g of lung for each group of mice and dividing the treated groups by the untreated group. The expected growth inhibition is subtracted from the observed growth inhibition to calculate the Bliss score for the combination.

Eq1: $Expected\ inhibition = y_A + y_B - (y_A)(y_B)$

Figure 2.7: Biological replicates of pairwise drug combination $\log_2 FIC_{50}$ measurements against (A) *Acinetobacter baumannii* ATCC17978, (B) *Pseudomonas aeruginosa* PaO1, and (C) *Klebsiella pneumoniae* ATCC43816, each grown in CAMHB (purple), M9Glu (green), and UMM (blue). Box plots depict the median (central circle), 25th and 75th percentiles (edges), and whiskers extend to the largest and smallest replicate values. Individual replicate values are marked with a black asterisk.

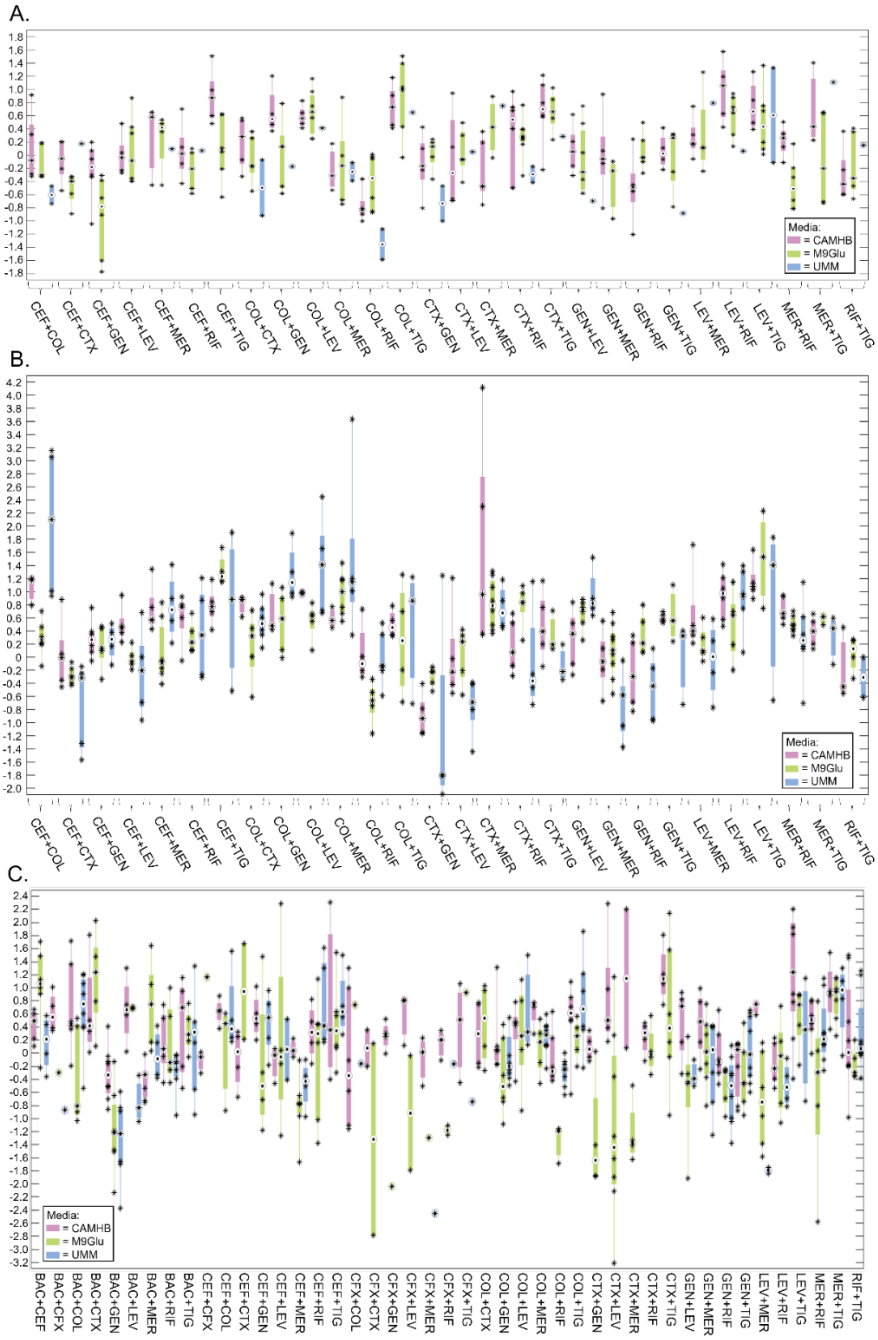

Figure 2.8: Biological replicates of drug combination $\log_2 FIC_{90}$ measurements against (A) *Acinetobacter baumannii* ATCC17978, (B) *Pseudomonas aeruginosa* PaO1, and (C) *Klebsiella pneumoniae* ATCC43816, each grown in CAMHB (purple), M9Glu (green), and UMM (blue). Box plots depict the median (central circle), 25th and 75th percentiles (edges), and whiskers extend to the largest and smallest replicate values. Individual replicate values are marked with a black asterisk.

2.5. Acknowledgements

We thank Nhi Van, Jonah Larkins-Ford, Yonatan Degefu, and Talia Greenstein for coding assistance and experimental advice. We thank Pathricia Leus and Rachel Ende for critical reading of manuscript. YM was supported by 4T32AI007422 award to Ralph Isberg from NIH (NIH NIAID); ALM was supported by NIGMS grant 1K12GM133314 awarded to Dr. Claire Moore. KPD, JM and BA were supported by NIH NIAID U19142780 awarded to Deborah T. Hung. JM was also supported by NIH NIAID AI169786.

2.6. Contributions

All work related to *Klebsiella* was performed by YM, including mouse work and *in vitro* assays. Work related to *Acinetobacter* and *Pseudomonas* was performed by KD.

Chapter 3: Deletion of thymidine kinase in Klebsiella pneumoniae enables an in vivo model of treatment with trimethoprim-sulfamethoxazole.[1]

[1]Morales, Y., Krasilnikov M,. Ende, R., Florence, I., Mecsas, J. To be submitted to *mBio*

3.1. Introduction

Klebsiella pneumoniae (Kp) is a leading cause of nosocomial infections and hospital outbreaks often complicated by high rates of drug resistance (Gupta, 2002). With the increasing prevalence of multi-drug resistant (MDR), and even pan-drug resistant, infections there is a rising need for novel therapies involving either new antibiotics or the repurposing of current antibiotics (Tumbarello et al., 2012). Fortuitously, up to one third of extended-spectrum-beta-lactamase (ESBL)-producing strains of Kp, resistant to most commonly used antibiotics, remain sensitive to treatment by the drug trimethoprim-sulfamethoxazole (TMP:SMX, also known as Bactrim) (Teklu et al., 2019). In fact, during an outbreak of a carbapenem and colistin-resistant strain of Kp, two antibiotics considered "drugs of last resort," 94% of isolates from patients were susceptible to TMP:SMX leading to its use to contain the spread of this highly drug-resistant Kp strain (Sili et al., 2015).

TMP:SMX is one of the recommended drugs for empirical first line therapy for many urinary tract infections (UTIs), including those caused by Kp (Gupta et al., 2011). This is due to low instances of side effects, high tissue penetration, low cost, and broad coverage of many causative pathogens (Masters et al., 2003). TMP:SMX is a combination of trimethoprim and sulfamethoxazole inhibiting dihydrofolate reductase and dihydropteroate synthase respectively, the two key enzymes in the folate synthesis pathway (Masters et al., 2003). Folate is an essential co-factor for many cellular processes including de novo synthesis of nucleotides. Unlike humans, bacteria cannot utilize folate from their environment making it an ideal pathway for drug targeting (Bourne, 2014). In fact, there are newer generation anti-folate antibiotics being tested,

such as icalaprim (Huang et al., 2019), that aim to take advantage of this pathway. Given the qualities of TMP:SMX, there is potential to exploit this drug to both help inform newer anti-folate drugs and be repurposed to help treat complex infections involving MDR-Kp.

Despite the effectiveness of TMP:SMX in humans (Brogden et al., 1982) and *in vitro*, there is currently no *in vivo* mouse model for treating Gram-negative infections with TMP:SMX or other anti-folate targeting drugs, including Kp. The lack of a mouse model for anti-folates has impeded exploration of ways to exploit TMP:SMX in addition to the development of novel folate inhibitors that function in Gram-negative bacteria. Mouse models provide several insights for antibiotic research including the kinetics of an infection and a novel compound, correlation between dose schedule and bacterial burden, and the availability of a drug at infection sites (Marra, 2012). While inhibition of this critical pathway may arise during large *in vitro* screening efforts of novel compounds it would be difficult to advance these potential drugs without evidence of *in vivo* efficacy with an animal model.

In murine infections of *E. coli*, trimethoprim is ineffective at clearing an *in vivo* infection despite susceptibility *in vitro* (Tokunaga et al., 1997). This ineffectiveness of TMP:SMX in rodent models to treat Gram-negative bacteria has been linked to high concentrations of thymidine present the plasma of mice unlike humans (Heinzmann et al., 2016; Tokunaga et al., 1997). Coincidentally, through salvage pathways that utilize exogenous nucleotides to bypass de novo synthesis, many bacteria can become resistant to TMP:SMX in the presence of thymidine (Heinzmann et al., 2016). The use of exogenous thymidine is mainly carried out by the enzyme thymidine kinase (Tdk) that

converts thymidine into thymidine-5'-phosphate which can supplement DNA synthesis (Saito et al., 1985). It has been previously demonstrated that a transposon insertion within the *tdk* gene of *E. coli* sensitizes the strain to trimethoprim in the presence of exogenous thymidine *in vitro* and during *in vivo* mouse infections (Tokunaga et al., 1997). Additionally, a deletion of *tdk* in a *Staphylococcus aureus* strain led to sensitization to an anti-folate, icaliprim, during mouse infection (Huang et al., 2019). Interestingly, in Kp, Tdk has an 11 fold higher level of activity compared to E. coli and several other Gram-negative bacteria (Saito et al., 1985). We hypothesized that the high levels of thymidine in mice combined with the ability for Kp to efficiently utilize exogenous thymidine creates a situation where TMP:SMX is unable to inhibit the growth of Kp in mouse models. We aimed to delete the *tdk* gene in a Kp strain in hopes of sensitizing it to TMP:SMX during a mouse infection. This would enable a model that may uncover potential combinations with TMP:SMX as well as novel vulnerabilities involving the folate synthesis pathway.

3.2. Results

3.2.1. TMP:SMX is unable to inhibit growth of TMP:SMX-sensitive *Klebsiella pneumoniae*

The clinical relevance of TMP:SMX for Kp infections and its distinct mechanism of action motivated testing TMP:SMX in combinations with additional antibiotics (Davis, Morales bioRvix). Initial testing demonstrated that for a hypervirulent and spectinomycin resistant strain of Kp derived from ATCC43816 (Wt_{specR}) (Pazcosa 2016), TMP:SMX had an inhibitory concentration of 90% (IC90) below 1μg/ml (Fig. 3.1A) when grown in

the rich medium, Cation Adjusted Mueller Hinton Broth (CAMHB). This falls below the EUCAST designation of sensitivity for Enterobacteriaceae of 4µg/ml, classifying this strain as sensitive to TMP:SMX.

To evaluate whether Wt_{specR} was sensitive to TMP:SMX during an *in vivo* mouse lung infection, mice were inoculated via an intranasal infection with 10,000 CFU of Wt_{specR} (Paczosa et al., 2020). At 14 hours post infection (hpi), mice were given a dose of 30mg/kg TMP:SMX via intraperitoneal injection and sacrificed 22 hpi. Strikingly, there was no appreciable reduction of lung bacterial burden (Fig 3.1B). These findings indicated that despite its *in vitro* sensitivity, Wt_{specR} was resistant to TMP:SMX during lung infection.

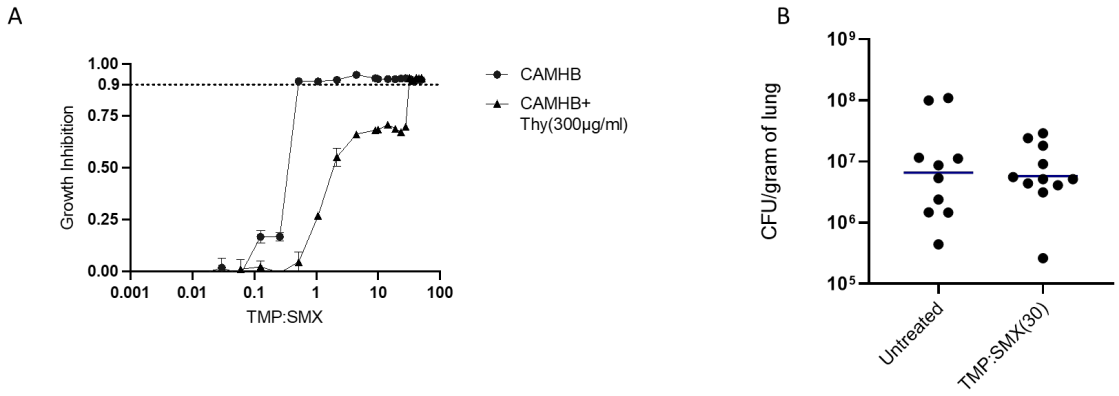

Figure 3.1 ***Klebsiella pneumoniae* was resistant to treatment by TMP:SMX *in vivo* despite *in vitro* sensitivity.** (A) Wt_{specR} grown overnight and back diluted in CAMHB media with (triangles) or without (circles) 300µg/ml of thymidine was exposed to various concentrations of trimethoprim:sulfamethoxazole (1:20) in 384-well plates. The y-axis indicates the growth inhibition based off untreated control wells. Inhibitory concentration for 90% were measured by OD 630nm after 16-18 hours of growth (dotted line on y-axis). The data in the figure is representative of three biological replicates. The error bars indicate the standard error of the mean of technical triplicates. (B) Swiss Webster mice were inoculated via the intranasal route with 10,000 CFU of Kp strain Wt_{specR}. At 14 hours post infection mice were given a dose of 30mg/kg of trimethoprim:sulfamethoxazole (1:5) diluted in DMSO via intraperitoneal injection. Each dot represents the CFU/gram lung recovered at 22 hrs post-infection a mouse with a line representing geometric mean. 3-4 mice per group were infected in three separate experiments. A two-way ANOVA with Tukeys correction was performed on log transform values and showed no significant difference.

3.2.2. Genomic deletion of *tdk* sensitizes *Klebsiella pneumoniae* specifically to TMP:SMX *in vitro* in the presence of thymidine.

We hypothesized that the inability for TMP:SMX to inhibit the growth of Kp during mouse lung infection was due to the high level of thymidine in mouse plasma (Heinzmann et al., 2016) coupled with the relatively high activity of Tdk in Kp (Saito et al., 1985). To test this hypothesis, we investigated whether exogenous thymidine would increase the IC90 of TMP:SMX. When Wt_{specR} was grown in CAMHB + 300µg/ml of thymidine, there was a 70-fold increase in the IC90 of TMP:SMX compared to growth in CAMHB alone (Fig 3.1A). These data paralleled the observation that TMP:SMX was ineffective in the mouse lung environment where exogenous thymidine is present (Fig 3.1B and Tokunaga, 1997).

To probe this hypothesis, lambda recombineering was used to delete *tdk* in Wt_{specR} (Huang et al., 2014). The IC90 of TMP:SMX was significantly lower (over 50-fold) for Wt_{specR}Δ*tdk* (Δ*tdk*) compared to Wt_{specR} when both strains were grown in CAMHB + 300µg/ml of thymidine (Fig. 3.2A). However, when Δ*tdk* was grown in CAMHB alone, the IC90 of TMP:SMX was similar to that of Wt_{specR} (Fig 3.2B, first column). To confirm that the effects on the IC90 of TMP:SMX were solely due to the loss of Tdk and its ability to utilize exogenous thymidine, *tdk* was cloned into pACYC184 and the resulting plasmid, pTdk1, transformed into Δ*tdk*. Both the IC90 and dose curve of TMP:SMX in Δ*tdk*+pTdk1, were indistinguishable from Wt_{specR} in either CAMHB or CAMHB+300µg/ml of thymidine (Fig 3.2A). These data showed that the deletion of *tdk* is sufficient to sensitize Kp to TMP:SMX in the presence of high levels of exogenous thymidine.

While deletion of *tdk* impacted to IC90 of TMP:SMX in the presence of thymidine (Fig 3.2A), it was unclear if this effect was specific to TMP:SMX alone or if the deletion would shift the IC90 of other drugs. A panel of nine drugs were used to test both Wt_{specR} and Δ*tdk*. This panel of antibiotics covered a diverse set of drug classes and included three cephalosporins cefixime (CFX), cefepime (CFP), and ceftriaxone (CTX); a polymyxin, colistin (COL); an aminoglycoside, gentamicin (GENT); a fluoroquinolone, levofloxacin (LEVO); an RNA polymerase inhibitor, rifampicin (RIF), and a glycylcycline (a tetracycline derivative) tigecycline (TIG). Previously, we showed that media growth conditions can impact the behavior of antibiotics in Kp (Davis & Morales et al., 2022). Specifically, we demonstrated that a media more nutritionally similar to the mouse lung environment (Silver et al., 2019), a minimal media with 0.5% glucose and 0.6μM FeSO4 (M9Glu), was a better predictor of drug interactions in an animal infection model. Therefore, measurements of IC90s were compared between Wt_{specR} and Δ*tdk* in CAMHB, CAMHB + 300ug/ml thymidine and M9Glu. There were no significant differences in IC90 between Wt_{specR} and Δ*tdk* for any of the drugs tested in either medium (Fig 3.2B, C), indicating that deletion of *tdk* does not alter the behavior of other drugs in these media. Additionally, the presence of thymidine did not reveal any significant differences in IC90s of these nine drugs between the two strains, suggesting that the effects of thymidine are specific to TMP:SMX (Fig 3.2D).

3.2.3. Δ*tdk* is sensitive to TMP:SMX *in vivo*

Given that growth of Δ*tdk* remained sensitive to TMP:SMX in the presence of exogeneous thymidine (Fig 3.2A) and that deletion of *tdk* did not affect sensitivity to nine

other antibiotics (Fig 3.2B, C, D), we next investigated the sensitivity of Δ*tdk* to TMP:SMX during mouse lung infection.

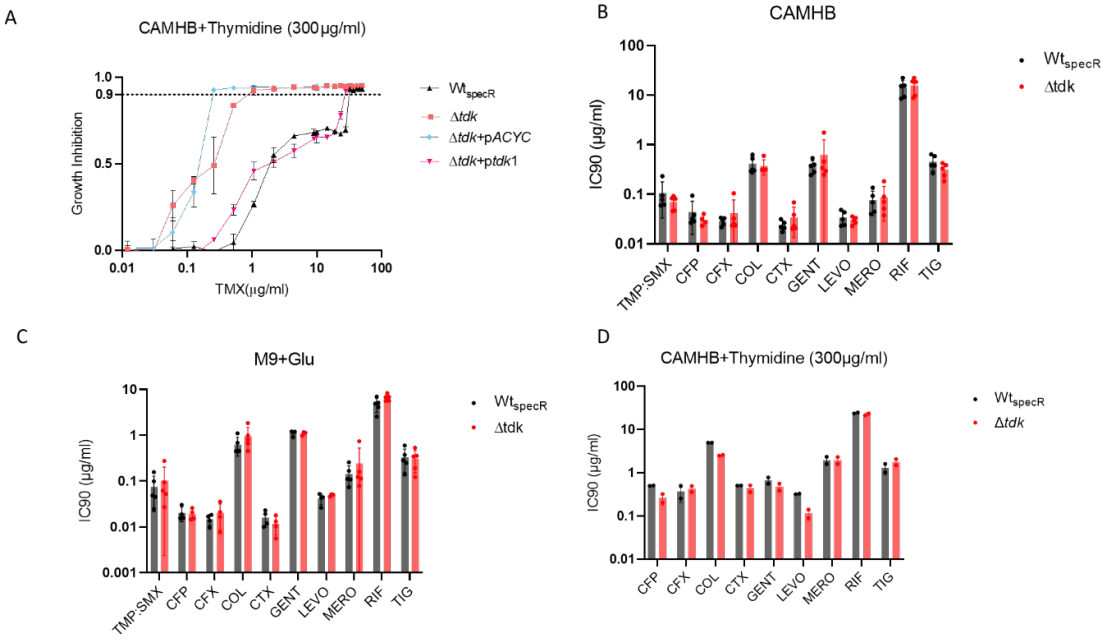

Figure 3.2: Deletion of *tdk* gene sensitizes *Klebsiella pneumoniae* specifically to TMP:SMX in the presence of exogenous thymidine. (A) The strains WtspecR, Δtdk, Δtdk transformed with pACYC184 (Δtdk+pACYC), and Δtdk transformed with pTdk1 (Δtdk+pTdk1) were grown overnight in CAMHB and back diluted in CAMHB. They were diluted to an OD630 of 0.01 and exposed to various concentrations of TMP:SMX (x-axis) in 384-well plates with the addition of 300µg/ml of thymidine. The y-axis indicates the growth inhibition and the IC90 is indicated by the dotted line across the y-axis. The data in the figure is one replicate performed in technical triplicate and is representative of three biological replicates. Error bars represent the standard deviation (B-D) IC90 measurements were made in both WtspecR and Δtdk in both CAMHB (B), (C) M9+0.5%glucose+0.6µMFeSO4,and (D) CAMHB + 300µg/ml thymidine. For the indicated drugs: trimethoprim:sulfamethoxazole (TMP:SMX) (B-C only), cefepime (CFP), cefixime (CFX), colistin (COL), ceftriaxone (CTX), gentamicin (GNT), levofloxacin (LEVO), meropenem (MERO), rifampicin (RIF), and tigecycline (TIG). Each point is a biological replicate. A two-way ANOVA with Tukey's correction was done to compare both strains for each drug and no significant differences were found. (2D) Both WtspecR and Δtdk were grown overnight and back diluted in CAMHB. They were exposed to the same antibiotics as in 2B and 2C in 385-well plates for IC90 measurements in the presence of 300µg/ml of thymidine.

Comparisons between the response to TMP:SMX by Wt_{specR} and Δ*tdk* were measured via a competition experiment. Here, mice were inoculated intranasally with a 1:1 ratio of the

spectinomycin sensitive ATCC43816 strain with either spectinomycin resistant Wt_{specR} or the isogenic Δ*tdk*. At 4 and 16 hpi mice were given 30 mg/kg of TMP:SMX. Mice were sacrificed at 22 hours and the competitive index (CI) was calculated. Only in the TMP:SMX-treated group did we observe a significant reduction in CI of Δ*tdk* indicating that Δ*tdk* is sensitive to TMP:SMX while Wt_{specR} is not (Fig 3.3). Importantly, Δ*tdk* competed as effectively as Wt_{specR} in the absence of TMP:SMX indicating the deletion of *tdk* does not reduce the fitness of the strain *in vivo*. These data are in accordance with our *in vitro* finding that Δ*tdk* remained sensitive to TMP:SMX in the presence of exogenous thymidine and demonstrate that Δ*tdk* can be used to evaluate drugs targeting folate production in murine infection models.

3.2.4. Δ*tdk* reveals an antagonistic interaction of TMP:SMX with meropenem during mouse infection

Recently, we have described that the same combinations of the antibiotics act synergistically or antagonistically *in vitro* when Kp is grown under different media conditions, such as CAMHB and M9Glu (Davis et al., 2022). We further tested several synergistic combinations in M9Glu and showed that the results from M9Glu matched observations after intranasal lung infection (Davis et al., 2022); ie two synergistic combinations in M9Glu but not CAMHB behaved synergistically after intranasal infection (Davis et al., 2022). However, we did not evaluate an antagonistic combination in M9Glu. Our previous work suggested that TMP-SMX in combination with meropenem was antagonistic. To further test this model, we first explored whether the loss in *tdk* impacted *in vitro* drug-drug interaction measurements using DiaMOND, a geometric

optimization of the traditional checkerboard assay (Diagonal Measurement of N-way Drug interactions) (Cokol et al., 2017). Drug interactions were measured in both WT_{specR} and Δ*tdk* grown in either CAMHB or M9Glu for pairwise combinations of TMP:SMX and the same panel of nine drugs used previously (Fig 3.2B- D).

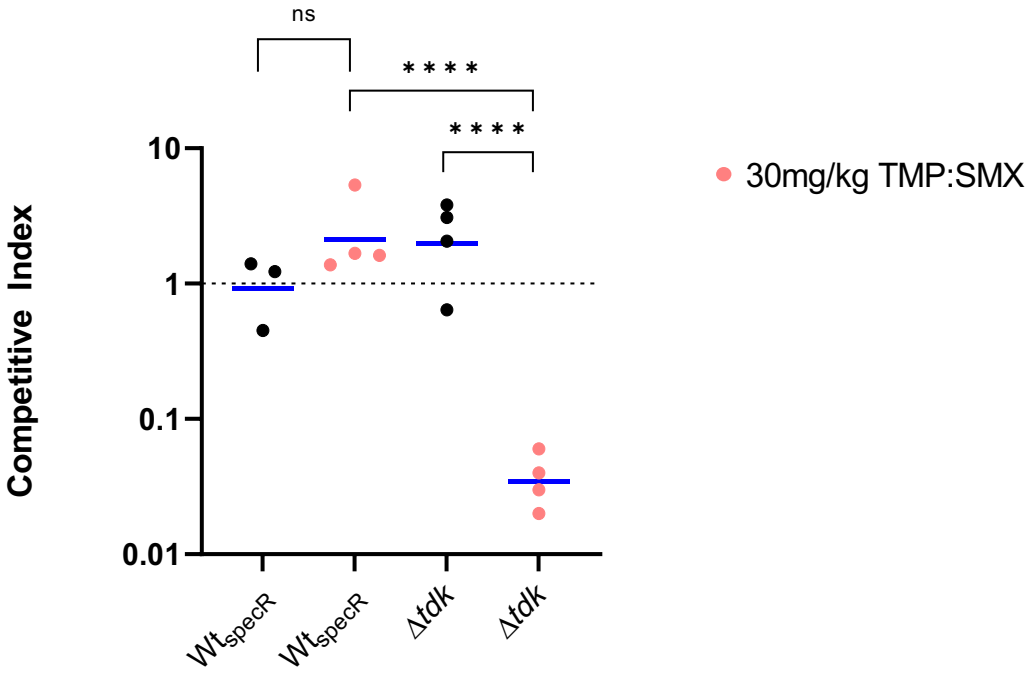

Figure 3.3. Deletion of *tdk* sensitizes *Klebsiella pneumoniae* to TMP:SMX during mouse lung infection. (3) A total 10,000 CFU of ATCC43816 (spectinomycin sensitive) mixed with eitherWt_{specR} or Δ*tdk* were inoculated at a 1:1 ratio into Swiss webster mice. For each group of mice, a subset (colored circles) were intraperitoneally injected with 100ul of 30mg/kg of TMP:SMX at a 1:5 ratio at 4 and 16hpi. Mice were euthanized at 22 hpi and lungs were harvested. Outputs from mice were plated on both selective (L+spectinomycin) and non-selective (L) plates. Competitive index was calculated as described in methods so that an index below one indicates that ATCC43816 out-competes the respective spectinomycin resistant strain. Each dot represents a mouse with the mean represented by the blue line. Two experiments with 1-2 mice per group were aggregated. Strains listed on the x-axis indicated those used in competition with the spectinomycin sensitive ATCC43816. Two-way ANOVA with Tukeys correction was used to determine statistical significance ($p<0.0001$ ****)

A comparison of the drug interactions using the fractional inhibitory concentration at 50% (FIC_{50}), showed no significant difference between wildtype and

Δ*tdk* in either CAMHB or M9Glu (Fig 3.4A). Consistent with single drugs, these data indicate that the deletion of *tdk* does not cause unexpected sensitivities or resistances to the action of other antibiotics. Importantly, the results with Δ*tdk* again confirmed that the combination of TMP-SMX and Meropenem were significantly different in CAMHB versus M9Glu and that there were antagonistic in M9Glu.

Based on these *in vitro* observations made in M9Glu, we expected that the combination of meropenem and TMP:SMX would behave antagonistically during mouse lung infection. We used a model similar to our previous study. This involves using non-sterilizing doses of antibiotics that kill between 90-99.9% of the bacteria during mouse lung infections to determine *in vivo*¬ drug-drug interactions of the combination meropenem + TMP:SMX (Davis, Morales 2022). In brief, mice were separated into five treatment groups consisting of 1X TMP:SMX, ½X TMP:SMX, 1X meropenem, ½X meropenem, and the combination of ½XTMP:SMX + ½X meropenem. 1X doses are designed to be partially effective but not sterilizing, while ½ doses allow for a more direct comparison between monotherapies and combination therapy. Mice were infected with Δ*tdk* and administered antibiotics at 14 hours post infection and lung bacterial burden was measured at 22 hpi. Interestingly, we observed a significant increase in lung bacterial burden in the combination therapy when compared to both 1X meropenem and ½X meropenem monotherapies (Fig 3.4B). We observed a significant decrease in lung bacterial burden in the combination group when compared to ½ X TMP-SMX

monotherapy, while no significance was detected between the combination and 1X TMP-SMX monotherapy.

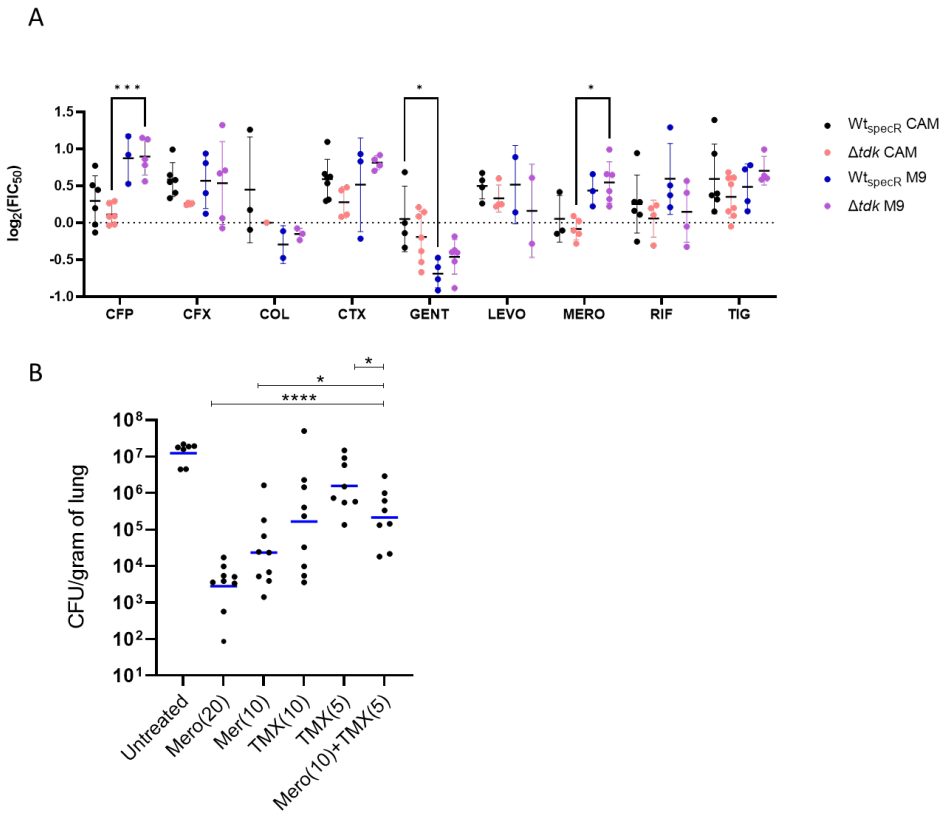

Figure 3.4. Use of Δ*tdk* allows for testing drug combinations *in vivo.*
(A) The indicated drugs were tested in combination with TMP-SMX for synergy or antagonism using DiaMOND for Wt_{specR} and Δ*tdk* grown in either CAMHB or M9+0.5%glucose+0.6μM FeSO4. Values plotted are the log_2FIC_{50} (fractional inhibitory concentration at 50%) so that negative values indicate synergistic interactions and positive values are antagonistic interactions. Cefepime (CFP), cefixime (CFX), colistin (COL), ceftriaxone (CTX), gentamicin (GENT), levofloxacin (LEVO), meropenem (MERO), rifampicin (RIF), tigecycline (TIG). Each dot is a biological replicate. An outlier correction was done using the ROUT test (Q=1%) in Graphpad prism followed by a two-way ANOVA with Tukey's correction to calculate significance between media conditions within a strain or between strains in a media condition ($p<0.05$ *). (B) Mice were inoculated with 10,000 CFU of Δ*tdk* via intranasal route. At 14 hours post infection antibiotics, trimethoprim:sulfamethoxazole (TMP:SMX, 1:5) and meropenem (Mero), were administered at the indicated dose in mg/kg. Meropenem was given a second time at 18 hours post infection due to its short half-life. Lungs were harvested at 24 hours post infection and plated for CFU. Bacterial burden was calculated in CFU per gram of lung (y-axis). Each dot represents a mouse with geometric mean represented by the blue line. To determine statistical significance, output values were log-transformed and used in a two-way ANOVA with Tukey's correction to calculate significance ($p<0.05$ *, $p<.0001$ ****)

Taken together, these data suggest that the aggregate effect of TMP:SMX and meropenem is antagonistic and a monotherapy of meropenem alone is more effective than the combination.

3.3. Discussion

To date there is no working model that utilizes TMP:SMX and presumably other folate targeting drugs to treat Kp infections in mice because the mouse lung environment has key differences that renders TMP:SMX ineffective (Tokunaga et al., 1997).The inability to utilize well established mouse models for Kp infections limits the potential discovery of both novel anti-folates and investigation of TMP:SMX with additional therapies to treat MDR-Kp. Previously, Tokunaga et.al demonstrated that a transposon insertion within the *tdk* gene of *E. coli* leads to the sensitization to trimethoprim during exposure to thymidine and during mouse lung infection (Tokunaga et al., 1997). Here, we showed that the deletion of *tdk*, similar to observations made by Tokunaga et.al, enabled testing of TMP:SMX during Kp mouse lung infection models. Since folate synthesis is a proven, useful target of anti-microbial therapies (Masters et al., 2003), this mutation may prove highly beneficial for testing strategies involving targeting folate in combating MDR infections by Kp and other Gram-negative infections, including the evaluation of novel compounds that inhibit folate synthesis. One such compound, iclaprim, is a new generation anti-folate inhibitor with increased *in vitro* activity in both Gram-positive and Gram-negative infections (Huang et al., 2019). However, *in vivo* activity for iclaprim has only been demonstrated for Gram-positive infections (Huang et al., 2019). Interestingly, studies using iclaprim have demonstrated that a deletion of *tdk* in a *Staphylococcus*

aureus strain increases the potency of iclaprim during mouse infection models (Huang et al., 2019). While iclaprim demonstrated broad spectrum *in vitro* activity against Gram-negative pathogens, the use of a Kp Δ*tdk* strain may show *in vivo* efficacy to complement observed *in vitro* findings.

In addition to iclaprim, other novel anti folates antibiotics are in development designed to target trimethoprim resistant strains. These compounds include propargyl-linked antifolates (PLAs) that target both Gram-positive and Gram-negative infections (Estrada et al., 2016). Several of these compounds have shown high levels of potency *in vitro*, however *in vivo* data is currently lacking for these early compounds (Estrada et al., 2016). Deletion of the *tdk* gene may facilitate testing these compounds with Kp *in vivo* models and potentially other Gram-negative pathogens.

Combination therapy for the treatment of Kp is an essential tool that clinicians turn to in highly complex infections involving extremely multi-drug resistant infections of Kp (Tumbarello et al., 2012). In particular, infection by carbapenem-resistant Kp are often cases where combination therapy has shown efficacy and value (Gomez-Simmonds et al., 2016). As rates of either CRE or pan-resistant strains of Kp continue to rise (Avgoulea et al., 2018; Chamieh et al., 2020), both utilization and relevance of combination therapy may follow. Our previous work demonstrated that combinations of antibiotic have different interactions dependent on both the species of bacteria and the environment of the bacteria (Davis et al., 2022). Furthermore, in the case of Kp testing combination *in vitro* in lung mimetic conditions proved beneficial for predicting which combinations would be effective in a mouse lung infection model. When considering combination therapy, TMP:SMX is an attractive option given its qualities (Masters et al.,

2003). However, in our previous study, it was not possible to link *in vitro* findings with *in vivo* studies involving TMP:SMX. Here, we showed how the deletion of *tdk* allowed for the testing of the combination of TMP:SMX with meropenem, a combination that on the surface is appealing. We found that the combination therapy was not as effective as monotherapy with meropenem alone. This finding supports previous data that indicate that *in vitro* measurements made in M9+Glu better correlated with *in vivo* findings in lungs (Davis et al., 2022) while also stressing the importance of *in vivo* data when considering combination regiments since some may do more harm than good. In summary, by deleting *tdk* and sensitizing Kp to TMP:SMX *in vivo*, we were able to link *in vitro* findings to an *in vivo* model which may aid in future efforts to improve clinical decision-making surrounding complex infections by Kp.

3.4. Materials and Methods

3.4.1. Bacterial strains and lambda recombineering

Klebsiella pneumoniae was obtained from ATCC (ATCC43816) and transformed with a spectinomycin resistance cassette yielding MKP220 (Wt_{specR}) (Paczosa et al., 2020). To generate a Δ*tdk* mutant, lambda recombineering was performed as described in (Huang et al., 2014). In brief, an apramycin resistance cassette flanked by complimentary regions of DNA was constructed, primers listed below, and transformed into cells already containing a plasmid encoding the lambda red system (pACBSR-hyg). After removal of the hygromycin resistance plasmid by passaging in absence of hygromycin, bacteria were transformed with plasmid encoding the gene for the flippase enzyme (pFLP-hyg) to remove the apramycin resistance cassette. Apramycin sensitive colonies were then

passaged for the removal of hygromycin resistance containing plasmid and sent for confirmation sequencing.

Primers used to construct apramycin cassette flanked by sequence homologous to region of chromosome containing *tdk*:

Forward: TAAAATATGGTACAATCGTCGCCGCGATAAAACACTTTGATTGGGG TCACGCAGCCG

Reverse: ACCTATAGCAGACATTAAAAAGGCGCCCACAGGCGCCTGTACGAGC TTCTGAGGGTA

For complementation experiments, the *tdk* gene and promoter region was amplified with PCR from genomic DNA extracted from Wt_{specR}. Products were then cloned into pACYC184 using BamH1 and Sac1 restriction digest and T4 ligation. Ligation products were transformed via electroporation into competent DH5α E. coli. Isolates that were chloramphenicol resistant and tetracycline sensitive were selected for confirmatory PCR and sequencing. The resulting plasmid, pACYC+tdk1, was transformed into the Δ*tdk* strain by electroporation.

3.4.2. Antibiotics and *in vitro* testing

Trimethoprim, sulfamethoxazole, cefixime, cefepime, colistin, gentamicin, levofloxacin, meropenem, and rifampicin were acquired from Sigma. Tigecycline was acquired from TCI chemicals. Gentamicin and colistin were prepared in PBS + 0.2% Tween20, all other drugs were diluted in DMSO. Thymidine was purchased from Sigma and diluted in PBS. For single drug dose curves, bacteria were grown overnight in CAMHB. Overnight cultures were diluted 1:2000 in CAMHB and allowed to grow to

mid-log growth to an optical density at OD_{630}nm of 0.2-0.4. $1x10^5$ CFUs of bacteria were inoculated into either CAMHB or CAMHB+300µg/ml of thymidine in 384-well plates where antibiotics were pre-dispensed by an HP liquid dispenser (Cokol et al., 2017). Plates were shaken overnight at 37˚C. The OD_{630} was read between 16 and 18 hours of growth. The controls included the OD630 of non-drug treated bacteria and wells were used to calculate levels of growth inhibition. Drug-drug interactions were measured using DiaMOND as described in Cokol, et.al., 2017 and Davis, et.al., 2022.

3.4.3. Mouse infections and competition experiments

For mouse infections, 7–9-week-old female Swiss Webster mice weighing between 25-30g were infected with 10,000 CFU of bacteria via intranasal route in 50µl of sterile PBS after exposure to isoflurane. Mice were weighed at the time of infection and bacteria used for inoculation were prepared by growth overnight in L medium. Overnight cultures were then diluted in sterile PBS to 10,000 CFU in 50µl. Antibiotics were prepared in DMSO and administered via a 100µl intraperitoneal injection using a 30gauge syringe needle at times indicated. At 22 hours post infection mice were euthanized using CO_2 and lungs were harvested, homogenized, and plated for CFUs on L agar plates.

For competition experiments bacterial strains were grown independently overnight and an equal amount of, ATCC43816 (spectinomycin sensitive) and either Δ*tdk (*spectinomycin resistant) or Wt_{specR} were mixed at a 1:1 ratio prior to inoculation. TMP:SMX was prepared at a 1:5 ratio of trimethoprim:sulfamethoxazole prior to injection and administered at 4 and 16 hours post infection. At 22 hours post infection

lungs were harvested, homogenized, and plated on both non-selective (L) and selective (L+50μg/ml of spectinomycin) plates. Colonies grown on L plates were patched on to L + 50μg/ml of spectinomycin. Competitive indices were calculated using the following equation:

$$\frac{(mutant/wildtype)_{output}}{(mutant/wildtype)_{input}}$$

Testing antibiotic combinations in mice was performed by infecting mice as described above. Mice were infected with 10,000 CFU of Δ*tdk* and given antibiotics at 14hpi. Meropenem was given again at 18 hpi. Mice were euthanized and lungs were harvested at 22 hpi.

3.5. Acknowledgements

We thank Pathricia Leus for critical reading of manuscript. YM and JM were supported by NIH NIAID U19142780 awarded to Deborah T. Hung. JM was also supported by NIH NIAID AI169786.

3.6. Contributions

Generation of Δ*tdk* strain was done by MK assisted by YM. Construction of pACYC-Tdk was done by IF with help by YM. All other work was done by YM.

Chapter 4: Discussion and Future Directions

4.1. Role of growth conditions for synergy testing during Kp infections

Rates of both pan-drug resistant (PDR) and difficult to treat-resistance (DTR) Kp infections have continued to rise in recent years garnering the attention from several public health groups, including the CDC and WHO (Wyres et al., 2020). Infections by these organisms have severely limited options for treatment and often lead to high levels of morbidity and mortality (Wyres et al., 2020). The current limited rate of antibiotic discovery has rekindled an interest in alternative treatment modalities, including the use of combination therapy. Unfortunately, guidance on implementing combination therapy clinically is limited (Tamma PD, 2022).

In this dissertation, we demonstrated that for Kp, antibiotic interactions can be significantly affected by specific environmental conditions. While there have been studies that highlight the effects of growth environments on antibiotic monotherapies for several bacterial species (Conrad et al., 1979; Meylan et al., 2017; Steixner et al., 2021), there is little understanding on how drug interactions are affected by different growth conditions. Here we showed that for Kp testing synergy in a media that is more similar to the site of infection resulted in stronger correlation between *in vitro* and *in vivo* results. It is therefore possible that past attempts to link synergy testing with clinical outcomes failed to account for the effects of the environment on interactions between drugs.

Unlike Kp, the three media conditions we tested did not seem to significantly impact drug interactions for *Pseudomonas.* A previous attempt to use *in vitro* synergy testing to treat patients with cystic fibrosis (CF) found no positive correlations between *in vitro* synergy testing and clinical microbiological outcomes (Aaron, 2007). Authors from

this study attribute this finding to the high variability found in CF sputum microbiology (Aaron, 2007). Conversely, our data would suggest that changes in growth condition should not impact the ability for synergy testing to correlate with CF patient outcomes. However, the environment and colonization of the CF lung environment is complex often involving biofilm formation, anaerobic growth, and chronic inflammation (Bhagirath et al., 2016). This complex environment likely exerts an effect on drug interaction however it is difficult to fully recapitulate *in vitro.*

For both multi-site and multi-species infections involving Kp, our data would suggest that the implementation of synergy testing should account for the growth environment of the bacteria. Moreover, special considerations may be needed for implementing combination therapy for these forms of complex infections. Overall, our data set did not reveal a "silver-bullet" combination that was synergistic in every condition and species. While such a combination would prove highly beneficial, there are still several benefits to combination therapy for both multi-site and multi-species infections. During multi-site infection, we postulate that it is possible for a specific combination to act synergistically in one tissue while behaving antagonistically in another. This may make it difficult for a combination to have overall positive clinical outcomes. Our dataset demonstrated that the majority of drug combinations are antagonist making it difficult to find combinations that work in one environment and complicates the likelihood for finding drugs that are synergistic in multiple growth environments. While examples of synergy in all growth environments was limited, cases of non-antagonism (either synergistic or additive) were observed. For Kp, several combinations exhibited this quality, including examples such as ceftriaxone +

gentamicin, tigecycline + rifampicin, and colistin + rifampicin (Fig 2.1). For multi-species infections, it may prove beneficial to identify overlapping synergies, avoid overlapping antagonisms, or prioritize the pathogen most responsible for poor clinical outcomes. Our data set did not reveal any combination that was synergistic in all the species and conditions tested. However, several combinations were non-antagonistic for the three species within one condition. Some examples in M9Glu included colistin + rifampicin, cefepime + meropenem, and tigecycline + rifampicin (Fig 2.1). It is possible that for combinations such as these, the drugs involved are acting on independent pathways common to all three species that do not interfere with each other.

It remains unclear what the clinical benefits are of drug synergy. However, it is thought that treatment with an antagonistic drug combination is more likely to lead to treatment failure or recurrence of infection (Ocampo et al., 2014). Therefore, the value in synergy testing may not come from the identification of universally synergistic combinations, but more so in avoiding antagonistic combinations. These non-antagonistic drug combinations may have several benefits including broader coverage of organisms, reduced rates of resistance, and shortened treatment periods (M. Zhu et al., 2021). Of these benefits, reductions in rates of resistance are of particular interest. The concept of multi-target therapy to reduce the emergence of drug resistance has been utilized for some non-bacterial pathogens. This includes both HIV and malaria, where combinations of drugs are used to both limit the growth of the pathogen and reduce rates of resistance for these infections (Bell, 2005; M. Zhu et al., 2021). In fact, recent studies suggest that even antagonistic combinations, while overall clinically harmful, repress the evolution of resistance (Baym et al., 2016).

Next, we showed that in the case of a lung infection model, a tissue mimetic condition correlated with *in vivo* outcomes more so than a standard rich medium. The capacity for a more tissue mimetic condition to predict *in vivo* outcomes was done by adapting previous Kp mouse lung infection models (Paczosa et al., 2020). Typically, testing antibiotics as either monotherapies or combination therapies in mice has the goal of achieving sterility in the tissue of interest. This is an ideal outcome for testing novel compounds or for testing combination against MDR isolates (Byrne et al., 1998; Hvidberg et al., 2000; Montero et al., 2002). However, full clearance of the bacteria creates a limited dynamic range to capture differences between combination therapies and monotherapies. In particular, detecting increased effectiveness in a combination therapy is impossible if the monotherapy alone is at a dose where outputs are near or below the limit of detection. Use of subtherapeutic doses gets around this issue by titrating drug doses so that lung bacterial burden is significantly lower than untreated controls but remaining well above the limit of detection for the assay. In conjunction with subtherapeutic doses, we also designed the combination therapy with each component consisting of half the dose of its respective monotherapy. This strategy allowed for the direct comparison between monotherapy and combination therapy while allowing for the identification of *in vivo* synergy or antagonism.

Our data demonstrated that for a drug-sensitive strain of Kp, growth conditions had a significant influence on drug interactions. Although these data gave many insights into how drug interactions change in different growth conditions as well as their correlation to *in vivo* outcomes, they should not be extrapolated to interpret how a clinical MDR Kp isolate would behave. This is in large part due to the high genetic heterogeneity

found amongst Kp isolates including heterogeneity in resistance profiles (Wyres et al., 2020). Rather, these data serve to guide future efforts to implement synergy testing for MDR clinical Kp isolates. Expanding this data to include MDR clinical isolates may involve key adaptations of the DiaMOND model to account for various resistance profiles. When testing isolates with high heterogeneity in resistance profiles, drug combinations can be sorted into three categories for testing *via* DiaMOND. First is a classical DiaMOND design, as described in this dissertation, using two or more susceptible drugs. Second, incorporation of non-susceptible drugs can be done using either a variable dose curve, similar to those used for susceptible drugs, or a given at a constant dose. When a drug is used at a constant dose, rather than testing for synergy it is being tested for the possible potentiation of a susceptible drug. This kind of interaction would be of clinical interest to improve the treatment of patients with MDR or XDR Kp infections by improving the potency of a susceptible drug reducing the chance of treatment failure or acquired resistance. Third, alongside the use of non-susceptible drugs inclusion of some newer beta-lactamase inhibitors such as avibactam, varobactam, relobactam may recapitulate some of the results found using beta-lactams in our studies in drug-sensitive Kp. Identifying antibiotics that combine with these newer drugs may aid in efforts to combat drug resistance to these agents.

Similar to our *in vitro* data, *in vivo* data collected using a drug-sensitive strain of Kp should not be used to predict how MDR clinical isolates would behave. Alongside the genetic heterogeneity found in Kp isolates, virulence in mice is also highly variable between clinical isolates (Kabha et al., 1995; Xiong et al., 2015). In particular, the drug-sensitive strain used in these studies was derived from ATCC43816, a mouse virulent

strain capable of robust exponential growth in the mouse lung (Paczosa et al., 2020). Generally, clinical Kp isolates are unable to rapidly expand in the mouse lung and require inoculation doses several logs higher (Xiong et al., 2015). These differences in growth pattern may have significant effects on antibiotics' ability to inhibit growth, in particular those antibiotics that are most effective on rapidly growing bacteria. Some strategies to overcome these obstacles include using immunocompromised mice, aligning drug dosing with windows of bacterial growth, or longer infections and treatments. Depleting mice of neutrophils, either *via* specific neutrophil antibodies (Paczosa et al., 2020) or cyclophosphamide treatment (Robertson et al., 2008), removes components of the immune system that suppresses Kp during mouse infection allowing for more robust growth (Nguyen et al., 2020). In addition to immunosuppressing the mice, timing antibiotic therapy so bacteria are in contact with the drug during exponential phase growth may better replicate *in vitro* testing conditions. This timing may vary for different mouse and Kp strains and would need to be experimentally determined. Lastly, to fully appreciate the differences in therapies a longer infection, such as 48 hours, may be needed to allow antibiotic to take effect and resolve outcomes. Together these optimizations may allow for the testing of antibiotic combinations in a mouse lung infection model using clinical Kp isolates. *In vivo* mouse data would help guide future efforts to implement *in vitro* synergy testing by providing insights into the correlation between testing conditions and outcomes.

Ultimately, we recognize that it may be impractical to incorporate synergy testing across tissue relevant medium for all individual Kp isolates or infections. However, it may be possible to create a data base encompassing several tissue relevant media with

many of the most common Kp isolates grouped by strain type and levels of drug resistance (Wyres et al., 2020). This may provide clinical guidance on which combinations are the most likely to be effective given specific genetic testing that could be done at the point of care for a patient. Already, traditional drug susceptibility testing as proven to be too slow in identifying the causative pathogen and resistance profile to prevent serious infections from developing (Bhattacharyya et al., 2019). This is limited by the time required to reliably grow a given bacterial strain while also differentiating between susceptible and non-susceptible drugs (Bhattacharyya et al., 2019). Recent strategies to overcome this has involved the incorporation of genetic information, namely RNAseq data, on a given strain to predict drug susceptibility. This technique, referred to as Genotypic and Phenotypic Antimicrobial Susceptibility Testing through RNA detection (GoPhAST-R), has been able to link changes in specific stress response pathways that can predict the resistance profile of bacteria to a panel of drugs (Bhattacharyya et al., 2019). This link between genetic and phenotypic data could potentially be used to predict drug synergies quickly and reliably in a clinical setting, something that would be required for its implementation as a clinical tool.

4.2. Δ*tdk* as a model for testing anti-folate therapy.

Our testing of antibiotic combinations involved a curated panel of ten antibiotics with class heterogeneity (Table 2.1). The primary criteria for selecting antibiotics were clinical relevance and coverage of different drug classes. Clinical relevance was guided by consideration of drugs that are either commonly used to treat Kp infections or are critical for MDR infections, including “last resort” drugs such as colistin, tigecycline, and

meropenem. One drug that piqued our interest was TMP:SMX. In vitro testing showed several synergistic combinations involving TMP:SMX as a component. Furthermore, TMP:SMX appeared in a significant portion of antibiotic combinations that switched between antagonistic in CAMHB and synergistic in M9Glu (Fig 2.4, 3.4). TMP:SMX is the only clinically used folate inhibitor and is a common empiric therapy for UTIs (Masters et al., 2003). TMP:SMX has qualities that are desirable when considering drugs for combination therapy and dose optimization, such as tissue penetrance and relatively low side effect profile (Masters et al., 2003). Collectively, this led us to test TMP:SMX in an *in vivo* mouse model for Kp. To do so however, it required the creation of a Δ*tdk* strain of Kp which remained sensitive to TMP:SMX during mouse lung infection.

By using a Δ*tdk* mutant in a drug-sensitive background we sensitized Kp to treatment by TMP:SMX during a mouse lung infection model (Fig 3.3). We also demonstrated that deletion of *tdk* does not affect the behavior of either single drugs or drug combinations that involve TMP:SMX *in vitro* (Fig 2.3). Thus we tested a drug combination that we had identified as antagonistic in M9Glu but synergistic in CAMHB, TMP:SMX + meropenem (Fig 2.1, 3.4). Testing this combination allowed us to challenge the hypothesis that M9Glu is a better predictor of *in vivo* outcomes than CAMHB. Concurrently, we probed if our mouse model could detect antagonism. We found that our mouse model had enough resolution to detect an antagonistic interaction *in vivo* and that this correlated with *in vitro* measurements taken in M9Glu (Fig 3.4). These data supported our hypothesis that measurements made in a tissue mimetic medium is better able to predict *in vivo* outcomes and emphasizes the value of an *in vivo* mouse model when considering advancing therapeutic options.

This murine model with Δ*tdk* mutant now enables us to test anti-folate therapy for Kp infection. Potentially, this not only benefits efforts to exploit TMP:SMX for novel clinical uses, but will also permit evaluation of novel anti-folates. In fact, the folate synthesis pathway is an ideal target for antimicrobial therapy. Unlike humans, bacteria are unable to utilize folate, an essential co-factor for many cellular processes, from their surroundings so they rely solely on the folate they produce (Birmingham, 2002). Despite being an ideal target for antimicrobial development, no anti-folates have been brought to the clinic since TMP:SMX (Masters et al., 2003).

Resistance to TMP:SMX has been detected and, similar to other forms of resistance, has also increased (Mahaney & Franklin, 2022). Recent efforts have centered on the development of anti-folates that maintain inhibitory effects on the pathway in the presence of resistance to TMP:SMX. This includes the development of iclaprim and PALs, which both target folate synthesis in TMP:SMX resistant strains (Estrada et al., 2016; Huang et al., 2019). Unfortunately, there is little support for their effectiveness in Gram-negative pathogens in murine models (Estrada et al., 2016; Huang et al., 2019). This discrepancy between Gram-positive and Gram-negative may be caused by differences in permeability or in the ability for Gram-negatives to scavenge and incorporate thymidine found in murine tissues. Utilization of a *tdk* deletion mutant, especially in TMP:SMX resistance isolates, would allow the testing of these compounds in mouse model of infection providing critical information needed to advance these drugs for the treatment of Kp and other Gram-negative bacteria.

Beyond the use of a Δ*tdk* mutant in drug discovery efforts, inhibition of Tdk during infection may be beneficial in some cases. While in healthy individuals'

thymidine levels remain relatively low (Holden et al., 1980) several disease states have been associated with elevated serum levels of thymidine. This includes malignancies such as leukemia, lymphomas, megaloblastic anemia, and small-cell lung cancers (Gronowitz et al., 1984; Holden et al., 1980). During these chronic disease thymidine levels in the plasma can double compared to a healthy individual (Holden et al., 1980). This is thought to be associated with chronic inflammation and lysis of cells releasing thymidine into the plasma. Besides malignancies, the viruses Ebstein-Barr virus, herpes simplex virus, cytomegalovirus, and rubella have also been linked to high levels of plasma thymidine in humans (Gronowitz et al., 1984). The link between these viral diseases and cancers seems to be chronic inflammation and a thrombotic state, thymidine and thymidine phosphorylase are involved in the platelet activation (Gronowitz et al., 1984; Spinazzola et al., 2002). In fact, rare genetic disorders causing dysfunction of thymidine phosphorylase are also linked to increased plasma thymidine levels (Spinazzola, 2020). Both cancer and viral infections have been identified as risk factors for infection and poor prognosis by Kp (Paczosa & Mecsas, 2016). It is possible that these increased thymidine levels in these patients would contribute to treatment failure by TMP:SMX. For patients with cancer, TMP:SMX and other antibiotics are often used as a prophylaxis for infections (van de Wetering, 2005). While TMP:SMX is effective at reducing rates of Gram-positive infections, it is less effective at preventing Gram-negative infection (van de Wetering, 2005). Furthermore, older studies observed that TMP:SMX often leads to treatment failure, even in the absence of resistance, in patients with cancer (Grose & Bodey, 1980; Grose et al., 1977). Specifically for infections caused by Kp, only a 45% response rate to Kp was observed in patients with advanced cancer disease (Grose et al.,

1977). In these cases a compound inhibitor of Tdk may synergize with TMP:SMX to improve clinical outcomes for these patients and increased the efficacy of TMP:SMX as a prophylaxis against Gram-negative infections in patients with cancer.

4.3. Summary and Final conclusions

In this dissertation, I describe two project that focus on understanding the potential of repurposing current antibiotics through combination therapy and highlight the importance of considering tissue conditions for testing of antibiotics. First, we explored the hypothesis that previous efforts to correlate synergy testing with clinical outcomes for Kp have not accounted for the possible influence that growth environments have on drug interactions. We specifically asked whether the medium used for *in vitro* testing accurately reflects the conditions experienced by the bacteria during an infection and whether these differences in conditions account for the difficulty correlating drug combinations with positive clinical outcomes. We accomplished this using the DiaMOND platform, which allowed us to efficiently test a panel of ten antibiotics in three separate media conditions: CAMHB, M9Glu, and UMM. Through a productive collaboration with the Dr. Kathleen Davis and other members of the Aldridge lab we were able to make comparisons between Kp, Ab, and Pa. Surprisingly, amongst these three species drug combinations in Kp were uniquely influenced by the growth conditions. Additionally, we were able to compare antibiotic combinations between the three species and found no correlation between them. Other key findings from this dataset include the lack of a “silver-bullet” drug combination, a predominance of antagonism

amongst drug combination, and numerous synergistic interactions that appear in either M9Glu or UMM but not in CAMHB.

Through our efforts to validate the *in vitro* DiaMOND data set we optimized a mouse model for Kp lung infection to incorporate the use of antibiotic therapy. Use of subtherapeutic dosing of antibiotics increased the resolution of the assay while use of combination doses consisting of half the dose of component monotherapies allowed for the direct comparison between monotherapies and combination therapies. This experimental design enabled the use of a modified Bliss score to quantify the drug interactions we observed in this mouse model. From this we identified that M9Glu was a better predictor of *in vivo* outcomes compared to CAMHB for a lung mouse infection model. These experiments also highlighted the potential for a combination such as cefixime + meropenem which repurposes a relatively under-utilized drug, cefixime, with meropenem, a drug often used for to treat MDR Kp infections. By raising our understanding of the intersection between bacterial metabolism and drug interactions we may continue to improve clinical guidance surrounding the implementation of combination therapy.

The second project covered in this dissertation was an extension of the first, where were interested in testing several key combinations involving the drug TMP:SMX. However, due to key differences between the human and mouse lung environment Kp is resistant to the effects of TMP:SMX despite having a sensitive phenotype *in vitro.* We created a strain of Kp with a deletion of the *tdk* gene, responsible for the utilization of exogenous thymidine. This Δ*tdk* mutant was sensitive to TMP:SMX during a mouse lung infection and was then used to test the combination of TMP:SMX + meropenem, a

combination that stood out during our initial DiaMOND testing for its differential behavior in CAMHB and M9Glu. We found that this combination, which was antagonistic in M9Glu and synergistic in CAMHB, behaved antagonistically in the mouse lung. Use this genetic mutant would allow a deeper exploration into the space of anti-folates as antimicrobial for Gram-negative pathogens. Taken together, these projects increase our understanding of how drug combinations interact with Kp in multiple environments, while creating tools that can be utilized to explore the combinatorial space in MDR Kp isolates.

Chapter 5: Bibliography

Aaron, S. D. (2007). Antibiotic synergy testing should not be routine for patients with cystic fibrosis who are infected with multiresistant bacterial organisms. *Paediatr Respir Rev*, *8*(3), 256-261. https://doi.org/10.1016/j.prrv.2007.04.005

Aathithan, S., & French, G. L. (2011). Prevalence and role of efflux pump activity in ciprofloxacin resistance in clinical isolates of Klebsiella pneumoniae. *Eur J Clin Microbiol Infect Dis*, *30*(6), 745-752. https://doi.org/10.1007/s10096-010-1147-0

Acar, J. F. (2000). Antibiotic synergy and antagonism. *Med Clin North Am*, *84*(6), 1391-1406. https://doi.org/10.1016/s0025-7125(05)70294-7

Aditi Priyadarshini, B., Mahalakshmi, K., & Naveen Kumar, V. (2019). Mutant Prevention Concentration of Ciprofloxacin against Klebsiella pneumoniae Clinical Isolates: An Ideal Prognosticator in Treating Multidrug-Resistant Strains. *Int J Microbiol*, *2019*, 6850108. https://doi.org/10.1155/2019/6850108

Agyeman, A. A., Bergen, P. J., Rao, G. G., Nation, R. L., & Landersdorfer, C. B. (2020). A systematic review and meta-analysis of treatment outcomes following antibiotic therapy among patients with carbapenem-resistant Klebsiella pneumoniae infections. *Int J Antimicrob Agents*, *55*(1), 105833. https://doi.org/10.1016/j.ijantimicag.2019.10.014

Al-Zalabani, A., AlThobyane, O. A., Alshehri, A. H., Alrehaili, A. O., Namankani, M. O., & Aljafri, O. H. (2020). Prevalence of Klebsiella pneumoniae Antibiotic Resistance in Medina, Saudi Arabia, 2014-2018. *Cureus*, *12*(8), e9714. https://doi.org/10.7759/cureus.9714

Alp, E., & Voss, A. (2006). Ventilator associated pneumonia and infection control. *Ann Clin Microbiol Antimicrob*, *5*, 7. https://doi.org/10.1186/1476-0711-5-7

Alteri, C. J., & Mobley, H. L. (2012). Escherichia coli physiology and metabolism dictates adaptation to diverse host microenvironments. *Curr Opin Microbiol*, *15*(1), 3-9. https://doi.org/10.1016/j.mib.2011.12.004

Antimicrobial Resistance, C. (2022). Global burden of bacterial antimicrobial resistance in 2019: a systematic analysis. *Lancet*, *399*(10325), 629-655. https://doi.org/10.1016/S0140-6736(21)02724-0

Arcari, G., & Carattoli, A. (2022). Global spread and evolutionary convergence of multidrug-resistant and hypervirulent Klebsiella pneumoniae high-risk clones. *Pathog Glob Health*, 1-14. https://doi.org/10.1080/20477724.2022.2121362

Ashurst, J. V., & Dawson, A. (2022). Klebsiella Pneumonia. In *StatPearls*. https://www.ncbi.nlm.nih.gov/pubmed/30085546

Avgoulea, K., Di Pilato, V., Zarkotou, O., Sennati, S., Politi, L., Cannatelli, A., Themeli-Digalaki, K., Giani, T., Tsakris, A., Rossolini, G. M., & Pournaras, S. (2018). Characterization of Extensively Drug-Resistant or Pandrug-Resistant Sequence Type 147 and 101 OXA-48-Producing Klebsiella pneumoniae Causing Bloodstream Infections in Patients in an Intensive Care Unit. *Antimicrob Agents Chemother*, *62*(7). https://doi.org/10.1128/AAC.02457-17

Bachman, M. A., Oyler, J. E., Burns, S. H., Caza, M., Lepine, F., Dozois, C. M., & Weiser, J. N. (2011). Klebsiella pneumoniae yersiniabactin promotes respiratory tract infection through evasion of lipocalin 2. *Infect Immun*, *79*(8), 3309-3316. https://doi.org/10.1128/IAI.05114-11

Baker, E. H., & Baines, D. L. (2018). Airway Glucose Homeostasis: A New Target in the Prevention and Treatment of Pulmonary Infection. *Chest*, *153*(2), 507-514. https://doi.org/10.1016/j.chest.2017.05.031

Bassetti, M., Giacobbe, D. R., Giamarellou, H., Viscoli, C., Daikos, G. L., Dimopoulos, G., De Rosa, F. G., Giamarellos-Bourboulis, E. J., Rossolini, G. M., Righi, E., Karaiskos, I., Tumbarello, M., Nicolau, D. P., Viale, P. L., Poulakou, G., Critically Ill Patients Study Group of the European Society of Clinical, M., Infectious, D., Hellenic Society of, C., & Societa Italiana di Terapia, A. (2018). Management of KPC-producing Klebsiella pneumoniae infections. *Clin Microbiol Infect*, *24*(2), 133-144. https://doi.org/10.1016/j.cmi.2017.08.030

Baym, M., Stone, L. K., & Kishony, R. (2016). Multidrug evolutionary strategies to reverse antibiotic resistance. *Science*, *351*(6268), aad3292. https://doi.org/10.1126/science.aad3292

Bell, A. (2005). Antimalarial drug synergism and antagonism: mechanistic and clinical significance. *FEMS Microbiol Lett*, *253*(2), 171-184. https://doi.org/10.1016/j.femsle.2005.09.035

Bengoechea, J. A., & Sa Pessoa, J. (2019). Klebsiella pneumoniae infection biology: living to counteract host defences. *FEMS Microbiol Rev*, *43*(2), 123-144. https://doi.org/10.1093/femsre/fuy043

Berenbaum, M. C. (1989). What is synergy? *Pharmacol Rev*, *41*(2), 93-141. https://www.ncbi.nlm.nih.gov/pubmed/2692037

Berlanga, M., Montero, M. T., Hernandez-Borrell, J., & Vinas, M. (2004). Influence of the cell wall on ciprofloxacin susceptibility in selected wild-type Gram-negative and Gram-positive bacteria. *Int J Antimicrob Agents*, *23*(6), 627-630. https://doi.org/10.1016/j.ijantimicag.2003.12.015

Bhagirath, A. Y., Li, Y., Somayajula, D., Dadashi, M., Badr, S., & Duan, K. (2016). Cystic fibrosis lung environment and Pseudomonas aeruginosa infection. *BMC Pulm Med*, *16*(1), 174. https://doi.org/10.1186/s12890-016-0339-5

Bharatham, N., Bhowmik, P., Aoki, M., Okada, U., Sharma, S., Yamashita, E., Shanbhag, A. P., Rajagopal, S., Thomas, T., Sarma, M., Narjari, R., Nagaraj, S., Ramachandran, V., Katagihallimath, N., Datta, S., & Murakami, S. (2021). Structure and function relationship of OqxB efflux pump from Klebsiella pneumoniae. *Nat Commun*, *12*(1), 5400. https://doi.org/10.1038/s41467-021-25679-0

Bhattacharyya, R. P., Bandyopadhyay, N., Ma, P., Son, S. S., Liu, J., He, L. L., Wu, L., Khafizov, R., Boykin, R., Cerqueira, G. C., Pironti, A., Rudy, R. F., Patel, M. M., Yang, R., Skerry, J., Nazarian, E., Musser, K. A., Taylor, J., Pierce, V. M., . . . Hung, D. T. (2019). Simultaneous detection of genotype and phenotype enables rapid and accurate antibiotic susceptibility determination. *Nat Med*, *25*(12), 1858-1864. https://doi.org/10.1038/s41591-019-0650-9

Blanco, P., Hernando-Amado, S., Reales-Calderon, J. A., Corona, F., Lira, F., Alcalde-Rico, M., Bernardini, A., Sanchez, M. B., & Martinez, J. L. (2016). Bacterial Multidrug Efflux Pumps: Much More Than Antibiotic Resistance Determinants. *Microorganisms*, *4*(1). https://doi.org/10.3390/microorganisms4010014

Bourne, C. R. (2014). Utility of the Biosynthetic Folate Pathway for Targets in Antimicrobial Discovery. *Antibiotics (Basel)*, *3*(1), 1-28. https://doi.org/10.3390/antibiotics3010001

Brauner, A., Fridman, O., Gefen, O., & Balaban, N. Q. (2016). Distinguishing between resistance, tolerance and persistence to antibiotic treatment. *Nat Rev Microbiol*, *14*(5), 320-330. https://doi.org/10.1038/nrmicro.2016.34

Brochado, A. R., Telzerow, A., Bobonis, J., Banzhaf, M., Mateus, A., Selkrig, J., Huth, E., Bassler, S., Zamarreno Beas, J., Zietek, M., Ng, N., Foerster, S., Ezraty, B., Py, B., Barras, F., Savitski, M. M., Bork, P., Gottig, S., & Typas, A. (2018). Species-specific activity of antibacterial drug combinations. *Nature*, *559*(7713), 259-263. https://doi.org/10.1038/s41586-018-0278-9

Brogden, R. N., Carmine, A. A., Heel, R. C., Speight, T. M., & Avery, G. S. (1982). Trimethoprim: a review of its antibacterial activity, pharmacokinetics and therapeutic use in urinary tract infections. *Drugs*, *23*(6), 405-430. https://doi.org/10.2165/00003495-198223060-00001

Brooks, T., & Keevil, C. W. (1997). A simple artificial urine for the growth of urinary pathogens. *Lett Appl Microbiol*, *24*(3), 203-206. https://doi.org/10.1046/j.1472-765x.1997.00378.x

Brown, A. N., Anderson, M. T., Bachman, M. A., & Mobley, H. L. T. (2022). The ArcAB Two-Component System: Function in Metabolism, Redox Control, and Infection. *Microbiol Mol Biol Rev*, *86*(2), e0011021. https://doi.org/10.1128/mmbr.00110-21

Bryan, L. E., & Kwan, S. (1983). Roles of ribosomal binding, membrane potential, and electron transport in bacterial uptake of streptomycin and gentamicin. *Antimicrob Agents Chemother*, *23*(6), 835-845. https://doi.org/10.1128/AAC.23.6.835

Bulik, C. C., Christensen, H., Li, P., Sutherland, C. A., Nicolau, D. P., & Kuti, J. L. (2010). Comparison of the activity of a human simulated, high-dose, prolonged infusion of meropenem against Klebsiella pneumoniae producing the KPC carbapenemase versus that against Pseudomonas aeruginosa in an *in vitro* pharmacodynamic model. *Antimicrob Agents Chemother*, *54*(2), 804-810. https://doi.org/10.1128/AAC.01190-09

Bush, K., & Bradford, P. A. (2016). beta-Lactams and beta-Lactamase Inhibitors: An Overview. *Cold Spring Harb Perspect Med*, *6*(8). https://doi.org/10.1101/cshperspect.a025247

Bush, K., & Bradford, P. A. (2019). Interplay between beta-lactamases and new beta-lactamase inhibitors. *Nat Rev Microbiol*, *17*(5), 295-306. https://doi.org/10.1038/s41579-019-0159-8

Butler, M. S., & Buss, A. D. (2006). Natural products--the future scaffolds for novel antibiotics? *Biochem Pharmacol*, *71*(7), 919-929. https://doi.org/10.1016/j.bcp.2005.10.012

Byrne, W. R., Welkos, S. L., Pitt, M. L., Davis, K. J., Brueckner, R. P., Ezzell, J. W., Nelson, G. O., Vaccaro, J. R., Battersby, L. C., & Friedlander, A. M. (1998). Antibiotic treatment of experimental pneumonic plague in mice. *Antimicrob Agents Chemother*, *42*(3), 675-681. https://doi.org/10.1128/AAC.42.3.675

Cai, S., Batra, S., Shen, L., Wakamatsu, N., & Jeyaseelan, S. (2009). Both TRIF- and MyD88-dependent signaling contribute to host defense against pulmonary

Klebsiella infection. *J Immunol*, *183*(10), 6629-6638. https://doi.org/10.4049/jimmunol.0901033

Calfee, D. P. (2017). Recent advances in the understanding and management of Klebsiella pneumoniae. *F1000Res*, *6*, 1760. https://doi.org/10.12688/f1000research.11532.1

Chamieh, A., El-Hajj, G., Zmerli, O., Afif, C., & Azar, E. (2020). Carbapenem resistant organisms: A 9-year surveillance and trends at Saint George University Medical Center. *J Infect Public Health*, *13*(12), 2101-2106. https://doi.org/10.1016/j.jiph.2019.02.019

Chandrasekaran, S., Cokol-Cakmak, M., Sahin, N., Yilancioglu, K., Kazan, H., Collins, J. J., & Cokol, M. (2016). Chemogenomics and orthology-based design of antibiotic combination therapies. *Mol Syst Biol*, *12*(5), 872. https://doi.org/10.15252/msb.20156777

cheng, D.-L., Liu, Y.-C., Yen, M.-Y., Liu, c.-Y., & Wang, R.-S. (1991). Septic Metastatic Lesions of Pyogenic Liver Abscess: Their Association With Klebsiella pneumoniae Bacteremia in Diabetic Patients. *Archives of Internal Medicine*, *151*(8), 1557-1559. https://doi.org/10.1001/archinte.1991.00400080059010

Chevereau, G., & Bollenbach, T. (2015). Systematic discovery of drug interaction mechanisms. *Mol Syst Biol*, *11*(4), 807. https://doi.org/10.15252/msb.20156098

Choby, J. E., Howard-Anderson, J., & Weiss, D. S. (2020). Hypervirulent Klebsiella pneumoniae - clinical and molecular perspectives. *J Intern Med*, *287*(3), 283-300. https://doi.org/10.1111/joim.13007

Choi, M., Hegerle, N., Nkeze, J., Sen, S., Jamindar, S., Nasrin, S., Sen, S., Permala-Booth, J., Sinclair, J., Tapia, M. D., Johnson, J. K., Mamadou, S., Thaden, J. T., Fowler, V. G., Jr., Aguilar, A., Teran, E., Decre, D., Morel, F., Krogfelt, K. A., . . . Tennant, S. M. (2020). The Diversity of Lipopolysaccharide (O) and Capsular Polysaccharide (K) Antigens of Invasive Klebsiella pneumoniae in a Multi-Country Collection. *Front Microbiol*, *11*, 1249. https://doi.org/10.3389/fmicb.2020.01249

Clegg, S., & Murphy, C. N. (2016). Epidemiology and Virulence of Klebsiella pneumoniae. *Microbiol Spectr*, *4*(1). https://doi.org/10.1128/microbiolspec.UTI-0005-2012

Cokol, M., Chua, H. N., Tasan, M., Mutlu, B., Weinstein, Z. B., Suzuki, Y., Nergiz, M. E., Costanzo, M., Baryshnikova, A., Giaever, G., Nislow, C., Myers, C. L., Andrews, B. J., Boone, C., & Roth, F. P. (2011). Systematic exploration of synergistic drug pairs. *Mol Syst Biol*, *7*, 544. https://doi.org/10.1038/msb.2011.71

Cokol, M., Kuru, N., Bicak, E., Larkins-Ford, J., & Aldridge, B. B. (2017). Efficient measurement and factorization of high-order drug interactions in Mycobacterium tuberculosis. *Sci Adv*, *3*(10), e1701881. https://doi.org/10.1126/sciadv.1701881

Collins, C. M., & D'Orazio, S. E. (1993). Bacterial ureases: structure, regulation of expression and role in pathogenesis. *Mol Microbiol*, *9*(5), 907-913. https://doi.org/10.1111/j.1365-2958.1993.tb01220.x

Conrad, R. S., Wulf, R. G., & Clay, D. L. (1979). Effects of carbon sources on antibiotic resistance in Pseudomonas aeruginosa. *Antimicrob Agents Chemother*, *15*(1), 59-66. https://doi.org/10.1128/AAC.15.1.59

Cristea, O. M., Avramescu, C. S., Balasoiu, M., Popescu, F. D., Popescu, F., & Amzoiu, M. O. (2017). Urinary tract infection with Klebsiella pneumoniae in Patients with Chronic Kidney Disease. *Curr Health Sci J*, *43*(2), 137-148. https://doi.org/10.12865/CHSJ.43.02.06

Daikos, G. L., Tsaousi, S., Tzouvelekis, L. S., Anyfantis, I., Psichogiou, M., Argyropoulou, A., Stefanou, I., Sypsa, V., Miriagou, V., Nepka, M., Georgiadou, S., Markogiannakis, A., Goukos, D., & Skoutelis, A. (2014). Carbapenemase-producing Klebsiella pneumoniae bloodstream infections: lowering mortality by antibiotic combination schemes and the role of carbapenems. *Antimicrob Agents Chemother*, *58*(4), 2322-2328. https://doi.org/10.1128/AAC.02166-13

Darras-Joly, C., Bedos, J. P., Sauve, C., Moine, P., Vallee, E., Carbon, C., & Azoulay-Dupuis, E. (1996). Synergy between amoxicillin and gentamicin in combination against a highly penicillin-resistant and -tolerant strain of Streptococcus pneumoniae in a mouse pneumonia model. *Antimicrob Agents Chemother*, *40*(9), 2147-2151. https://doi.org/10.1128/AAC.40.9.2147

Davies, J., & Davies, D. (2010). Origins and evolution of antibiotic resistance. *Microbiol Mol Biol Rev*, *74*(3), 417-433. https://doi.org/10.1128/MMBR.00016-10

Davis, K., Greenstein, T., Viau Colindres, R., & Aldridge, B. B. (2021). Leveraging laboratory and clinical studies to design effective antibiotic combination therapy. *Curr Opin Microbiol*, *64*, 68-75. https://doi.org/10.1016/j.mib.2021.09.006

Davis, K. P., Morales, Y., McCabe, A. L., Mecsas, J., & Aldridge, B. B. (2022). Critical role of growth medium for detecting drug interactions in Gram-negative bacteria that model in vivo responses. *bioRxiv*, 2022.2009.2020.508761. https://doi.org/10.1101/2022.09.20.508761

De Oliveira, D. M. P., Forde, B. M., Kidd, T. J., Harris, P. N. A., Schembri, M. A., Beatson, S. A., Paterson, D. L., & Walker, M. J. (2020). Antimicrobial Resistance in ESKAPE Pathogens. *Clin Microbiol Rev*, *33*(3). https://doi.org/10.1128/CMR.00181-19

Demidenko, E., & Miller, T. W. (2019). Statistical determination of synergy based on Bliss definition of drugs independence. *PLoS One*, *14*(11), e0224137. https://doi.org/10.1371/journal.pone.0224137

Dillon, N., Holland, M., Tsunemoto, H., Hancock, B., Cornax, I., Pogliano, J., Sakoulas, G., & Nizet, V. (2019). Surprising synergy of dual translation inhibition vs. Acinetobacter baumannii and other multidrug-resistant bacterial pathogens. *EBioMedicine*, *46*, 193-201. https://doi.org/10.1016/j.ebiom.2019.07.041

Doern, C. D. (2014). When does 2 plus 2 equal 5? A review of antimicrobial synergy testing. *J Clin Microbiol*, *52*(12), 4124-4128. https://doi.org/10.1128/JCM.01121-14

Dourakis, S. P., Alexopoulou, A., Metallinos, G., Thanos, L., & Archimandritis, A. J. (2006). Pubic osteomyelitis due to Klebsiella pneumoniae in a patient with diabetes mellitus. *Am J Med Sci*, *331*(6), 322-324. https://doi.org/10.1097/00000441-200606000-00006

Drusano, G. L., Liu, W., Fregeau, C., Kulawy, R., & Louie, A. (2009). Differing effects of combination chemotherapy with meropenem and tobramycin on cell kill and suppression of resistance of wild-type Pseudomonas aeruginosa PAO1 and its

isogenic MexAB efflux pump-overexpressed mutant. *Antimicrob Agents Chemother*, *53*(6), 2266-2273. https://doi.org/10.1128/AAC.01680-08

Effah, C. Y., Sun, T., Liu, S., & Wu, Y. (2020). Klebsiella pneumoniae: an increasing threat to public health. *Ann Clin Microbiol Antimicrob*, *19*(1), 1. https://doi.org/10.1186/s12941-019-0343-8

El-Badawy, M. F., Tawakol, W. M., El-Far, S. W., Maghrabi, I. A., Al-Ghamdi, S. A., Mansy, M. S., Ashour, M. S., & Shohayeb, M. M. (2017). Molecular Identification of Aminoglycoside-Modifying Enzymes and Plasmid-Mediated Quinolone Resistance Genes among Klebsiella pneumoniae Clinical Isolates Recovered from Egyptian Patients. *Int J Microbiol*, *2017*, 8050432. https://doi.org/10.1155/2017/8050432

Elgazzar, D., Aboubakr, M., Bayoumi, H., Ibrahim, A. N., Sorour, S. M., El-Hewaity, M., Elsayed, A. M., Shehata, S. A., Bayoumi, K. A., Alsieni, M., Behery, M., Abdelrahaman, D., Ibrahim, S. F., & Abdeen, A. (2022). Tigecycline and Gentamicin-Combined Treatment Enhances Renal Damage: Oxidative Stress, Inflammatory Reaction, and Apoptosis Interplay. *Pharmaceuticals (Basel)*, *15*(6). https://doi.org/10.3390/ph15060736

Escudero Siosi, A., Al Ani, H., Chaudhry, N., Brady, S., & Chan, A. (2021). Multifocal reactive myositis induced by Klebsiella pneumoniae. *Rheumatol Adv Pract*, *5*(2), rkab025. https://doi.org/10.1093/rap/rkab025

Estrada, A., Wright, D. L., & Anderson, A. C. (2016). Antibacterial Antifolates: From Development through Resistance to the Next Generation. *Cold Spring Harb Perspect Med*, *6*(8). https://doi.org/10.1101/cshperspect.a028324

Fan, B., Guan, J., Wang, X., & Cong, Y. (2016). Activity of Colistin in Combination with Meropenem, Tigecycline, Fosfomycin, Fusidic Acid, Rifampin or Sulbactam against Extensively Drug-Resistant Acinetobacter baumannii in a Murine Thigh-Infection Model. *PLoS One*, *11*(6), e0157757. https://doi.org/10.1371/journal.pone.0157757

Fang, C. T., Chen, Y. C., Chang, S. C., Sau, W. Y., & Luh, K. T. (2000). Klebsiella pneumoniae meningitis: timing of antimicrobial therapy and prognosis. *QJM*, *93*(1), 45-53. https://doi.org/10.1093/qjmed/93.1.45

Fang, C. T., Chuang, Y. P., Shun, C. T., Chang, S. C., & Wang, J. T. (2004). A novel virulence gene in Klebsiella pneumoniae strains causing primary liver abscess and septic metastatic complications. *J Exp Med*, *199*(5), 697-705. https://doi.org/10.1084/jem.20030857

Foschi, C., Salvo, M., Laghi, L., Zhu, C., Ambretti, S., Marangoni, A., & Re, M. C. (2018). Impact of meropenem on Klebsiella pneumoniae metabolism. *PLoS One*, *13*(11), e0207478. https://doi.org/10.1371/journal.pone.0207478

Foster, T. J. (2017). Antibiotic resistance in Staphylococcus aureus. Current status and future prospects. *FEMS Microbiol Rev*, *41*(3), 430-449. https://doi.org/10.1093/femsre/fux007

Galani, I., Anagnostoulis, G., Chatzikonstantinou, M., Petrikkos, G., & Souli, M. (2016). Emergence of Klebsiella pneumoniae co-producing OXA-48, CTX-M-15, and ArmA in Greece. *Clin Microbiol Infect*, *22*(10), 898-899. https://doi.org/10.1016/j.cmi.2016.08.002

Galani, I., Karaiskos, I., Souli, M., Papoutsaki, V., Galani, L., Gkoufa, A., Antoniadou, A., & Giamarellou, H. (2020). Outbreak of KPC-2-producing Klebsiella pneumoniae endowed with ceftazidime-avibactam resistance mediated through a VEB-1-mutant (VEB-25), Greece, September to October 2019. *Euro Surveill*, *25*(3). https://doi.org/10.2807/1560-7917.ES.2020.25.3.2000028

Ganz, T., & Nemeth, E. (2015). Iron homeostasis in host defence and inflammation. *Nat Rev Immunol*, *15*(8), 500-510. https://doi.org/10.1038/nri3863

Garcia-Menino, I., Forcelledo, L., Rosete, Y., Garcia-Prieto, E., Escudero, D., & Fernandez, J. (2021). Spread of OXA-48-producing Klebsiella pneumoniae among COVID-19-infected patients: The storm after the storm. *J Infect Public Health*, *14*(1), 50-52. https://doi.org/10.1016/j.jiph.2020.11.001

Giamarellou, H., & Karaiskos, I. (2022). Current and Potential Therapeutic Options for Infections Caused by Difficult-to-Treat and Pandrug Resistant Gram-Negative Bacteria in Critically Ill Patients. *Antibiotics (Basel)*, *11*(8). https://doi.org/10.3390/antibiotics11081009

Giamarellou, H., Zissis, N. P., Tagari, G., & Bouzos, J. (1984). In vitro synergistic activities of aminoglycosides and new beta-lactams against multiresistant Pseudomonas aeruginosa. *Antimicrob Agents Chemother*, *25*(4), 534-536. https://doi.org/10.1128/AAC.25.4.534

Gomez-Simmonds, A., Nelson, B., Eiras, D. P., Loo, A., Jenkins, S. G., Whittier, S., Calfee, D. P., Satlin, M. J., Kubin, C. J., & Furuya, E. Y. (2016). Combination Regimens for Treatment of Carbapenem-Resistant Klebsiella pneumoniae Bloodstream Infections. *Antimicrob Agents Chemother*, *60*(6), 3601-3607. https://doi.org/10.1128/AAC.03007-15

Gomez, M., Valverde, A., Del Campo, R., Rodriguez, J. M., & Maldonado-Barragan, A. (2021). Phenotypic and Molecular Characterization of Commensal, Community-Acquired and Nosocomial Klebsiella spp. *Microorganisms*, *9*(11). https://doi.org/10.3390/microorganisms9112344

Graham, J. P., Eisenberg, J. N. S., Trueba, G., Zhang, L., & Johnson, T. J. (2017). Small-Scale Food Animal Production and Antimicrobial Resistance: Mountain, Molehill, or Something in-between? *Environ Health Perspect*, *125*(10), 104501. https://doi.org/10.1289/EHP2116

Greco, W. R., Bravo, G., & Parsons, J. C. (1995). The search for synergy: a critical review from a response surface perspective. *Pharmacol Rev*, *47*(2), 331-385. https://www.ncbi.nlm.nih.gov/pubmed/7568331

Gronowitz, J. S., Kallander, F. R., Diderholm, H., Hagberg, H., & Pettersson, U. (1984). Application of an *in vitro* assay for serum thymidine kinase: results on viral disease and malignancies in humans. *Int J Cancer*, *33*(1), 5-12. https://doi.org/10.1002/ijc.2910330103

Grose, W. E., & Bodey, G. P. (1980). Intravenous trimethoprim-sulfamethoxazole alone or combined with tobramycin for infections in cancer patients. *The American Journal of the Medical Sciences*, *279*(1), 4-13. https://doi.org/https://doi.org/10.1097/00000441-198001000-00001

Grose, W. E., Bodey, G. P., & Rodriguez, V. (1977). Sulfamethoxazole-Trimethoprim for Infections in Cancer Patients. *JAMA*, *237*(4), 352-354. https://doi.org/10.1001/jama.1977.03270310036004

Grousd, J. A., Rich, H. E., & Alcorn, J. F. (2019). Host-Pathogen Interactions in Gram-Positive Bacterial Pneumonia. *Clin Microbiol Rev*, *32*(3). https://doi.org/10.1128/CMR.00107-18

Gupta, A. (2002). Hospital-acquired infections in the neonatal intensive care unit--Klebsiella pneumoniae. *Semin Perinatol*, *26*(5), 340-345. https://doi.org/10.1053/sper.2002.36267

Gupta, K., Hooton, T. M., Naber, K. G., Wullt, B., Colgan, R., Miller, L. G., Moran, G. J., Nicolle, L. E., Raz, R., Schaeffer, A. J., Soper, D. E., Infectious Diseases Society of, A., European Society for, M., & Infectious, D. (2011). International clinical practice guidelines for the treatment of acute uncomplicated cystitis and pyelonephritis in women: A 2010 update by the Infectious Diseases Society of America and the European Society for Microbiology and Infectious Diseases. *Clin Infect Dis*, *52*(5), e103-120. https://doi.org/10.1093/cid/ciq257

Hancock, R. E., Raffle, V. J., & Nicas, T. I. (1981). Involvement of the outer membrane in gentamicin and streptomycin uptake and killing in Pseudomonas aeruginosa. *Antimicrob Agents Chemother*, *19*(5), 777-785. https://doi.org/10.1128/AAC.19.5.777

Hansen, D. S., Mestre, F., Alberti, S., Hernandez-Alles, S., Alvarez, D., Domenech-Sanchez, A., Gil, J., Merino, S., Tomas, J. M., & Benedi, V. J. (1999). Klebsiella pneumoniae lipopolysaccharide O typing: revision of prototype strains and O-group distribution among clinical isolates from different sources and countries. *J Clin Microbiol*, *37*(1), 56-62. https://doi.org/10.1128/JCM.37.1.56-62.1999

Hasdemir, U. O., Chevalier, J., Nordmann, P., & Pages, J. M. (2004). Detection and prevalence of active drug efflux mechanism in various multidrug-resistant Klebsiella pneumoniae strains from Turkey. *J Clin Microbiol*, *42*(6), 2701-2706. https://doi.org/10.1128/JCM.42.6.2701-2706.2004

Heineman, H. S., & Lofton, W. M. (1978). Unpredictable response of Pseudomonas aeruginosa to synergistic antibiotic combinations *in vitro*. *Antimicrob Agents Chemother*, *13*(5), 827-831. https://doi.org/10.1128/AAC.13.5.827

Heinzmann, K., Honess, D. J., Lewis, D. Y., Smith, D. M., Cawthorne, C., Keen, H., Heskamp, S., Schelhaas, S., Witney, T. H., Soloviev, D., Williams, K. J., Jacobs, A. H., Aboagye, E. O., Griffiths, J. R., & Brindle, K. M. (2016). The relationship between endogenous thymidine concentrations and [(18)F]FLT uptake in a range of preclinical tumour models. *EJNMMI Res*, *6*(1), 63. https://doi.org/10.1186/s13550-016-0218-3

Hernando-Amado, S., Coque, T. M., Baquero, F., & Martinez, J. L. (2019). Defining and combating antibiotic resistance from One Health and Global Health perspectives. *Nat Microbiol*, *4*(9), 1432-1442. https://doi.org/10.1038/s41564-019-0503-9

Hirsch, E. B., Guo, B., Chang, K. T., Cao, H., Ledesma, K. R., Singh, M., & Tam, V. H. (2013). Assessment of antimicrobial combinations for Klebsiella pneumoniae carbapenemase-producing K. pneumoniae. *J Infect Dis*, *207*(5), 786-793. https://doi.org/10.1093/infdis/jis766

Holden, L., Hoffbrand, A. V., & Tattersall, M. H. (1980). Thymidine concentrations in human sera: variations in patients with leukaemia and megaloblastic anaemia. *Eur J Cancer (1965)*, *16*(1), 115-121. https://doi.org/10.1016/0014-2964(80)90116-4

Huang, D. B., Park, J. H., & Murphy, T. M. (2019). Iclaprim activity against wild-type and corresponding thymidine kinase-deficient Staphylococcus aureus in a mouse protection model. *Eur J Clin Microbiol Infect Dis*, *38*(2), 409-412. https://doi.org/10.1007/s10096-018-3440-2

Huang, T. W., Lam, I., Chang, H. Y., Tsai, S. F., Palsson, B. O., & Charusanti, P. (2014). Capsule deletion via a lambda-Red knockout system perturbs biofilm formation and fimbriae expression in Klebsiella pneumoniae MGH 78578. *BMC Res Notes*, *7*, 13. https://doi.org/10.1186/1756-0500-7-13

Huang, Y., Sokolowski, K., Rana, A., Singh, N., Wang, J., Chen, K., Lang, Y., Zhou, J., Kadiyala, N., Krapp, F., Ozer, E. A., Hauser, A. R., Li, J., Bulitta, J. B., & Bulman, Z. P. (2021). Generating Genotype-Specific Aminoglycoside Combinations with Ceftazidime/Avibactam for KPC-Producing Klebsiella pneumoniae. *Antimicrob Agents Chemother*, *65*(9), e0069221. https://doi.org/10.1128/AAC.00692-21

Hvidberg, H., Struve, C., Krogfelt, K. A., Christensen, N., Rasmussen, S. N., & Frimodt-Moller, N. (2000). Development of a long-term ascending urinary tract infection mouse model for antibiotic treatment studies. *Antimicrob Agents Chemother*, *44*(1), 156-163. https://doi.org/10.1128/AAC.44.1.156-163.2000

Jacobs, D. M., Safir, M. C., Huang, D., Minhaj, F., Parker, A., & Rao, G. G. (2017). Triple combination antibiotic therapy for carbapenemase-producing Klebsiella pneumoniae: a systematic review. *Ann Clin Microbiol Antimicrob*, *16*(1), 76. https://doi.org/10.1186/s12941-017-0249-2

Jain, K., & Saini, S. (2016). MarRA, SoxSR, and Rob encode a signal dependent regulatory network in Escherichia coli. *Mol Biosyst*, *12*(6), 1901-1912. https://doi.org/10.1039/c6mb00263c

Jawetz, E., & Gunnison, J. B. (1952). Studies on antibiotic synergism and antagonism: a scheme of combined antibiotic action. *Antibiot Chemother (Northfield)*, *2*(5), 243-248.

Ji, S., Lv, F., Du, X., Wei, Z., Fu, Y., Mu, X., Jiang, Y., & Yu, Y. (2015). Cefepime combined with amoxicillin/clavulanic acid: a new choice for the KPC-producing K. pneumoniae infection. *Int J Infect Dis*, *38*, 108-114. https://doi.org/10.1016/j.ijid.2015.07.024

Johnson, D. I. (2018). Bacterial Virulence Factors. In D. I. Johnson (Ed.), *Bacterial Pathogens and Their Virulence Factors* (pp. 1-38). Springer International Publishing. https://doi.org/10.1007/978-3-319-67651-7_1

Joly-Guillou, M. L., Wolff, M., Farinotti, R., Bryskier, A., & Carbon, C. (2000). In vivo activity of levofloxacin alone or in combination with imipenem or amikacin in a mouse model of Acinetobacter baumannii pneumonia. *J Antimicrob Chemother*, *46*(5), 827-830. https://doi.org/10.1093/jac/46.5.827

Joshi, P., Shrivastava, R., Bhagwat, S., & Patel, M. (2021). Activity of beta-lactam plus beta-lactam-enhancer combination cefepime/zidebactam against Klebsiella pneumoniae harbouring defective OmpK35/36 porins and carbapenemases. *Diagn Microbiol Infect Dis*, *101*(2), 115481. https://doi.org/10.1016/j.diagmicrobio.2021.115481

Kabha, K., Nissimov, L., Athamna, A., Keisari, Y., Parolis, H., Parolis, L. A., Grue, R. M., Schlepper-Schafer, J., Ezekowitz, A. R., Ohman, D. E., & et al. (1995).

Relationships among capsular structure, phagocytosis, and mouse virulence in Klebsiella pneumoniae. *Infect Immun*, *63*(3), 847-852. https://doi.org/10.1128/iai.63.3.847-852.1995

Khurana, S., Singh, P., Sharad, N., Kiro, V. V., Rastogi, N., Lathwal, A., Malhotra, R., Trikha, A., & Mathur, P. (2021). Profile of co-infections & secondary infections in COVID-19 patients at a dedicated COVID-19 facility of a tertiary care Indian hospital: Implication on antimicrobial resistance. *Indian J Med Microbiol*, *39*(2), 147-153. https://doi.org/10.1016/j.ijmmb.2020.10.014

Kishibe, S., Okubo, Y., Morino, S., Hirotaki, S., Tame, T., Aoki, K., Ishii, Y., Ota, N., Shimomura, S., Sakakibara, H., Terakawa, T., & Horikoshi, Y. (2016). Pediatric hypervirulent Klebsiella pneumoniae septic arthritis. *Pediatr Int*, *58*(5), 382-385. https://doi.org/10.1111/ped.12806

Klemm, P., & Schembri, M. A. (2000). Bacterial adhesins: function and structure. *Int J Med Microbiol*, *290*(1), 27-35. https://doi.org/10.1016/S1438-4221(00)80102-2

Knight, S. D., & Bouckaert, J. (2009). Structure, function, and assembly of type 1 fimbriae. *Top Curr Chem*, *288*, 67-107. https://doi.org/10.1007/128_2008_13

Ko, W. C., Paterson, D. L., Sagnimeni, A. J., Hansen, D. S., Von Gottberg, A., Mohapatra, S., Casellas, J. M., Goossens, H., Mulazimoglu, L., Trenholme, G., Klugman, K. P., McCormack, J. G., & Yu, V. L. (2002). Community-acquired Klebsiella pneumoniae bacteremia: global differences in clinical patterns. *Emerg Infect Dis*, *8*(2), 160-166. https://doi.org/10.3201/eid0802.010025

Kumar, V., & Park, S. (2018). Potential and limitations of Klebsiella pneumoniae as a microbial cell factory utilizing glycerol as the carbon source. *Biotechnol Adv*, *36*(1), 150-167. https://doi.org/10.1016/j.biotechadv.2017.10.004

Lan, P., Yan, R., Lu, Y., Zhao, D., Shi, Q., Jiang, Y., Yu, Y., & Zhou, J. (2021). Genetic diversity of siderophores and hypermucoviscosity phenotype in Klebsiella pneumoniae. *Microb Pathog*, *158*, 105014. https://doi.org/10.1016/j.micpath.2021.105014

Langevin, A. M., El Meouche, I., & Dunlop, M. J. (2020). Mapping the Role of AcrAB-TolC Efflux Pumps in the Evolution of Antibiotic Resistance Reveals Near-MIC Treatments Facilitate Resistance Acquisition. *mSphere*, *5*(6). https://doi.org/10.1128/mSphere.01056-20

Larkins-Ford, J., Greenstein, T., Van, N., Degefu, Y. N., Olson, M. C., Sokolov, A., & Aldridge, B. B. (2021). Systematic measurement of combination-drug landscapes to predict in vivo treatment outcomes for tuberculosis. *Cell Syst*, *12*(11), 1046-1063 e1047. https://doi.org/10.1016/j.cels.2021.08.004

Lery, L. M., Frangeul, L., Tomas, A., Passet, V., Almeida, A. S., Bialek-Davenet, S., Barbe, V., Bengoechea, J. A., Sansonetti, P., Brisse, S., & Tournebize, R. (2014). Comparative analysis of Klebsiella pneumoniae genomes identifies a phospholipase D family protein as a novel virulence factor. *BMC Biol*, *12*, 41. https://doi.org/10.1186/1741-7007-12-41

Lewis, K. (2020). The Science of Antibiotic Discovery. *Cell*, *181*(1), 29-45. https://doi.org/10.1016/j.cell.2020.02.056

Li, J., Zhang, H., Ning, J., Sajid, A., Cheng, G., Yuan, Z., & Hao, H. (2019). The nature and epidemiology of OqxAB, a multidrug efflux pump. *Antimicrob Resist Infect Control*, *8*, 44. https://doi.org/10.1186/s13756-019-0489-3

Li, W., Sun, G., Yu, Y., Li, N., Chen, M., Jin, R., Jiao, Y., & Wu, H. (2014). Increasing occurrence of antimicrobial-resistant hypervirulent (hypermucoviscous) Klebsiella pneumoniae isolates in China. *Clin Infect Dis*, *58*(2), 225-232. https://doi.org/10.1093/cid/cit675

Lin, C. T., Chen, Y. C., Jinn, T. R., Wu, C. C., Hong, Y. M., & Wu, W. H. (2013). Role of the cAMP-dependent carbon catabolite repression in capsular polysaccharide biosynthesis in Klebsiella pneumoniae. *PLoS One*, *8*(2), e54430. https://doi.org/10.1371/journal.pone.0054430

Lin, D., Fan, J., Wang, J., Liu, L., Xu, L., Li, F., Yang, J., & Li, B. (2018). The Fructose-Specific Phosphotransferase System of Klebsiella pneumoniae Is Regulated by Global Regulator CRP and Linked to Virulence and Growth. *Infect Immun*, *86*(8). https://doi.org/10.1128/IAI.00340-18

Linhares, I., Raposo, T., Rodrigues, A., & Almeida, A. (2013). Frequency and antimicrobial resistance patterns of bacteria implicated in community urinary tract infections: a ten-year surveillance study (2000-2009). *BMC Infect Dis*, *13*, 19. https://doi.org/10.1186/1471-2334-13-19

Liu, Q., Yin, X., Languino, L. R., & Altieri, D. C. (2018). Evaluation of drug combination effect using a Bliss independence dose-response surface model. *Stat Biopharm Res*, *10*(2), 112-122. https://doi.org/10.1080/19466315.2018.1437071

Livermore, D. M. (2002). Multiple mechanisms of antimicrobial resistance in Pseudomonas aeruginosa: our worst nightmare? *Clin Infect Dis*, *34*(5), 634-640. https://doi.org/10.1086/338782

Louie, A., Liu, W., VanGuilder, M., Neely, M. N., Schumitzky, A., Jelliffe, R., Fikes, S., Kurhanewicz, S., Robbins, N., Brown, D., Baluya, D., & Drusano, G. L. (2015). Combination treatment with meropenem plus levofloxacin is synergistic against Pseudomonas aeruginosa infection in a murine model of pneumonia. *J Infect Dis*, *211*(8), 1326-1333. https://doi.org/10.1093/infdis/jiu603

Ma, D., Alberti, M., Lynch, C., Nikaido, H., & Hearst, J. E. (1996). The local repressor AcrR plays a modulating role in the regulation of acrAB genes of Escherichia coli by global stress signals. *Mol Microbiol*, *19*(1), 101-112. https://doi.org/10.1046/j.1365-2958.1996.357881.x

Mahaney, A. P., & Franklin, R. B. (2022). Persistence of wastewater-associated antibiotic resistant bacteria in river microcosms. *Sci Total Environ*, *819*, 153099. https://doi.org/10.1016/j.scitotenv.2022.153099

Maraki, S., Mavromanolaki, V. E., Moraitis, P., Stafylaki, D., Kasimati, A., Magkafouraki, E., & Scoulica, E. (2021). Ceftazidime-avibactam, meropenen-vaborbactam, and imipenem-relebactam in combination with aztreonam against multidrug-resistant, metallo-beta-lactamase-producing Klebsiella pneumoniae. *Eur J Clin Microbiol Infect Dis*, *40*(8), 1755-1759. https://doi.org/10.1007/s10096-021-04197-3

Marra, A. (2012). A Review of Animal Models Used for Antibiotic Evaluation. In T. J. Dougherty & M. J. Pucci (Eds.), *Antibiotic Discovery and Development* (pp. 1009-1033). Springer US. https://doi.org/10.1007/978-1-4614-1400-1_33

Mason, D. J., Stott, I., Ashenden, S., Weinstein, Z. B., Karakoc, I., Meral, S., Kuru, N., Bender, A., & Cokol, M. (2017). Prediction of Antibiotic Interactions Using

Descriptors Derived from Molecular Structure. *J Med Chem*, *60*(9), 3902-3912. https://doi.org/10.1021/acs.jmedchem.7b00204

Masters, P. A., O'Bryan, T. A., Zurlo, J., Miller, D. Q., & Joshi, N. (2003). Trimethoprim-sulfamethoxazole revisited. *Arch Intern Med*, *163*(4), 402-410. https://doi.org/10.1001/archinte.163.4.402

Matuschek, E., Longshaw, C., Takemura, M., Yamano, Y., & Kahlmeter, G. (2022). Cefiderocol: EUCAST criteria for disc diffusion and broth microdilution for antimicrobial susceptibility testing. *J Antimicrob Chemother*, *77*(6), 1662-1669. https://doi.org/10.1093/jac/dkac080

McInnes, R. S., McCallum, G. E., Lamberte, L. E., & van Schaik, W. (2020). Horizontal transfer of antibiotic resistance genes in the human gut microbiome. *Curr Opin Microbiol*, *53*, 35-43. https://doi.org/10.1016/j.mib.2020.02.002

Mead, A., Lees, P., Mitchell, J., Rycroft, A., Standing, J. F., Toutain, P. L., & Pelligand, L. (2019). Differential susceptibility to tetracycline, oxytetracycline and doxycycline of the calf pathogens Mannheimia haemolytica and Pasteurella multocida in three growth media. *J Vet Pharmacol Ther*, *42*(1), 52-59. https://doi.org/10.1111/jvp.12719

Meatherall, B. L., Gregson, D., Ross, T., Pitout, J. D., & Laupland, K. B. (2009). Incidence, risk factors, and outcomes of Klebsiella pneumoniae bacteremia. *Am J Med*, *122*(9), 866-873. https://doi.org/10.1016/j.amjmed.2009.03.034

Merino, S., Camprubi, S., Alberti, S., Benedi, V. J., & Tomas, J. M. (1992). Mechanisms of Klebsiella pneumoniae resistance to complement-mediated killing. *Infect Immun*, *60*(6), 2529-2535. https://doi.org/10.1128/iai.60.6.2529-2535.1992

Meylan, S., Porter, C. B. M., Yang, J. H., Belenky, P., Gutierrez, A., Lobritz, M. A., Park, J., Kim, S. H., Moskowitz, S. M., & Collins, J. J. (2017). Carbon Sources Tune Antibiotic Susceptibility in Pseudomonas aeruginosa via Tricarboxylic Acid Cycle Control. *Cell Chem Biol*, *24*(2), 195-206. https://doi.org/10.1016/j.chembiol.2016.12.015

Miethke, M., & Marahiel, M. A. (2007). Siderophore-based iron acquisition and pathogen control. *Microbiol Mol Biol Rev*, *71*(3), 413-451. https://doi.org/10.1128/MMBR.00012-07

Miftode, I. L., Nastase, E. V., Miftode, R. S., Miftode, E. G., Iancu, L. S., Lunca, C., Anton Paduraru, D. T., Costache, II, Stafie, C. S., & Dorneanu, O. S. (2021). Insights into multidrug-resistant K. pneumoniae urinary tract infections: From susceptibility to mortality. *Exp Ther Med*, *22*(4), 1086. https://doi.org/10.3892/etm.2021.10520

Miller, M. H., Feinstein, S. A., & Chow, R. T. (1987). Early effects of beta-lactams on aminoglycoside uptake, bactericidal rates, and turbidimetrically measured growth inhibition in Pseudomonas aeruginosa. *Antimicrob Agents Chemother*, *31*(1), 108-110. https://doi.org/10.1128/AAC.31.1.108

Moellering, R. C., Jr., & Weinberg, A. N. (1971). Studies on antibiotic syngerism against enterococci. II. Effect of various antibiotics on the uptake of 14 C-labeled streptomycin by enterococci. *J Clin Invest*, *50*(12), 2580-2584. https://doi.org/10.1172/JCI106758

Moellering, R. C., Jr., Wennersten, C., & Weinberg, A. N. (1971). Studies on antibiotic synergism against enterococci. I. Bacteriologic studies. *J Lab Clin Med*, *77*(5), 821-828. https://www.ncbi.nlm.nih.gov/pubmed/4997545

Mohr, K. I. (2016). History of Antibiotics Research. *Curr Top Microbiol Immunol*, *398*, 237-272. https://doi.org/10.1007/82_2016_499

Montero, A., Ariza, J., Corbella, X., Domenech, A., Cabellos, C., Ayats, J., Tubau, F., Ardanuy, C., & Gudiol, F. (2002). Efficacy of colistin versus beta-lactams, aminoglycosides, and rifampin as monotherapy in a mouse model of pneumonia caused by multiresistant Acinetobacter baumannii. *Antimicrob Agents Chemother*, *46*(6), 1946-1952. https://doi.org/10.1128/AAC.46.6.1946-1952.2002

Montero, A., Ariza, J., Corbella, X., Domenech, A., Cabellos, C., Ayats, J., Tubau, F., Borraz, C., & Gudiol, F. (2004). Antibiotic combinations for serious infections caused by carbapenem-resistant Acinetobacter baumannii in a mouse pneumonia model. *J Antimicrob Chemother*, *54*(6), 1085-1091. https://doi.org/10.1093/jac/dkh485

Motsch, J., Murta de Oliveira, C., Stus, V., Koksal, I., Lyulko, O., Boucher, H. W., Kaye, K. S., File, T. M., Brown, M. L., Khan, I., Du, J., Joeng, H. K., Tipping, R. W., Aggrey, A., Young, K., Kartsonis, N. A., Butterton, J. R., & Paschke, A. (2020). RESTORE-IMI 1: A Multicenter, Randomized, Double-blind Trial Comparing Efficacy and Safety of Imipenem/Relebactam vs Colistin Plus Imipenem in Patients With Imipenem-nonsusceptible Bacterial Infections. *Clin Infect Dis*, *70*(9), 1799-1808. https://doi.org/10.1093/cid/ciz530

Murphy, C. N., & Clegg, S. (2012). Klebsiella pneumoniae and type 3 fimbriae: nosocomial infection, regulation and biofilm formation. *Future Microbiol*, *7*(8), 991-1002. https://doi.org/10.2217/fmb.12.74

Nagy, T. A., Crooks, A. L., Quintana, J. L. J., & Detweiler, C. S. (2020). Clofazimine Reduces the Survival of Salmonella enterica in Macrophages and Mice. *ACS Infect Dis*, *6*(5), 1238-1249. https://doi.org/10.1021/acsinfecdis.0c00023

Nassif, X., & Sansonetti, P. J. (1986). Correlation of the virulence of Klebsiella pneumoniae K1 and K2 with the presence of a plasmid encoding aerobactin. *Infect Immun*, *54*(3), 603-608. https://doi.org/10.1128/iai.54.3.603-608.1986

Navon-Venezia, S., Kondratyeva, K., & Carattoli, A. (2017). Klebsiella pneumoniae: a major worldwide source and shuttle for antibiotic resistance. *FEMS Microbiol Rev*, *41*(3), 252-275. https://doi.org/10.1093/femsre/fux013

Nguyen, G. T., Shaban, L., Mack, M., Swanson, K. D., Bunnell, S. C., Sykes, D. B., & Mecsas, J. (2020). SKAP2 is required for defense against K. pneumoniae infection and neutrophil respiratory burst. *Elife*, *9*. https://doi.org/10.7554/eLife.56656

Nichols, R. J., Sen, S., Choo, Y. J., Beltrao, P., Zietek, M., Chaba, R., Lee, S., Kazmierczak, K. M., Lee, K. J., Wong, A., Shales, M., Lovett, S., Winkler, M. E., Krogan, N. J., Typas, A., & Gross, C. A. (2011). Phenotypic landscape of a bacterial cell. *Cell*, *144*(1), 143-156. https://doi.org/10.1016/j.cell.2010.11.052

Ocampo, P. S., Lazar, V., Papp, B., Arnoldini, M., Abel zur Wiesch, P., Busa-Fekete, R., Fekete, G., Pal, C., Ackermann, M., & Bonhoeffer, S. (2014). Antagonism between bacteriostatic and bactericidal antibiotics is prevalent. *Antimicrob Agents Chemother*, *58*(8), 4573-4582. https://doi.org/10.1128/AAC.02463-14

Ohno, A., Isii, Y., Tateda, K., Matumoto, T., Miyazaki, S., Yokota, S., & Yamaguchi, K. (1995). Role of LPS length in clearance rate of bacteria from the bloodstream in mice. *Microbiology (Reading)*, *141 (Pt 10)*, 2749-2756. https://doi.org/10.1099/13500872-141-10-2749

Oliveira, R., Castro, J., Silva, S., Oliveira, H., Saavedra, M. J., Azevedo, N. F., & Almeida, C. (2022). Exploring the Antibiotic Resistance Profile of Clinical Klebsiella pneumoniae Isolates in Portugal. *Antibiotics (Basel)*, *11*(11). https://doi.org/10.3390/antibiotics11111613

Ota, K., Kaku, N., & Yanagihara, K. (2020). Efficacy of meropenem and amikacin combination therapy against carbapenemase-producing Klebsiella pneumoniae mouse model of pneumonia. *J Infect Chemother*, *26*(12), 1237-1243. https://doi.org/10.1016/j.jiac.2020.07.002

Paczosa, M. K., & Mecsas, J. (2016). Klebsiella pneumoniae: Going on the Offense with a Strong Defense. *Microbiol Mol Biol Rev*, *80*(3), 629-661. https://doi.org/10.1128/MMBR.00078-15

Paczosa, M. K., Silver, R. J., McCabe, A. L., Tai, A. K., McLeish, C. H., Lazinski, D. W., & Mecsas, J. (2020). Transposon Mutagenesis Screen of Klebsiella pneumoniae Identifies Multiple Genes Important for Resisting Antimicrobial Activities of Neutrophils in Mice. *Infect Immun*, *88*(4). https://doi.org/10.1128/IAI.00034-20

Panjaitan, N. S. D., Horng, Y. T., Chien, C. C., Yang, H. C., You, R. I., & Soo, P. C. (2021). The PTS Components in Klebsiella pneumoniae Affect Bacterial Capsular Polysaccharide Production and Macrophage Phagocytosis Resistance. *Microorganisms*, *9*(2). https://doi.org/10.3390/microorganisms9020335

Pantopoulou, A., Giamarellos-Bourboulis, E. J., Raftogannis, M., Tsaganos, T., Dontas, I., Koutoukas, P., Baziaka, F., Giamarellou, H., & Perrea, D. (2007). Colistin offers prolonged survival in experimental infection by multidrug-resistant Acinetobacter baumannii: the significance of co-administration of rifampicin. *Int J Antimicrob Agents*, *29*(1), 51-55. https://doi.org/10.1016/j.ijantimicag.2006.09.009

Patel, P. K., Russo, T. A., & Karchmer, A. W. (2014). Hypervirulent Klebsiella pneumoniae. *Open Forum Infect Dis*, *1*(1), ofu028. https://doi.org/10.1093/ofid/ofu028

Patel, T. S., Pogue, J. M., Mills, J. P., & Kaye, K. S. (2018). Meropenem-vaborbactam: a new weapon in the war against infections due to resistant Gram-negative bacteria. *Future Microbiol*, *13*(9), 971-983. https://doi.org/10.2217/fmb-2018-0054

Pendleton, J. N., Gorman, S. P., & Gilmore, B. F. (2013). Clinical relevance of the ESKAPE pathogens. *Expert Rev Anti Infect Ther*, *11*(3), 297-308. https://doi.org/10.1586/eri.13.12

Podschun, R., & Ullmann, U. (1998). Klebsiella spp. as nosocomial pathogens: epidemiology, taxonomy, typing methods, and pathogenicity factors. *Clin Microbiol Rev*, *11*(4), 589-603. https://doi.org/10.1128/CMR.11.4.589

Polse, R. F., Qarani, S. M., Assafi, M. S., Sabaly, N., & Ali, F. (2020). Incidence and Antibiotic Sensitivity of Klebsiella pneumonia isolated from urinary tract infection patients in Zakho emergency hospital / Iraq. *Journal of Education and Science*, *29*(3), 257-268. https://doi.org/10.33899/edusj.2020.126827.1056

Poudel, S., Tsunemoto, H., Meehan, M., Szubin, R., Olson, C. A., Lamsa, A., Seif, Y., Dillon, N., Vrbanac, A., Sugie, J., Dahesh, S., Monk, J. M., Dorrestein, P. C., Pogliano, J., Knight, R., Nizet, V., Palsson, B. O., & Feist, A. M. (2019). Characterization of CA-MRSA TCH1516 exposed to nafcillin in bacteriological and physiological media. *Sci Data*, *6*(1), 43. https://doi.org/10.1038/s41597-019-0051-4

Pranita D. Tamma*, S. L. A., Robert A. Bonomo, Amy J. Mathers, David van Duin, Cornelius J. Clancy. (2022, 03/31/2022). *IDSA Guidance on the Treatment of Antimicrobial-Resistant Gram-Negative Infections: Version 2.0*. https://www.idsociety.org/practice-guideline/amr-guidance-2.0/

Prokesch, B. C., TeKippe, M., Kim, J., Raj, P., TeKippe, E. M., & Greenberg, D. E. (2016). Primary osteomyelitis caused by hypervirulent Klebsiella pneumoniae. *Lancet Infect Dis*, *16*(9), e190-e195. https://doi.org/10.1016/S1473-3099(16)30021-4

Rahim, G. R., Gupta, N., Maheshwari, P., & Singh, M. P. (2019). Monomicrobial Klebsiella pneumoniae necrotizing fasciitis: an emerging life-threatening entity. *Clin Microbiol Infect*, *25*(3), 316-323. https://doi.org/10.1016/j.cmi.2018.05.008

Ramirez, M. S., & Tolmasky, M. E. (2010). Aminoglycoside modifying enzymes. *Drug Resist Updat*, *13*(6), 151-171. https://doi.org/10.1016/j.drup.2010.08.003

Regueiro, V., Moranta, D., Frank, C. G., Larrarte, E., Margareto, J., March, C., Garmendia, J., & Bengoechea, J. A. (2011). Klebsiella pneumoniae subverts the activation of inflammatory responses in a NOD1-dependent manner. *Cell Microbiol*, *13*(1), 135-153. https://doi.org/10.1111/j.1462-5822.2010.01526.x

Richards, R., Schwartz, H. R., Honeywell, M. E., Stewart, M. S., Cruz-Gordillo, P., Joyce, A. J., Landry, B. D., & Lee, M. J. (2020). Drug antagonism and single-agent dominance result from differences in death kinetics. *Nat Chem Biol*, *16*(7), 791-800. https://doi.org/10.1038/s41589-020-0510-4

Rivera-Espinar, F., Machuca, I., Tejero, R., Rodriguez, J., Mula, A., Marfil, E., Cano, A., Gutierrez-Gutierrez, B., Rodriguez, M., Pozo, J. C., De la Fuente, C., Rodriguez-Bano, J., Martinez-Martinez, L., Leon, R., & Torre-Cisneros, J. (2020). Impact of KPC Production and High-Level Meropenem Resistance on All-Cause Mortality of Ventilator-Associated Pneumonia in Association with Klebsiella pneumoniae. *Antimicrob Agents Chemother*, *64*(6). https://doi.org/10.1128/AAC.02164-19

Robertson, C. M., Perrone, E. E., McConnell, K. W., Dunne, W. M., Boody, B., Brahmbhatt, T., Diacovo, M. J., Van Rooijen, N., Hogue, L. A., Cannon, C. L., Buchman, T. G., Hotchkiss, R. S., & Coopersmith, C. M. (2008). Neutrophil depletion causes a fatal defect in murine pulmonary Staphylococcus aureus clearance. *J Surg Res*, *150*(2), 278-285. https://doi.org/10.1016/j.jss.2008.02.009

Rossol, M., Heine, H., Meusch, U., Quandt, D., Klein, C., Sweet, M. J., & Hauschildt, S. (2011). LPS-induced cytokine production in human monocytes and macrophages. *Crit Rev Immunol*, *31*(5), 379-446. https://doi.org/10.1615/critrevimmunol.v31.i5.20

Ryan, M. A., Akinbi, H. T., Serrano, A. G., Perez-Gil, J., Wu, H., McCormack, F. X., & Weaver, T. E. (2006). Antimicrobial activity of native and synthetic surfactant protein B peptides. *J Immunol*, *176*(1), 416-425. https://doi.org/10.4049/jimmunol.176.1.416

Sahly, H., & Podschun, R. (1997). Clinical, bacteriological, and serological aspects of Klebsiella infections and their spondylarthropathic sequelae. *Clin Diagn Lab Immunol*, *4*(4), 393-399. https://doi.org/10.1128/cdli.4.4.393-399.1997

Saito, H., Tomioka, H., & Ohkido, S. (1985). Further studies on thymidine kinase: distribution pattern of the enzyme in bacteria. *J Gen Microbiol*, *131*(11), 3091-3098. https://doi.org/10.1099/00221287-131-11-3091

Sanchez, G. V., Master, R. N., Clark, R. B., Fyyaz, M., Duvvuri, P., Ekta, G., & Bordon, J. (2013). Klebsiella pneumoniae antimicrobial drug resistance, United States, 1998-2010. *Emerg Infect Dis*, *19*(1), 133-136. https://doi.org/10.3201/eid1901.120310

Sande, M. A., & Irvin, R. G. (1974). Penicillin-aminoglycoside synergy in experimental Streptococcus viridans endocarditis. *J Infect Dis*, *129*(5), 572-576. https://doi.org/10.1093/infdis/129.5.572

Sande, M. A., & Johnson, M. L. (1975). Antimicrobial therapy of experimental endocarditis caused by Staphylococcus aureus. *J Infect Dis*, *131*(4), 367-375. https://doi.org/10.1093/infdis/131.4.367

Schofield, C. B. (2012). Updating antimicrobial susceptibility testing: introduction. *Clin Lab Sci*, *25*(4), 230-232. https://www.ncbi.nlm.nih.gov/pubmed/23330513

Scudeller, L., Righi, E., Chiamenti, M., Bragantini, D., Menchinelli, G., Cattaneo, P., Giske, C. G., Lodise, T., Sanguinetti, M., Piddock, L. J. V., Franceschi, F., Ellis, S., Carrara, E., Savoldi, A., & Tacconelli, E. (2021). Systematic review and meta-analysis of *in vitro* efficacy of antibiotic combination therapy against carbapenem-resistant Gram-negative bacilli. *Int J Antimicrob Agents*, *57*(5), 106344. https://doi.org/10.1016/j.ijantimicag.2021.106344

Serban, D., Popa Cherecheanu, A., Dascalu, A. M., Socea, B., Vancea, G., Stana, D., Smarandache, G. C., Sabau, A. D., & Costea, D. O. (2021). Hypervirulent Klebsiella pneumoniae Endogenous Endophthalmitis-A Global Emerging Disease. *Life (Basel)*, *11*(7). https://doi.org/10.3390/life11070676

Shbaklo, N., Corcione, S., Vicentini, C., Giordano, S., Fiorentino, D., Bianco, G., Cattel, F., Cavallo, R., Zotti, C. M., & De Rosa, F. G. (2022). An Observational Study of MDR Hospital-Acquired Infections and Antibiotic Use during COVID-19 Pandemic: A Call for Antimicrobial Stewardship Programs. *Antibiotics (Basel)*, *11*(5). https://doi.org/10.3390/antibiotics11050695

Shon, A. S., Bajwa, R. P., & Russo, T. A. (2013). Hypervirulent (hypermucoviscous) Klebsiella pneumoniae: a new and dangerous breed. *Virulence*, *4*(2), 107-118. https://doi.org/10.4161/viru.22718

Sili, U., Tekin, A., Karadag, H., Altinkanat, G., Gul, F., Bilgili, B., Arslantas, M. K., Ay, P., Soyletir, G., Cinel, I., & Korten, V. (2015). An Outbreak With Colistin- and Carbapenem-Resistant Klebsiella pneumoniae in an Intensive Care Unit. *Open Forum Infectious Diseases*, *2*(suppl_1). https://doi.org/10.1093/ofid/ofv133.1344

Silver, R. J., Paczosa, M. K., McCabe, A. L., Balada-Llasat, J. M., Baleja, J. D., & Mecsas, J. (2019). Amino Acid Biosynthetic Pathways Are Required for Klebsiella pneumoniae Growth in Immunocompromised Lungs and Are Druggable Targets during Infection. *Antimicrob Agents Chemother*, *63*(8). https://doi.org/10.1128/AAC.02674-18

Sobel, J. D. (1997). Pathogenesis of urinary tract infection. Role of host defenses. *Infect Dis Clin North Am*, *11*(3), 531-549. https://doi.org/10.1016/s0891-5520(05)70372-x

Song, J. Y., Cheong, H. J., Lee, J., Sung, A. K., & Kim, W. J. (2009). Efficacy of monotherapy and combined antibiotic therapy for carbapenem-resistant Acinetobacter baumannii pneumonia in an immunosuppressed mouse model. *Int J Antimicrob Agents*, *33*(1), 33-39. https://doi.org/10.1016/j.ijantimicag.2008.07.008

Spapen, H., Jacobs, R., Van Gorp, V., Troubleyn, J., & Honore, P. M. (2011). Renal and neurological side effects of colistin in critically ill patients. *Ann Intensive Care*, *1*(1), 14. https://doi.org/10.1186/2110-5820-1-14

Spinazzola, A., Marti, R., Nishino, I., Andreu, A. L., Naini, A., Tadesse, S., Pela, I., Zammarchi, E., Donati, M. A., Oliver, J. A., & Hirano, M. (2002). Altered thymidine metabolism due to defects of thymidine phosphorylase. *J Biol Chem*, *277*(6), 4128-4133. https://doi.org/10.1074/jbc.M111028200

Steixner, S. J. M., Spiegel, C., Dammerer, D., Wurm, A., Nogler, M., & Coraca-Huber, D. C. (2021). Influence of Nutrient Media Compared to Human Synovial Fluid on the Antibiotic Susceptibility and Biofilm Gene Expression of Coagulase-Negative Staphylococci In Vitro. *Antibiotics (Basel)*, *10*(7). https://doi.org/10.3390/antibiotics10070790

Stokes, J. M., Lopatkin, A. J., Lobritz, M. A., & Collins, J. J. (2019). Bacterial Metabolism and Antibiotic Efficacy. *Cell Metab*, *30*(2), 251-259. https://doi.org/10.1016/j.cmet.2019.06.009

Struve, C., Bojer, M., & Krogfelt, K. A. (2009). Identification of a conserved chromosomal region encoding Klebsiella pneumoniae type 1 and type 3 fimbriae and assessment of the role of fimbriae in pathogenicity. *Infect Immun*, *77*(11), 5016-5024. https://doi.org/10.1128/IAI.00585-09

Struve, C., Roe, C. C., Stegger, M., Stahlhut, S. G., Hansen, D. S., Engelthaler, D. M., Andersen, P. S., Driebe, E. M., Keim, P., & Krogfelt, K. A. (2015). Mapping the Evolution of Hypervirulent Klebsiella pneumoniae. *mBio*, *6*(4), e00630. https://doi.org/10.1128/mBio.00630-15

Sullivan, G. J., Delgado, N. N., Maharjan, R., & Cain, A. K. (2020). How antibiotics work together: molecular mechanisms behind combination therapy. *Curr Opin Microbiol*, *57*, 31-40. https://doi.org/10.1016/j.mib.2020.05.012

Sun, X., Vilar, S., & Tatonetti, N. P. (2013). High-throughput methods for combinatorial drug discovery. *Sci Transl Med*, *5*(205), 205rv201. https://doi.org/10.1126/scitranslmed.3006667

Sun, Y., Wang, L., Li, J., Zhao, C., Zhao, J., Liu, M., Wang, S., Lu, C., Shang, G., Jia, Y., & Wen, A. (2014). Synergistic efficacy of meropenem and rifampicin in a murine model of sepsis caused by multidrug-resistant Acinetobacter baumannii. *Eur J Pharmacol*, *729*, 116-122. https://doi.org/10.1016/j.ejphar.2014.02.015

Talebi Bezmin Abadi, A., Rizvanov, A. A., Haertlé, T., & Blatt, N. L. (2019). World Health Organization Report: Current Crisis of Antibiotic Resistance. *BioNanoScience*, *9*(4), 778-788. https://doi.org/10.1007/s12668-019-00658-4

Tamma, P. D., Aitken, S. L., Bonomo, R. A., Mathers, A. J., van Duin, D., & Clancy, C. J. (2021). Infectious Diseases Society of America Guidance on the Treatment of

Extended-Spectrum beta-lactamase Producing Enterobacterales (ESBL-E), Carbapenem-Resistant Enterobacterales (CRE), and Pseudomonas aeruginosa with Difficult-to-Treat Resistance (DTR-P. aeruginosa). *Clin Infect Dis*, *72*(7), e169-e183. https://doi.org/10.1093/cid/ciaa1478

Tamma PD, A. S., Bonomo RA, Mathers AJ, van Duin D, Clancy CJ. (2022). *Infectious Diseases Society of America Antimicrobial-Resistant Treatment Guidance: Gram-Negative Bacterial Infections*. Retrieved 03/20/2023 from

Tarkkanen, A. M., Allen, B. L., Williams, P. H., Kauppi, M., Haahtela, K., Siitonen, A., Orskov, I., Orskov, F., Clegg, S., & Korhonen, T. K. (1992). Fimbriation, capsulation, and iron-scavenging systems of Klebsiella strains associated with human urinary tract infection. *Infect Immun*, *60*(3), 1187-1192. https://doi.org/10.1128/iai.60.3.1187-1192.1992

Teklu, D. S., Negeri, A. A., Legese, M. H., Bedada, T. L., Woldemariam, H. K., & Tullu, K. D. (2019). Extended-spectrum beta-lactamase production and multi-drug resistance among Enterobacteriaceae isolated in Addis Ababa, Ethiopia. *Antimicrob Resist Infect Control*, *8*, 39. https://doi.org/10.1186/s13756-019-0488-4

Tokunaga, T., Oka, K., Takemoto, A., Ohtsubo, Y., Gotoh, N., & Nishino, T. (1997). Efficacy of trimethoprim in murine experimental infection with a thymidine kinase-deficient mutant of Escherichia coli. *Antimicrob Agents Chemother*, *41*(5), 1042-1045. https://doi.org/10.1128/AAC.41.5.1042

Tooke, C. L., Hinchliffe, P., Bragginton, E. C., Colenso, C. K., Hirvonen, V. H. A., Takebayashi, Y., & Spencer, J. (2019). beta-Lactamases and beta-Lactamase Inhibitors in the 21st Century. *J Mol Biol*, *431*(18), 3472-3500. https://doi.org/10.1016/j.jmb.2019.04.002

Tumbarello, M., Trecarichi, E. M., De Rosa, F. G., Giannella, M., Giacobbe, D. R., Bassetti, M., Losito, A. R., Bartoletti, M., Del Bono, V., Corcione, S., Maiuro, G., Tedeschi, S., Celani, L., Cardellino, C. S., Spanu, T., Marchese, A., Ambretti, S., Cauda, R., Viscoli, C., . . . Isgri, S. (2015). Infections caused by KPC-producing Klebsiella pneumoniae: differences in therapy and mortality in a multicentre study. *J Antimicrob Chemother*, *70*(7), 2133-2143. https://doi.org/10.1093/jac/dkv086

Tumbarello, M., Viale, P., Viscoli, C., Trecarichi, E. M., Tumietto, F., Marchese, A., Spanu, T., Ambretti, S., Ginocchio, F., Cristini, F., Losito, A. R., Tedeschi, S., Cauda, R., & Bassetti, M. (2012). Predictors of mortality in bloodstream infections caused by Klebsiella pneumoniae carbapenemase-producing K. pneumoniae: importance of combination therapy. *Clin Infect Dis*, *55*(7), 943-950. https://doi.org/10.1093/cid/cis588

Van, N., Degefu, Y. N., & Aldridge, B. B. (2021). Efficient Measurement of Drug Interactions with DiaMOND (Diagonal Measurement of N-Way Drug Interactions). *Methods Mol Biol*, *2314*, 703-713. https://doi.org/10.1007/978-1-0716-1460-0_30

Vernet, V., Philippon, A., Madoulet, C., Vistelle, R., Jaussaud, R., & Chippaux, C. (1995). Virulence factors (aerobactin and mucoid phenotype) in Klebsiella pneumoniae and Escherichia coli blood culture isolates. *FEMS Microbiol Lett*, *130*(1), 51-57. https://doi.org/10.1016/0378-1097(95)00141-Q

Walker, K. A., & Miller, V. L. (2020). The intersection of capsule gene expression, hypermucoviscosity and hypervirulence in Klebsiella pneumoniae. *Curr Opin Microbiol*, *54*, 95-102. https://doi.org/10.1016/j.mib.2020.01.006

Walter, J., Haller, S., Quinten, C., Karki, T., Zacher, B., Eckmanns, T., Abu Sin, M., Plachouras, D., Kinross, P., Suetens, C., & group, E. P. s. (2018). Healthcare-associated pneumonia in acute care hospitals in European Union/European Economic Area countries: an analysis of data from a point prevalence survey, 2011 to 2012. *Euro Surveill*, *23*(32). https://doi.org/10.2807/1560-7917.ES.2018.23.32.1700843

Wang, G., Zhao, G., Chao, X., Xie, L., & Wang, H. (2020). The Characteristic of Virulence, Biofilm and Antibiotic Resistance of Klebsiella pneumoniae. *Int J Environ Res Public Health*, *17*(17). https://doi.org/10.3390/ijerph17176278

Weber, B. S., De Jong, A. M., Guo, A. B. Y., Dharavath, S., French, S., Fiebig-Comyn, A. A., Coombes, B. K., Magolan, J., & Brown, E. D. (2020). Genetic and Chemical Screening in Human Blood Serum Reveals Unique Antibacterial Targets and Compounds against Klebsiella pneumoniae. *Cell Rep*, *32*(3), 107927. https://doi.org/10.1016/j.celrep.2020.107927

Willsey, G. G., Ventrone, S., Schutz, K. C., Wallace, A. M., Ribis, J. W., Suratt, B. T., & Wargo, M. J. (2018). Pulmonary Surfactant Promotes Virulence Gene Expression and Biofilm Formation in Klebsiella pneumoniae. *Infect Immun*, *86*(7). https://doi.org/10.1128/IAI.00135-18

Wiskirchen, D. E., Crandon, J. L., & Nicolau, D. P. (2013). Impact of various conditions on the efficacy of dual carbapenem therapy against KPC-producing Klebsiella pneumoniae. *Int J Antimicrob Agents*, *41*(6), 582-585. https://doi.org/10.1016/j.ijantimicag.2013.02.015

Woodford, N., & Ellington, M. J. (2007). The emergence of antibiotic resistance by mutation. *Clin Microbiol Infect*, *13*(1), 5-18. https://doi.org/10.1111/j.1469-0691.2006.01492.x

Wright, G. D. (1999). Aminoglycoside-modifying enzymes. *Curr Opin Microbiol*, *2*(5), 499-503. https://doi.org/10.1016/s1369-5274(99)00007-7

Wunderink, R. G., Giamarellos-Bourboulis, E. J., Rahav, G., Mathers, A. J., Bassetti, M., Vazquez, J., Cornely, O. A., Solomkin, J., Bhowmick, T., Bishara, J., Daikos, G. L., Felton, T., Furst, M. J. L., Kwak, E. J., Menichetti, F., Oren, I., Alexander, E. L., Griffith, D., Lomovskaya, O., . . . Kaye, K. S. (2018). Effect and Safety of Meropenem-Vaborbactam versus Best-Available Therapy in Patients with Carbapenem-Resistant Enterobacteriaceae Infections: The TANGO II Randomized Clinical Trial. *Infect Dis Ther*, *7*(4), 439-455. https://doi.org/10.1007/s40121-018-0214-1

Wyres, K. L., Lam, M. M. C., & Holt, K. E. (2020). Population genomics of Klebsiella pneumoniae. *Nat Rev Microbiol*, *18*(6), 344-359. https://doi.org/10.1038/s41579-019-0315-1

Xiao, Y., & Hu, Y. (2012). The major aminoglycoside-modifying enzyme AAC(3)-II found in Escherichia coli determines a significant disparity in its resistance to gentamicin and amikacin in China. *Microb Drug Resist*, *18*(1), 42-46. https://doi.org/10.1089/mdr.2010.0190

Xiong, H., Carter, R. A., Leiner, I. M., Tang, Y. W., Chen, L., Kreiswirth, B. N., & Pamer, E. G. (2015). Distinct Contributions of Neutrophils and CCR2+ Monocytes to Pulmonary Clearance of Different Klebsiella pneumoniae Strains. *Infect Immun*, *83*(9), 3418-3427. https://doi.org/10.1128/IAI.00678-15

Yadav, B., Wennerberg, K., Aittokallio, T., & Tang, J. (2015). Searching for Drug Synergy in Complex Dose-Response Landscapes Using an Interaction Potency Model. *Comput Struct Biotechnol J*, *13*, 504-513. https://doi.org/10.1016/j.csbj.2015.09.001

Yamane, K., Wachino, J., Suzuki, S., Kimura, K., Shibata, N., Kato, H., Shibayama, K., Konda, T., & Arakawa, Y. (2007). New plasmid-mediated fluoroquinolone efflux pump, QepA, found in an Escherichia coli clinical isolate. *Antimicrob Agents Chemother*, *51*(9), 3354-3360. https://doi.org/10.1128/AAC.00339-07

Yeh, P., Tschumi, A. I., & Kishony, R. (2006). Functional classification of drugs by properties of their pairwise interactions. *Nat Genet*, *38*(4), 489-494. https://doi.org/10.1038/ng1755

Yen, C. H., Wu, S. Y., & Liao, Y. L. (2018). Klebsiella pneumoniae Orbital Cellulitis: Clinical Manifestations and Outcomes in a Tertiary Medical Center in Taiwan. *J Ophthalmol*, *2018*, 4237573. https://doi.org/10.1155/2018/4237573

Yilmaz, G. R., Bastug, A. T., But, A., Yildiz, S., Yetkin, M. A., Kanyilmaz, D., Akinci, E., & Bodur, H. (2013). Clinical and microbiological efficacy and toxicity of colistin in patients infected with multidrug-resistant gram-negative pathogens. *J Infect Chemother*, *19*(1), 57-62. https://doi.org/10.1007/s10156-012-0451-2

Yoshida, K., Matsumoto, T., Tateda, K., Uchida, K., Tsujimoto, S., & Yamaguchi, K. (2000). Role of bacterial capsule in local and systemic inflammatory responses of mice during pulmonary infection with Klebsiella pneumoniae. *J Med Microbiol*, *49*(11), 1003-1010. https://doi.org/10.1099/0022-1317-49-11-1003

Yoshida, K., Matsumoto, T., Tateda, K., Uchida, K., Tsujimoto, S., & Yamaguchi, K. (2001). Induction of interleukin-10 and down-regulation of cytokine production by Klebsiella pneumoniae capsule in mice with pulmonary infection. *J Med Microbiol*, *50*(5), 456-461. https://doi.org/10.1099/0022-1317-50-5-456

Yu, W. L., Ko, W. C., Cheng, K. C., Lee, C. C., Lai, C. C., & Chuang, Y. C. (2008). Comparison of prevalence of virulence factors for Klebsiella pneumoniae liver abscesses between isolates with capsular K1/K2 and non-K1/K2 serotypes. *Diagn Microbiol Infect Dis*, *62*(1), 1-6. https://doi.org/10.1016/j.diagmicrobio.2008.04.007

Zhang, X., Qi, S., Duan, X., Han, B., Zhang, S., Liu, S., Wang, H., Zhang, H., & Sun, T. (2021). Clinical outcomes and safety of polymyxin B in the treatment of carbapenem-resistant Gram-negative bacterial infections: a real-world multicenter study. *J Transl Med*, *19*(1), 431. https://doi.org/10.1186/s12967-021-03111-x

Zhu, J., Wang, T., Chen, L., & Du, H. (2021). Virulence Factors in Hypervirulent Klebsiella pneumoniae. *Front Microbiol*, *12*, 642484. https://doi.org/10.3389/fmicb.2021.642484

Zhu, M., Tse, M. W., Weller, J., Chen, J., & Blainey, P. C. (2021). The future of antibiotics begins with discovering new combinations. *Ann N Y Acad Sci*, *1496*(1), 82-96. https://doi.org/10.1111/nyas.14649